

UNIVERSIDADE FEDERAL DE MINAS GERAIS
Programa de Pós-Graduação em Engenharia Elétrica

Daniel Almeida Godinho

**DISTRIBUTED CONTROL AND REORGANIZATION OF HETEROGENEOUS
VEHICLE PLATOONS SUBJECT TO TIME DELAY AND LIMITED
COMMUNICATION RANGE**

Belo Horizonte

2023

Daniel Almeida Godinho

**DISTRIBUTED CONTROL AND REORGANIZATION OF
HETEROGENEOUS VEHICLE PLATOONS SUBJECT TO TIME DELAY
AND LIMITED COMMUNICATION RANGE**

A thesis presented to the Graduate Program in Electrical Engineering (PPGEE) of the Federal University of Minas Gerais (UFMG) in partial fulfillment of the requirements to obtain the degree of Doctor in Electrical Engineering.

Advisor: Fernando de Oliveira Souza

Co-Advisor: Armando Alves Neto

Belo Horizonte

2023

G585d	<p>Godinho, Daniel Almeida. Distributed control and reorganization of heterogeneous vehicle platoons subject to time delay and limited communication range [recurso eletrônico] / Daniel Almeida Godinho. – 2023. 1 recurso online (88 f. : il., color.) : pdf.</p>
	<p>Orientador: Fernando de Oliveira Souza. Coorientador: Armando Alves Neto.</p>
	<p>Tese (doutorado) – Universidade Federal de Minas Gerais, Escola de Engenharia.</p>
	<p>Inclui bibliografia.</p>
	<p>1. Engenharia elétrica – Teses. 2. Direção de automóveis – Teses. 3. Veículos autônomos – Teses. 4. Sensores – Processamento de dados – Teses. I. Souza, Fernando de Oliveira. II. Alves Neto, Armando. III. Universidade Federal de Minas Gerais. Escola de Engenharia. IV. Título.</p>
	<p>CDU: 621.3(043)</p>



UNIVERSIDADE FEDERAL DE MINAS GERAIS
ESCOLA DE ENGENHARIA
PROGRAMA DE PÓS-GRADUAÇÃO EM ENGENHARIA ELÉTRICA

FOLHA DE APROVAÇÃO

"DISTRIBUTED CONTROL AND REORGANIZATION OF HETEROGENEOUS VEHICLE PLATOONS SUBJECT TO TIME DELAY AND LIMITED COMMUNICATION RANGE"

DANIEL ALMEIDA GODINHO

Tese de Doutorado submetida à Banca Examinadora designada pelo Colegiado do Programa de Pós-Graduação em Engenharia Elétrica da Escola de Engenharia da Universidade Federal de Minas Gerais, como requisito para obtenção do grau de Doutor em Engenharia Elétrica. Aprovada em 26 de junho de 2023. Por:

Prof. Dr. Fernando de Oliveira Souza
DELT (UFMG) - Orientador

Prof. Dr. Armando Alves Neto
DELT (UFMG) - Coorientador

Prof. Dr. Leonardo Amaral Mozelli
DELT (UFMG)

Prof. Dr. Luciano Cunha de Araújo Pimenta
DELT (UFMG)

Prof. Dr. José Mário Araújo
PPGESP (IFBA)

Prof. Dr. David Saldaña
Department of Computer Science and Engineering (Lehigh University)



Documento assinado eletronicamente por **Frederico Gadelha Guimaraes, Coordenador(a) de curso de pós-graduação**, em 04/07/2023, às 16:22, conforme horário oficial de Brasília, com fundamento no art. 5º do [Decreto nº 10.543, de 13 de novembro de 2020](#).



A autenticidade deste documento pode ser conferida no site https://sei.ufmg.br/sei/controlador_externo.php?acao=documento_conferir&id_orgao_acesso_externo=0, informando o código verificador **2436379** e o código CRC **F27FB160**.

Dedico a minha Mãe.

ACKNOWLEDGEMENTS

First of all, I would like to thank my advisor Professor Fernando for the opportunity to open my horizons to other areas of knowledge and Professor Armando for his important contributions. Remembering, and already thanking Professor Leo Torres, for his dedication to expanding my abstraction capacity. I would like to thank Professor Reinaldo Palhares for motivating me during the first morning classes and for accessing D!FCOM, where I had the opportunity to make friends: Caio, Gabriela, Daniela, Pedro, Iury, Márcia, Murilo, Mariella and Emerson. I would also like to thank my colleagues Alesi and José. The professors for their example and dedication in writing the articles: Armando for the important contribution and programming expertise for simulation results, Mozelli for his synergy with the group, Fernando for his care and perfection in his corrections. Special thanks to Professors Leonardo Frezzatto, Victor, Frederico, Adorno and Aguirre for the excellent classes.

I thank Izabela, my wife, who travels by my side through the infinite universe of life. For always participating in my studies, research, experiences in the physical/metaphysical, exact/inaccurate sciences; social and philosophical. Much love and thanks for all the interest, encouragement and active participation in understanding and suggestions for clearer expositions and aggregators of broad meanings of greater accessibility to knowledge.

Special thanks to professors José Mario Araújo from the Federal Institute of Bahia and David Saldaña at Lehigh University in Bethlehem, Pennsylvania for their suggestions that improved this work.

Special thanks to Ian for teaching me to live life again with the perspective and understanding of children. For strengthening my patience and helping me develop a broader sense of social responsibility. For you, my son, my eternal love!

I thank the Brazilian agencies that invested in this work: CNPq, CAPES, and FAPEMIG.

*“A beleza de ser um eterno aprendiz”
(Gonzaguinha)*

RESUMO

A cooperação entre veículos autônomos no tráfego urbano e no transporte em estradas, dispostos em comboios, constitui uma solução para um trânsito mais seguro e organizado, promovendo maior eficiência energética. Neste contexto, este trabalho aborda o controle distribuído e a reorganização de comboios heterogêneos de veículos, considerando restrições de comunicação, incluindo limitação do alcance e atrasos fixos e heterogêneos, bem como eventos de reconfiguração ao longo do deslocamento. Os veículos são equipados com sensores, atuadores e unidades de processamento e controle, o que possibilita a formação e a manutenção dos comboios por meio do consenso sobre as posições relativas entre veículos conectados. Este trabalho propõe soluções para o problema de controle distribuído aplicado à formação de comboios heterogêneos, adotando uma política de espaçamento constante e alcance de comunicação limitado. Como principais resultados, são apresentadas estratégias para a recuperação automática da distância desejada, garantindo a resiliência do comboio independentemente do número de veículos. O controle dos veículos é projetado segundo uma estrutura hierárquica de dois níveis. No primeiro nível, a lei de controle implementada em um sistema de automação regula o movimento do veículo a partir de dados de posição, velocidade e aceleração recebidos dos veículos à sua frente, caracterizando uma topologia de comunicação do tipo *predecessor-seguidor*. O segundo nível da hierarquia é regido por protocolos que modificam entradas de dados e a estrutura de controle diante de mudanças na configuração do comboio, abrangendo a reconfiguração para eventos de entrada e saída de veículos e a recuperação após perda completa de comunicação e segmentação, viabilizando a recomposição do sistema. Os resultados obtidos são aplicáveis a sistemas lineares invariantes no tempo. O modelo de cada veículo é obtido por meio de uma técnica de linearização aplicada a um modelo não linear da dinâmica longitudinal. A conectividade entre os veículos é descrita utilizando a teoria de grafos. A estabilidade do sistema é assegurada pela convergência da distância de espaçamento em relação aos veículos vizinhos para valores desejados. As análises consideram cenários de comunicação sem atraso e com atraso fixo e heterogêneo, utilizando a teoria de controle clássica, com ganhos de controle selecionados de acordo com o critério de *Routh-Hurwitz*, o qual garante a estabilidade assintótica. Os resultados demonstram que a estabilização de todos os veículos do comboio heterogêneo é assegurada pela estabilidade individual de cada veículo, utilizando apenas variáveis locais. Exemplos numéricos, implementados em linguagem *Python*, e testes realizados no simulador *CARLA*, emulando condições realistas de condução dos veículos, demonstram a eficácia das metodologias propostas.

Palavras-chave: comboios de veículos autônomos; controle distribuído; veículos heterogêneos; distância interveicular; perda de comunicação.

ABSTRACT

The cooperation between autonomous vehicles in urban traffic and highway transportation, arranged in platoons, constitutes a solution for safer and more organized traffic conditions, promoting greater energy efficiency. In this context, this work addresses the distributed control and reorganization of heterogeneous vehicle platoons, considering communication constraints, including limited communication range and fixed and heterogeneous delays, as well as reconfiguration events during motion. Vehicles are equipped with sensors, actuators, and processing and control units, which enable the formation and maintenance of platoons through consensus on the relative positions among connected vehicles. This work proposes solutions to the distributed control problem applied to the formation of heterogeneous platoons, adopting a constant spacing policy and limited communication range. As the main results, strategies for the automatic recovery of the desired spacing distance are presented, ensuring platoon resilience regardless of the number of vehicles. Vehicle control is designed according to a two-level hierarchical structure. At the first level, the control law implemented in an automation system regulates the vehicle's motion based on position, velocity, and acceleration data received from preceding vehicles, characterizing a predecessor–follower communication topology. The second level of the hierarchy is governed by protocols that modify data inputs and control structure in response to changes in the platoon configuration, encompassing reconfiguration for vehicle entry and exit events and recovery after complete communication loss and platoon segmentation, enabling system recomposition. The obtained results are applicable to linear time-invariant systems. The model of each vehicle is obtained through a linearization technique applied to a nonlinear longitudinal dynamics model. Inter-vehicle connectivity is described using graph theory. System stability is ensured by the convergence of inter-vehicle spacing relative to neighboring vehicles to desired values. The analyses consider communication scenarios without delay and with fixed and heterogeneous delays, using classical control theory, with control gains selected according to the *Routh-Hurwitz* criterion, which guarantees asymptotic stability. The results demonstrate that stabilization of all vehicles in the heterogeneous platoon is ensured through the individual stability of each vehicle using only local variables. Numerical examples implemented in *Python* and tests conducted in the *CARLA* simulator, emulating realistic vehicle driving conditions, demonstrate the effectiveness of the proposed methodologies.

Keywords: autonomous vehicle platoons; distributed control; heterogeneous vehicles; inter-vehicle distance; communication loss.

LIST OF FIGURES

Figure 1.1 – The platoon must reorganize itself to fill/vacate some spots, keeping stability and ensuring the desired inter-vehicle space in steady-state.	22
Figure 1.2 – Heterogeneous vehicular platoons under limited communication range and time-delay: when a vehicle, or a subset of vehicles, loses connection with the team, it must be able to re-connect, maintaining the original formation.	23
Figure 3.1 – Example: direct graph – > connections communication topology of the vehicles in a platoon formed by five follower vehicles ($i = 1, \dots, 5$) plus the leader ($i = 0$).	33
Figure 3.2 – Metric parameters in the platoon. The position p_i of the i – th vehicle is referenced on its rear bumper. The vehicle i must keep the fixed distance $d_{i,i-1} = \gamma_i + \ell_i$ from its first immediately preceding neighbor, the distance $d_{i,i-2} = \gamma_i + \ell_i + \gamma_{i-1} + \ell_{i-1}$ to its second immediately preceding neighbor ($i - 2$), and so on.	36
Figure 5.1 – Vehicles position with multiple entries and exits.	57
Figure 5.2 – Formation error. At 150 s, 3 vehicles exit simultaneously splitting the platoon.	57
Figure 5.3 – Weighted-Mean-Subsequence-Reduced (W-MSR) method in (PIRANI <i>et al.</i> , 2018). Comparative analysis between (PIRANI <i>et al.</i> , 2018) and our approach: position over time.	59
Figure 5.4 – Our reconfiguration protocol. Comparative analysis between (PIRANI <i>et al.</i> , 2018) and our approach: position over time.	59
Figure 5.5 – Comparative analysis between (PIRANI <i>et al.</i> , 2018) and our approach: spacing over time. W-MSR method in (PIRANI <i>et al.</i> , 2018).	59
Figure 5.6 – Comparative analysis between (PIRANI <i>et al.</i> , 2018) and our approach: spacing over time. Our reconfiguration protocol.	60
Figure 6.1 – Switching protocol: in the <i>Virtual Reference</i> state, the vehicle is completely disconnected from the platoon; when it reaches one agent at its front, it switches to the <i>Transitory Condition</i> , using the state information provided by its new neighbor to reduce the state error; when the error is small enough, the vehicle goes to the <i>Stationary Condition</i> , following the entire platoon.	62
Figure 6.2 – Virtual agent used to ensure connectivity with the platoon in the <i>Virtual Reference</i> state: when no communication is available and there is a free path, vehicle i uses a virtual neighbor traveling ahead to run the proposed control law. R_i represents the vehicle i communication range.	64

Figure 6.3 – (experiment 1) position of the vehicles over time. All agents start disconnected and, over time, they are capable of stabilizing the platoon. After the exit of three vehicles simultaneously, there is a momentary split, but a new steady state condition is reached.	68
Figure 6.4 – (experiment 1) spacing error of the vehicles over time according to the leader. All followers start disconnected, but they can reach their forwarding neighbors. The platoon presented a null error when three vehicles exited, but the disturbance is quickly compensated.	69
Figure 6.5 – (experiment 1) state behavior of the vehicles over time. After the stabilization, all followers reach the stationary condition, until the disturbance, when vehicle 7 assumes the <i>Virtual Reference</i> state and accelerates to reach again the <i>Stationary Condition</i> state.	69
Figure 6.6 – (experiment 1) speed of the vehicles over time. Even with the disturbances caused by the disconnection, the followers were able to track the leader’s speed.	70
Figure 6.7 – (experiment 2) position of the vehicles over time. The agents start connected and the platoon moves on until 40 s when a traffic light splits it. Then, the leader and the first 4 followers travel freely, while the rest are held at the red light during 20 s. Even so, after the green light, the platooning formation is reestablished.	70
Figure 6.8 – (experiment 2) spacing error of the vehicles over time according to the leader. After some members are stuck at the traffic light, they manage to reach the vehicles ahead.	71
Figure 6.9 – (Experiment 2) Vehicle state evolution over time. After stabilization, all followers reach the <i>Stationary</i> state until the traffic light event, when vehicle 5 assumes the <i>Virtual Reference</i> state. At the green light, this vehicle accelerates and returns to the <i>Stationary</i> state.	72
Figure 6.10–(Experiment 2) Vehicle speeds over time. After leaving the traffic light, the follower vehicles successfully track the leader speed.	73
Figure 6.11–experiment 3) platoon composed of the leader and 9 followers implemented in the <i>CARLA</i> simulator: (a) the robots start connected, but the fourth follower (an Human-driven Vehicle (HDV)) delays its predecessors with a low speed;	74
Figure 6.12–experiment 3) platoon composed of the leader and 9 followers implemented in the <i>CARLA</i> simulator: (b) the HDV leaves the road	74
Figure 6.13–experiment 3) platoon composed of the leader and 9 followers implemented in the <i>CARLA</i> simulator: (c) the last agents recover connection and reaches null spacing error.	75

Figure 6.14–(Experiment 3) Vehicle positions in the <i>CARLA</i> simulator. All agents start connected. After $t = 20$ s, the HDV splits the platoon, leaving the road at $t = 50$ s and allowing the predecessor vehicles to recover communication after approximately $t = 70$ s.	76
Figure 6.15–(Experiment 3) Spacing error of the vehicles with respect to the leader in the <i>CARLA</i> simulator. After the initial stationary condition of the platoon, the HDV enters and leaves the road; however, the resulting disturbance is completely rejected by the proposed protocol.	77
Figure 6.16–(Experiment 3) Vehicle states in the <i>CARLA</i> simulator. All agents remain in the <i>Stationary</i> state until the interference of the HDV, whose lower speed forces the disconnection of follower 5. This vehicle remains in the <i>Virtual</i> state until it rejoins the platoon, after the exit of the disturbing agent at $t = 50$ s.	78
Figure 6.17–(Experiment 3) Vehicle speeds in the <i>CARLA</i> simulator. All follower vehicles track the leader speed before and after the exit of the HDV.	79

LIST OF TABLES

Table 5.1 – Vehicle parameters extracted from (ZHENG <i>et al.</i> , 2019).	56
Table 5.2 – Parameters extracted from the CoppeliaSim.	58
Table 6.1 – Vehicle parameters extracted from (ZHENG <i>et al.</i> , 2019).	68

LIST OF ABBREVIATIONS

ADRC	Approximate Distributed Robust Convergence
DAG	Directed Acyclic Graph
DAGs	Directed Acyclic Graphs
DoS	Denial-of-Service
HDV	Human-driven Vehicle
HDVs	Human-driven Vehicles
LTI	linear time-invariant
VANETs	Vehicular Ad-hoc Network
W-MSR	Weighted-Mean-Subsequence-Reduced

LIST OF SYMBOLS

\mathbb{R}^n	The n -dimensional Euclidean space
$\mathbb{R}^{n \times m}$	The set of $n \times m$ real matrix
$\det(\dots)$	Determinant matrix
\otimes	Kronecker product
\mathbf{x}	The vector is written in bold
0	Null matrix of appropriate dimension
I	Identity matrix of appropriate dimension
I_n	Identity matrix of n -th order
$\text{diag}\{\dots\}$	Block-diagonal matrix
A	Matrix $A = [a_{ij}]$
A^\top	Transpose of matrix A
$*$	Transpose element inside of a symmetric matrix
$p_i(t)$	position of i -th follower vehicle
$v_i(t)$	velocity of i -th follower vehicle
$a_i(t)$	acceleration of i -th follower vehicle
m_i	mass
η_i	efficiency
r_i	tire radius
g	gravity acceleration
μ_i	friction constant
ρ	density
C_i	drag coefficient
T_i	torque of the actuators on the movement of the vehicle
\tilde{T}_i	desired torque

ζ_i	powertrain time constant
\mathbf{K}_i	control gain vector
τ	fixed communication time-delay between connected vehicles and your follower
τ_{i0}	communication time-delay between the follower and the lead vehicle
τ_{ij}	communication time-delay between the i-th follower and the j-th followed vehicle

CONTENTS

1	INTRODUCTION	18
1.1	Control of connected vehicles in platoons	18
1.2	Motivation	20
1.2.1	Reorganization of platoon after vehicle exits and entrances	21
1.2.2	Vehicular Platoon under connection loss	22
1.3	Objectives	23
1.4	Thesis outline and contributions	23
2	RELATED WORKS	25
2.1	Autonomous ground vehicles in platoons	25
2.2	Resilience applied in control of vehicles in platoons	25
2.3	Limited communication ranges	27
2.4	Graph theory	28
2.5	Distributed Control and Stability of Vehicle Platoons	28
2.6	Reorganization of platoons	29
3	THEORETICAL FORMALIZATION	31
3.1	Longitudinal vehicle dynamics	31
3.2	Network communication model	32
3.3	Definitions for the steady state: Platoon formation	36
4	HETEROGENEOUS PLATOON VEHICLES WITH FIXED COMMUNICATION TOPOLOGY	37
4.1	Decentralized Control Law	37
4.1.1	A: Platoon free of communication delay	37
4.1.2	B: Communication with fixed constant delay	38
4.1.3	C: Communication with heterogeneous constant delay	41
4.2	Formation error dynamics	43
4.2.1	A: Platoon free of communication delay	43
4.2.2	B: Communication with fixed constant delay	44
4.2.3	C: Communication with heterogeneous constant delay	45
4.3	Platoon under fixed communication topology	47
4.3.1	A: Platoon free of communication delay	47
4.3.2	B: Communication with fixed constant delay	49
4.4	Structural Properties of Local Stabilization under a Predecessor–Follower Topology	51
5	PROTOCOL OF RECONFIGURATION AFTER ENTRY AND EXIT OF VEHICLES.	53
5.1	Resilience condition for platoon stability	55
5.2	Numerical examples	56

5.2.1	Linear simulation: multiple entries and exits	56
5.2.2	Nonlinear simulation: comparative analysis	58
6	PROTOCOL FOR RECOVERY OF VEHICLE TO THE PLATOON	61
6.1	Problem definition	61
6.2	Main results	61
6.2.1	Proposed approach	61
6.2.2	Reconnection protocol	63
6.2.3	Formation error	65
6.3	Simulation and analysis results for the platoon of vehicles with communication with heterogeneous delay.	67
6.3.1	Simulation: disconnection	67
6.3.2	Simulation: traffic light	69
6.3.3	Nonlinear simulation: human-driven vehicle	71
7	CONCLUSIONS AND FUTURE DIRECTIONS	80
7.1	Conclusions	80
7.2	Future research directions	81
7.3	Publications	82
	BIBLIOGRAPHY	83

1 INTRODUCTION

This chapter provides an overview of the entire thesis. The proposed approach for the decentralized control of vehicles connected in platoons is first introduced, highlighting the formation error as the main performance variable and its modeling through graph-based augmented state-space representations. The motivations and objectives of this research are then presented, followed by a summary of the main contributions and an outline of the organization of the thesis.

1.1 Control of connected vehicles in platoons

The cooperation between autonomous vehicles in urban traffic and road transport, organized in platoons, is an intelligent solution for greater safety, time savings, energy efficiency (PI *et al.*, 2023), and consequently lower pollutant emissions (LI *et al.*, 2015). The growing demand for efficient and safe transportation systems in urban and highway scenarios has fostered extensive research on autonomous vehicle platoons (LIU; KAMEL, 2016; GAO; DANG; LI, 2015; JIN; OROSZ, 2016; XU *et al.*, 2018).

From the perspective of control theory, the concept of self-recovery explored in this thesis is associated with the stability properties of interconnected systems, particularly their ability to reorganize and recompose vehicle formations under a consensus-based strategy (SILJAK, 1978; MESBAHI; EGERSTEDT, 2010; BULLO; CORTÉS; MARTÍNEZ, 2009a). Platoon stabilization is achieved when a decentralized control approach enables each vehicle to regulate its motion and relative spacing within the formation based on locally available information.

A representative scenario addressed in this work occurs when a vehicle leaves the platoon. Assuming that all vehicles are initially at the desired spacing from their predecessors, the departure of one vehicle creates an increase in the inter-vehicle distance for the following vehicle, which acts as a disturbance in the system. This disturbance gives rise to a spacing error, arising when relative position information is updated to account for the new preceding vehicle. The decentralized control law, once updated with this new local information, enables the self-recovery of the spacing error through cooperative interaction among vehicles (GUNGOR *et al.*, 2020).

Platoons can be viewed as a particular class of *networked robotic systems*, emerging at the intersection of robotics and control engineering, in which each vehicle follows its predecessors by exchanging information and executing automated control algorithms (Hu *et al.*, 2020). The progressive automation of vehicular fleets enhances autonomy with respect to human driving and enables tighter integration with other traffic agents and infrastructure, fostering cooperative behavior aligned with consensus objectives.

In this context, vehicles rely on onboard sensing and communication systems to obtain information such as position, velocity, and acceleration from neighboring vehicles. Such variables may be obtained through onboard sensors, such as sonar or infrared devices, or through wireless communication by transmitting measurements from preceding vehicles.

This work adopts predecessor–follower (or look-ahead) communication topologies, in which each vehicle receives information only from vehicles ahead. Such topologies are particularly attractive due to their practical relevance and their suitability for analytical treatment using classical control theory, allowing rigorous proofs of spacing error convergence to zero (FENG *et al.*, 2019).

Beyond coordination benefits, close inter-vehicle spacing also contributes to improved traffic flow efficiency and reduced aerodynamic drag, leading to energy savings. The nonlinear nature of longitudinal vehicle dynamics, in part due to aerodynamic effects, motivates the use of feedback linearization to obtain adequate linear models for control design within the scope of linear time-invariant (LTI) systems considered in this thesis.

The developments presented throughout this thesis extend control conditions commonly applied to homogeneous platoons, enabling their application to formations composed of vehicles with heterogeneous characteristics.

To better reflect realistic operating conditions, this work considers limited communication ranges that may vary among vehicles, leading to heterogeneous connectivity conditions within the platoon. Based on the information received from neighboring vehicles located within the communication radius, the control law is computed according to a consensus strategy on the inter-vehicle spacing among connected agents.

A platoon is initially conceived as a system composed of a finite number of vehicles, forming a closed group in which all members are known. The proposed methodology models the communication network using graph theory, where the leading vehicle is indexed as $i = 0$, and the following vehicles are indexed from $i = 1$ to the n -th vehicle in the queue.

By adopting a decentralized control approach and performing appropriate algebraic manipulations—together with properties of triangular matrix determinants—it follows that each vehicle can be governed by a control law that depends only on local information exchanged with its neighboring vehicles. Consequently, platoon formation and maintenance rely on the stabilization of the spacing error of each vehicle with respect to its neighbors.

Since communication networks are inherently imperfect, delays arise in the transmission of state information between vehicles. These delays may originate from onboard sensing processes or from wireless communication links. When a vehicle receives relative position measurements from a neighboring vehicle, this information typically arrives with a delay.

The analysis and design of the proposed control laws therefore account for scenarios without delay, with fixed delays, and with heterogeneous delays. Classical control tools are

employed to ensure stability, with control gains selected according to the Routh–Hurwitz criterion, providing guarantees of asymptotic stability and bounds on admissible delay values.

Finally, two complementary resilience mechanisms are considered. The first addresses platoon reconfiguration following vehicle entry and exit events, aiming to preserve stability under structural changes. The second concerns the recovery of vehicles that temporarily lose communication due to limited sensing or communication range, enabling their reconnection and reintegration into the platoon. Together, these mechanisms provide a foundation for resilient and scalable control of heterogeneous vehicular platoons, which is further developed in the subsequent chapters.

1.2 Motivation

The motivation for this work arises from the potential application of control engineering techniques to the coordination of autonomous vehicles organized in platoons for the transportation of people and freight (cargo). Such coordination aims to contribute to traffic efficiency by alleviating congestion and reducing the stress associated with low-speed driving conditions in urban and road environments.

To reflect realistic traffic scenarios and promote diversity in platoon formation, this thesis considers vehicles with different dynamic characteristics, giving rise to the concept of heterogeneous vehicle platoons. Any vehicle equipped with automatic longitudinal control, appropriate actuators, and sensing or communication capabilities to identify and exchange information with preceding vehicles may become part of a platoon.

Through the use of distributed controllers, control theory provides the necessary tools to regulate the motion of each vehicle autonomously while maintaining coordination with the overall platoon objectives. A key assumption adopted in this work is that each vehicle governs its motion using only local variables obtained from neighboring vehicles, without reliance on global or centralized information.

To further enhance realism, limitations on the communication range of each vehicle are explicitly considered. Additionally, imperfections inherent to communication networks are taken into account, such as the presence of information delays. These constraints reflect practical conditions encountered in real vehicular communication systems and motivate the development of robust distributed control strategies.

Another central motivation of this thesis is to ensure the resilience of vehicular platoons in the presence of structural changes and adverse communication conditions. Specifically, the platoon should be capable of autonomously recovering its desired formation following vehicle entry and exit events, as well as after complete communication loss caused by limited communication range. The objective is to maintain the desired inter-vehicle spacing and functional integrity of the platoon regardless of the number of participating vehicles.

To clarify these motivations, two illustrative scenarios are introduced in the following subsections. The first concerns the reorganization of the platoon following the entry and exit of vehicles, while the second addresses situations in which a vehicle temporarily loses communication with the platoon due to limited communication range.

1.2.1 Reorganization of platoon after vehicle exits and entrances

It is common in platooning scenarios that one or more vehicles need to leave the group due to mechanical issues, route changes, lane selection, unplanned stops, or individual driving decisions that differ from those of the remaining platoon members.

From a broader perspective, vehicles that were not originally part of the platoon may also request to join the formation, provided they are equipped with appropriate sensing, communication, and automation capabilities. Such vehicle entry and exit events introduce structural changes in the platoon configuration and must be handled without compromising stability.

Figure 1.1 illustrates the platoon reorganization process considered in this thesis.

In the first frame, the platoon is depicted in a steady-state configuration, with the leader (red truck) defining the reference velocity. In the second frame, the yellow truck exits the platoon, creating a gap in the formation. As a result, the remaining vehicles autonomously adjust their inter-vehicle spacing, forming a shorter platoon.

After reaching a new equilibrium condition, the platoon receives a request for the entry of a new vehicle (blue truck), which approaches from an adjacent lane. In the subsequent frames, the vehicles incorporate the information associated with the new member and reorganize the formation accordingly.

This entire process is carried out in a distributed and autonomous manner, with each vehicle relying solely on local information exchanged with neighboring vehicles. The optimization variable, defined as the inter-vehicle spacing error, converges to zero, preserving platoon stability throughout the reorganization process.

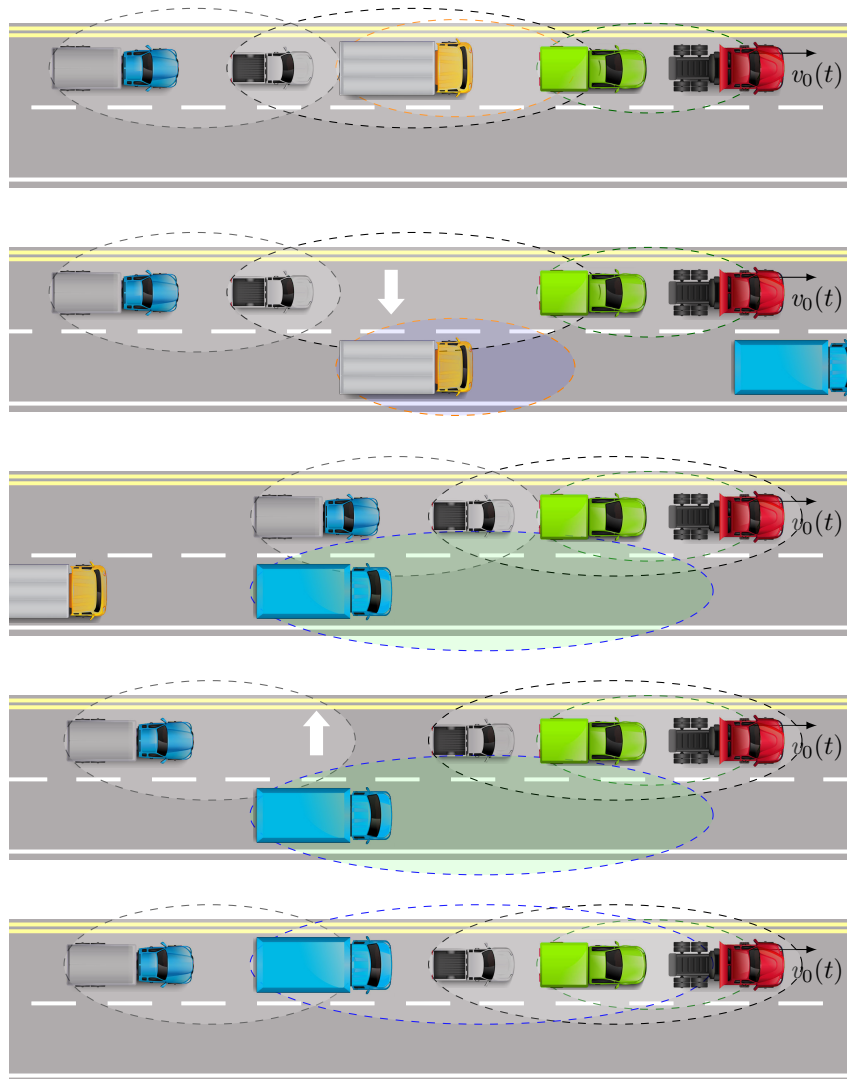


Figure 1.1 – The platoon must reorganize itself to fill/vacate some spots, keeping stability and ensuring the desired inter-vehicle space in steady-state.

1.2.2 Vehicular Platoon under connection loss

In practical vehicular communication networks, connectivity is subject to limitations and failures. A particularly critical situation arises when a vehicle, or a subset of vehicles, loses communication with the platoon due to limited communication range or adverse operating conditions.

In such cases, it is essential that the affected vehicle be able to autonomously respond to the loss of connectivity, modifying its operational mode in order to recover communication and reestablish its participation in the platoon, while preserving system stability.

Figure 1.2 presents a representative scenario in which communication loss leads to the segmentation of a heterogeneous vehicular platoon.

When communication is lost, the affected vehicle may no longer receive the information required to compute the distributed control law under the nominal platooning mode. Without

appropriate corrective actions, this situation may compromise the maintenance of the desired formation.

To address this issue, this thesis considers a recovery strategy in which the control law is modified to enable the disconnected vehicle to regain connectivity and reintegrate into the platoon.

The proposed approach allows the desired formation to be restored after communication loss, ensuring platoon resilience under realistic communication constraints.

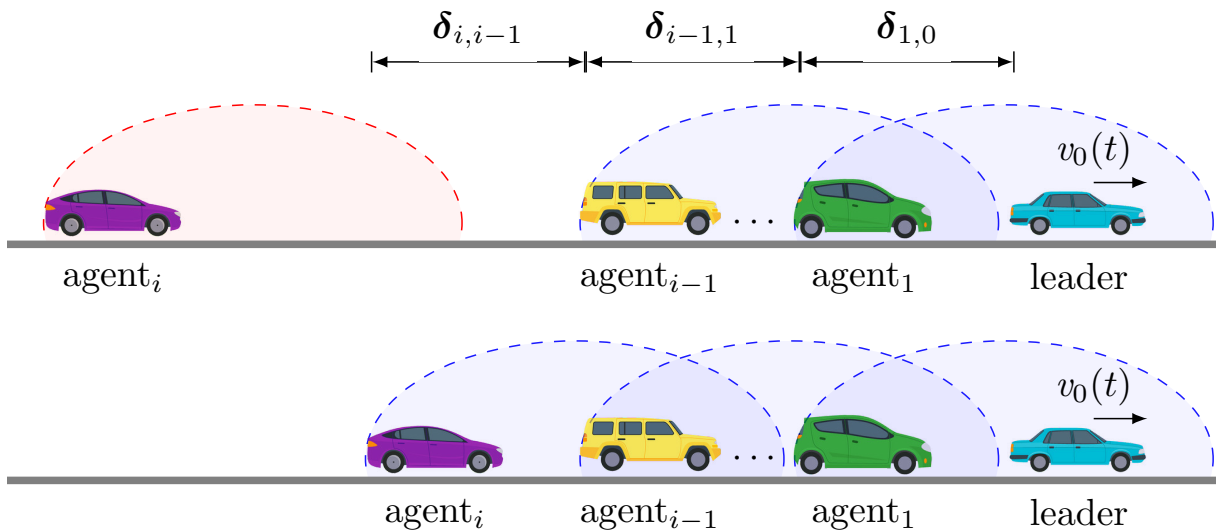


Figure 1.2 – Heterogeneous vehicular platoons under limited communication range and time-delay: when a vehicle, or a subset of vehicles, loses connection with the team, it must be able to re-connect, maintaining the original formation.

1.3 Objectives

- To develop a distributed control framework for the formation of heterogeneous autonomous vehicles organized in platoons;
- To design reorganization protocols that preserve platoon stability under vehicle entry and exit events;
- To develop recovery strategies for vehicle reintegration into the platoon under communication constraints, including limited communication range and time delay.

1.4 Thesis outline and contributions

This thesis is organized into seven chapters, following a continuous methodological progression from problem formulation to the development of control strategies and their analysis under realistic communication constraints.

Chapter 1 introduces the research problem, providing the motivation, objectives, and scope of the work. It also presents illustrative scenarios that highlight the challenges associated with vehicle platoon formation, reorganization, and recovery under communication limitations.

Chapter 2 reviews the relevant literature on vehicle platoons, distributed control strategies, communication topologies, limited communication ranges, graph-theoretic modeling, and stability analysis.

Chapter 3 presents the modeling and problem formulation adopted in this thesis. This chapter describes the longitudinal dynamics of individual vehicles, the communication network modeled using graph theory, and the definition of the formation error used as the main control objective.

Chapter 4 addresses the design and analysis of distributed control laws under fixed communication topology. Stability conditions are derived and analyzed for scenarios without communication delay, as well as for cases with fixed and heterogeneous communication delays.

Chapter 5 presents a reorganization protocol that enables the platoon to preserve stability following vehicle entry and exit events. Numerical simulations are provided to validate the effectiveness of the proposed approach.

Chapter 6 introduces a recovery protocol that allows a vehicle to reintegrate into the platoon after communication loss caused by limited communication range. The chapter includes analysis and simulation results demonstrating the resilience of the platoon under such conditions.

Finally, Chapter 7 summarizes the main results of the thesis, highlights the achieved objectives, and discusses possible directions for future research.

2 RELATED WORKS

This chapter presents a literature review and fundamental concepts that form the basis of this thesis. The discussion focuses on resilience, cooperative autonomous vehicles, and platoon control, with particular emphasis on communication constraints such as topology changes, time delays, and limited communication ranges.

2.1 Autonomous ground vehicles in platoons

Research and development efforts on autonomous ground vehicles operating in platoons have increased in recent years. Platoons can be seen as vehicles organized into groups for transport, travel, or in traffic jam conditions. The vehicles, to maintain formation, are equipped with propulsion and braking automation to control their movement. In addition, a communication device is necessary, with reception or measurements of the variables, to update the control law and thus maintain fixed distances from the other vehicles in the group. As the control is decentralized, the consensus law input information comes from the vehicle itself and from the variables measured and transmitted by other vehicles in the vicinity, within a limited connection distance. Due to the complexity involved, the control of this type of system is divided into stages, from the modeling of the individual dynamics of the vehicles, the modeling of the connections network, and finally the design and tuning of the controller of each vehicle. In (Dey et al., 2016), the authors provide an overview of the literature on platoons, covering the following subjects: communication structures, driver interference, and control strategies ranging from modeling to controller design.

The project to control connected vehicles in a resilient manner must be fault-tolerant and mitigate effects that may destabilize the platoon, considering technological limitations such as imperfect network effects, as well as structural changes in the communication topology, and human interaction.

2.2 Resilience applied in control of vehicles in platoons

The failures and technological limitations that are part of the real world scenario can make the platoon unstable. Considering connected vehicles as robots in a communication network, we can treat platoon stabilization with the concept of robotic resilience. In (ALEXIS, 2020), robotic resilience is divided into three areas of study: robustness, redundancy and resourcefulness.

Robustness is related to the ability of the system to absorb or withstand unpredictable disturbances or adverse situations. Meanwhile, *redundancy* concerns the capacity of maintaining

the core functionality of the system by backing up its components. And finally, *resourcefulness* addresses the ability of the system to adapt to changes or evolving operational conditions. This aspect is particularly relevant in the context of platoon reconfiguration and distributed operation.

Resourcefulness represents the main challenge in ensuring resilient autonomy in adverse environments. Changes in the platoon structure (planned or not) may lead to critical situations, such as collision, lack of network connectivity, or internal instability. In the paper (Antonelli; Chiaverini, 2006) the authors work with the formation of multi-robots proposing a controller to deal with obstacles. In this context, resilient platoons have attracted the attention of the community because of situations that can affect team performance. The authors of (Parkinson *et al.*, 2017), for example, describe weaknesses in vehicle components, human interaction and communication network infrastructure and strategies to deal with these problems. In (PIRANI *et al.*, 2018), the authors propose a control algorithm for k -nearest neighbor platoons modeled as k -connected graphs, ensuring resilience by employing the W-MSR algorithm (LeBlanc *et al.*, 2013) against up to k malicious or failing agents. These results are derived under the assumption of strong network connectivity, which characterizes a specific class of resilient platooning problems. Other classes of problems arise when connectivity conditions are relaxed or subject to structural changes. Redundancy is another resilience aspect considered in platoon missions. In (Patounas; Zhang; Gjessing, 2015), for example, the authors use a protocol to propagate redundant data among the agents, being able to confirm the information of its neighbors and reduce team vulnerability. In (Abunei *et al.*, 2019), redundant low-cost communication devices are used with the same goal. In both papers, heterogeneity and reconfiguration changes are not mentioned. Upon addressing networked robotic topologies, the authors of (PARK; HUTCHINSON, 2017) considered the rendezvous problem. Under appropriate connectivity conditions, the proposed Approximate Distributed Robust Convergence (ADRC) algorithm ensures the convergence of the agents to a region in the workspace, even if faulty robots are present, which can be outright malicious. Nevertheless, these approaches are not suitable for platoon reorganization, since misinformation from malicious (or faulty) agents remains part of the network. Concerning connectivity management, a switching strategy is applied by (SAULNIER *et al.*, 2017) to ensure that the network of agents stays above a critical resilience threshold. However, there is a limitation concerning access to the global properties of the graph.

Many works investigate more complex information flow topologies to improve performance, where the agent receives information from a set of neighbors, instead of only sensing the immediate preceding vehicle. Associated drawbacks are the possibilities of network disturbances, like Denial-of-Service (DoS) and communication delays, requiring robust control laws and resilient protocols. DoS mitigation strategies for platoons are presented as a hybrid controller in (Merco; Ferrante; Pisu, 2019), as a linear control law with estimators in (BIRON; DEY; PISU, 2017), and as a fuzzy controller in (NOEI *et al.*, 2016).

The paper (SEN; MATOLAK, 2008) provides information on experiments performed on V2V (Vehicle to Vehicle) communication that help in choosing communication delay values for the models used. On the other hand, effects of communication delay on platoons have been studied for second-order systems in (GHAEDSHARAF; SOMARAKIS; MOTEE, 2018), considering constant time-delay and exogenous noise, and in (Li *et al.*, 2019; Zhang; Orosz, 2016), considering heterogeneous time-varying delays and nonlinear spacing policies. Also, third-order systems subject to constant and time-varying delays have been studied in (LIU *et al.*, 2018; YANG *et al.*, 2019; Souza *et al.*, 2019; ELAHI; ALFI; MODARES, 2022), respectively. Heterogeneous platoons with switching topologies and time-varying communication delays have been faced in (CHEHARDOLI; HOMAEINEZHAD, 2017). In common, the aforementioned works consider platoons composed of a fixed number of vehicles and analyze resilience under predefined communication and interaction structures. As discussed in (ALEXIS, 2020), such formulations are closely related to robustness-oriented resilience, where the focus lies on maintaining stability under disturbances rather than on accommodating structural reconfigurations.

2.3 Limited communication ranges

Due to technological limitations involving electronic circuits and obstacles in real-world scenarios, both communication and sensing ranges are inherently limited. Another constraint is the limited communication ranges in mobile networks. Limited sensing capabilities are addressed in (GUO; YUE, 2012), considering sensors like sonars and radars, which have sensitive and non-sensitive zones, both defined by their detection capability. The proposed conditions ensure string stability whenever some agents travel within the detection ranges of others. Similarly, (MIDDLETON; BRASLAVSKY, 2010) investigates the effects of a limited range of forwarding and backward communication on string stability. However, these works focus on string stability under fixed communication assumptions and do not explicitly address scenarios involving changes in platoon composition. Disconnection has been recently addressed in the context of Vehicular Ad-hoc Network (VANETs) in (Huang; Tseng, 2018), where authors use temporary relay information to keep the system connected, while internal stability aspects are not explicitly addressed.

The authors of (ZHENG *et al.*, 2019) treat the heterogeneity of the platoon by considering different inertial time lags for ground vehicle power trains. Similarly, in our previous work (NETO; MOZELLI; SOUZA, 2019), we used the same parameter to model air-ground cooperative platoons. In this article, however, a more realistic scenario structure is studied, allowing heterogeneous vehicles with limited communication ranges.

The thesis (SAVINO, 2016) presents concepts from the consensus theory of multi-agent systems that we use as techniques for calculating the control law of each agent seen as a vehicle that is part of the platoon. In (GRAVINA, 2017) the consensus theory is applied to

homogeneous platoons of connected vehicles. Heterogeneity among platoon agents can be a possible source of instability, demanding robust control strategies as demonstrated in (Zhang; Orosz, 2016; CHEHARDOLI; HOMAEINEZHAD, 2017).

Regarding connectivity management, a switching strategy is applied in (SAULNIER *et al.*, 2017) ensuring that the resilience on the agents network stays above a critical threshold. However, it has the shortcoming of needing access to the global properties of the graph.

2.4 Graph theory

Graph theory provides a mathematical framework for modeling the communication topology used in information exchange among vehicles. By representing agents as nodes and communication links as directed edges, graph-based models are widely employed in platoon control, where the exchanged information typically includes position, velocity, and acceleration variables.

For information flow originating from predecessor vehicles, look-ahead communication networks are commonly modeled using directed graphs oriented from the leader to the last follower. In this context, directed acyclic graphs (Directed Acyclic Graphs (DAGs)) have been employed to represent both homogeneous and heterogeneous platoons in (Yan *et al.*, 2012; BIAN *et al.*, 2019; ZHENG *et al.*, 2019).

The impact of DAGs on the performance of consensus algorithms is analyzed in (Zhang; Chen; Mo, 2017), where different directed topologies are evaluated with respect to convergence properties.

Directed graphs have also been considered in (SANTINI *et al.*, 2019), in which the authors formally prove the stability of a control law under topology changes associated with vehicle insertion or disengagement. These results are obtained under the assumption that communication links among the involved vehicles are preserved.

Another challenge arises in mixed traffic scenarios, where autonomous and human-driven vehicles coexist. In (ZHOU *et al.*, 2019), a car-following strategy is investigated for strings composed of both vehicle types, in which autonomous agents receive distance, velocity, and acceleration information from the preceding vehicle. Stability is analyzed in the frequency domain by identifying predominant acceleration frequencies of human-driven vehicles through FFT-based analysis of experimental data.

2.5 Distributed Control and Stability of Vehicle Platoons

Distributed control of vehicle platoons has been widely investigated as a scalable alternative to centralized coordination architectures (BULLO; CORTÉS; MARTÍNEZ, 2009b; MESBAHI; EGERSTEDT, 2010). In this context, each vehicle computes its control action

using locally available information, typically obtained from onboard sensors and communication with neighboring vehicles. This paradigm reduces communication requirements, mitigates single points of failure, and naturally accommodates variations in platoon size, making it suitable for realistic traffic scenarios.

Early studies on longitudinal platoon control established fundamental stability concepts and performance limitations associated with inter-vehicle interactions. In particular, classical works introduced the notion of string stability to characterize how disturbances propagate along a vehicle chain and highlighted the importance of appropriate feedback structures to prevent amplification effects (SWAROOP; HEDRICK, 1996). These results provided a theoretical foundation for understanding platoon behavior under decentralized control laws and influenced subsequent developments in cooperative vehicular systems.

With the advent of vehicle-to-vehicle communication, consensus-based formulations emerged as a powerful framework for platoon coordination. By modeling the platoon as a networked multi-agent system, graph-theoretic tools have been employed to analyze convergence, stability, and robustness properties under different communication topologies (OLFATI-SABER; FAX; MURRAY, 2007; REN; BEARD, 2008). In this setting, predecessor–follower structures have received significant attention due to their simplicity and compatibility with local information exchange, while still allowing formal stability analysis.

More recent contributions extended these frameworks to address practical challenges such as communication delays, packet losses, and heterogeneous vehicle dynamics. Several studies demonstrated that stability and formation maintenance can be preserved under bounded delays and limited communication ranges, provided that suitable control gains and interaction structures are adopted (PLOEG *et al.*, 2014). These results reinforce the relevance of decentralized strategies for real-world platooning applications, where ideal communication assumptions are rarely satisfied.

Despite the extensive literature on distributed platoon control, different studies place emphasis on distinct aspects of stability and performance. While many works focus on global convergence properties and collective platoon metrics, other approaches investigate how specific communication topologies influence the local stabilization of individual vehicles. In this context, the present work complements existing studies by examining how, under a predecessor–follower configuration, stability and coordinated behavior arise from locally regulated dynamics without requiring explicit knowledge of the full platoon model.

2.6 Reorganization of platoons

Platoon reorganization arises as a consequence of interaction maneuvers among different vehicle groups, such as split and merge events or the entry and exit of vehicles from the formation. These maneuvers typically involve changes in inter-vehicle spacing, as well as

temporary disconnections and reconnections within the communication topology.

Regarding structural reorganization, high-level management protocols have been proposed to coordinate merge and split maneuvers. In (AMOOZADEH *et al.*, 2015), a supervisory protocol incorporating merge and split operations combined with lane changes is presented, with the objective of improving road utilization by managing platoon length. While simulation results support the feasibility of these maneuvers, low-level stability analysis and dynamic consequences of reorganization are outside the scope of that study.

Similarly, (PARANJOTHI; ATIQUZZAMAN; KHAN, 2020) describes a protocol for vehicle entry into platoons without addressing low-level control aspects. The impact of merge and lane-change maneuvers on different platoon positions is evaluated in (Maiti *et al.*, 2020), where it is shown that, under low traffic conditions, vehicles entering the middle of the platoon require longer stabilization times than those joining at the front or tail; however, stability analysis is not explicitly considered. A comprehensive review of merge and split control protocols is presented in (BADNAVA *et al.*, 2021).

Fusion maneuvers combining longitudinal and lateral control with high-level coordination strategies are addressed in (GOLI; ESKANDARIAN, 2020). Most of these works focus on homogeneous platoons and assume unlimited communication ranges. Extensions to heterogeneous platoons with variable time delays and limited communication ranges are considered in (WANG; WU; BARTH, 2017), although the analysis is restricted to early topologies involving a single follower.

A central objective in platoon reorganization is the preservation of string stability during transitional phases. While several studies address stability under idealized conditions, fewer works explicitly consider the combined effects of human-driven vehicles, mixed traffic, and communication failures in the controller design process (BADNAVA *et al.*, 2021).

Robust control approaches based on \mathcal{H}_∞ theory have also been employed to analyze and mitigate disturbance propagation in vehicle platoons. In (ZHENG *et al.*, 2018), the influence of communication topology on platoon stability is investigated using \mathcal{H}_∞ norms, leading to performance insights for large-scale formations. Mixed traffic scenarios are addressed in (ZHOU *et al.*, 2019), where string stability criteria and controller synthesis methods account for the dominant acceleration frequencies of human-driven vehicles. Distributed \mathcal{H}_∞ control strategies accommodating communication delays, packet losses, and topology uncertainties are further explored in (ELAHI; ALFI; MODARES, 2022).

3 THEORETICAL FORMALIZATION

This chapter presents the fundamental aspects related to the modeling of the problem addressed in this thesis. First, a model for the longitudinal dynamics of the vehicles is introduced. Then, a graph-theoretic framework is employed to describe the communication network among vehicles. The chapter concludes with the definition of the controlled variables for platoon formation. These variables, associated with spacing and cruising speed errors, converge to zero in steady state, ensuring BIBO (Bounded-Input Bounded-Output) stability of the formation error dynamics.

3.1 Longitudinal vehicle dynamics

The individual vehicle longitudinal dynamics model is obtained from (RAJAMANI, 2011; RAJAMANI; RAJAMANI, 2012), similarly to (Souza *et al.*, 2019), our platoon is composed of vehicles whose longitudinal dynamics is ruled based on the following assumptions: bodies are rigid and symmetrical; longitudinal sliding of tires is disregarded; wind effects are not considered; and the three dimensions of movement, pitch, yaw and roll moments do not affect the longitudinal navigation.

The main forces influencing the longitudinal motion of a land vehicle are considered in the modeling process. Each vehicle is assumed to be equipped with an engine capable of generating rotational energy, which is transmitted to the wheels. In addition, dissipative forces due to aerodynamic drag and friction are taken into account.

In such conditions, the dynamics of the i -th vehicle in the team is:

$$\begin{aligned} v_i(t) &= \dot{p}_i(t), \\ m_i a_i(t) &= \frac{\eta_i}{r_i} T_i(t) - \frac{1}{2} \rho C_i v_i^2(t) - m_i g \mu_i, \end{aligned} \quad (3.1)$$

where m_i is the mass, η_i is the motor efficiency, r_i is the tire radius, g is the gravity acceleration, μ_i is the friction constant, ρ is the air density, and C_i is the drag coefficient (proportional to the frontal area of the vehicle). And the variables related to the movement of vehicles are: $p_i(t)$ is the position, $v_i(t)$ is the velocity and $a_i(t)$ is the follower vehicle acceleration. The torque T_i of the driving/braking actuators is given by the first-order dynamics associated with the desired torque \tilde{T}_i ,

$$\zeta_i \dot{T}_i(t) = \tilde{T}_i(t) - T_i(t), \quad (3.2)$$

with ζ_i being the powertrain time constant. Although the control input u_i appears in the acceleration dynamics, it does not correspond to a direct jerk command, but rather to a filtered input acting on the longitudinal acceleration through the powertrain dynamics. Further,

manipulating (3.1) yields

$$\begin{aligned} T_i(t) &= \frac{r_i}{\eta_i} \left(m_i a_i(t) + m_i g \mu_i + \frac{1}{2} \rho_i C_i v_i^2(t) \right) \quad \text{and} \\ \dot{T}_i(t) &= \frac{r_i}{\eta_i} \left(m_i \dot{a}_i(t) + \rho_i C_i v_i(t) a_i(t) \right). \end{aligned}$$

Then the vehicle dynamics can be linearized by the following control law (see (Souza *et al.*, 2019) and references therein)

$$\tilde{T}_i(t) = \frac{r_i}{\eta_i} \left(\rho_i C_i v_i(t) (\zeta_i a_i(t) + \frac{1}{2} v_i(t)) + m_i g \mu_i + m_i u_i(t) \right),$$

where u_i is a new control input used to regulate the vehicle acceleration in order to maintain the desired inter-vehicle spacing. Substituting the latter equations into (3.2) yields $\zeta_i \dot{a}_i(t) = -a_i(t) + u_i(t)$, showing that the control input u_i governs the acceleration dynamics.¹ Therefore, by defining the state vector $\mathbf{x}_i(t) = [p_i(t) \ v_i(t) \ a_i(t)]^\top$, the i -th vehicle dynamics can be written in state-space form as the third-order linear time-invariant model (3.3).

$$\dot{\mathbf{x}}_i(t) = \mathbf{A}_i \mathbf{x}_i(t) + \mathbf{B}_i u_i(t), \quad \text{with} \quad (3.3)$$

$$\mathbf{A}_i = \begin{bmatrix} 0 & 1 & 0 \\ 0 & 0 & 1 \\ 0 & 0 & -\frac{1}{\zeta_i} \end{bmatrix}, \quad \mathbf{B}_i = \begin{bmatrix} 0 \\ 0 \\ \frac{1}{\zeta_i} \end{bmatrix}, \quad \mathbf{x}_i(t) = \begin{bmatrix} p_i(t) \\ v_i(t) \\ a_i(t) \end{bmatrix}.$$

This third-order model captures position, velocity, and acceleration dynamics, which are sufficient to describe longitudinal platoon behavior under the considered operating conditions.

3.2 Network communication model

The model described hereafter considers nominal operating conditions, under which the platoon is composed of a constant number of vehicles and a fixed communication network topology. Accordingly, DAGs are used to model the communication network of the heterogeneous platoon. Generally speaking, a Directed Acyclic Graph (DAG) is a finite directed graph with no directed cycles and admitting a topological ordering among its vertices. It is a convenient property on vehicular platoons because, if an agent only receives information from hierarchically superior (predecessor) neighbors, it is not influenced by failing successor agents, thereby improving the resilience of the formation, see, e.g., (BIAN *et al.*, 2019) and (ZHENG *et al.*,

¹ Although the control input u_i does not explicitly represent jerk, it effectively acts on the time derivative of the acceleration. As a result, the closed-loop behavior implicitly regulates jerk, which is known to be relevant for ride comfort and smooth longitudinal motion.

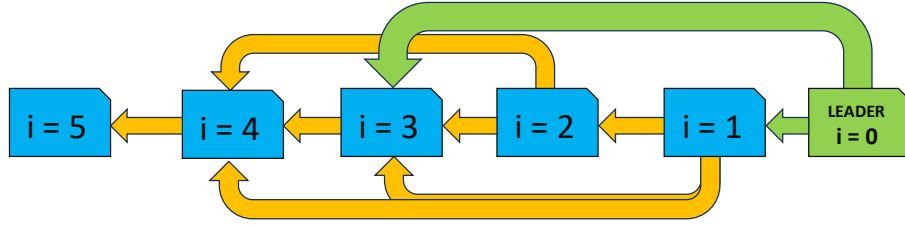


Figure 3.1 – Example: direct graph \rightarrow connections communication topology of the vehicles in a platoon formed by five follower vehicles ($i = 1, \dots, 5$) plus the leader ($i = 0$).

2019). In other words, DAGs can be used to model *predecessor-follower* topologies subject to limited communication range, as follows.

Formally, a DAG is defined by a graph $\mathcal{G} = \{\mathcal{V}, \mathcal{E}\}$, composed of $n + 1$ nodes $\mathcal{V} = \{v_0, v_1, v_2, \dots, v_n\}$, and a set of edges $\mathcal{E} \subseteq \mathcal{V} \times \mathcal{V}$. The edge set \mathcal{E} represents only the active communication links determined by the communication range constraints.

Here, we assume a topological ordering $v_0, v_1, v_2, \dots, v_n$, such that, for every directed edge $e_{ij} = (v_i, v_j) \in \mathcal{E}$, we have $i > j$. By definition, vertex v_0 constitutes the platoon leader.

The existence of each edge e_{ij} is conditioned by the longitudinal distance between v_i and v_j , whose positions are given by p_i and p_j . If this distance is smaller than the communication range R_i , whose reference point is given by the rear bumper of the vehicle i , to the rear bumper of the predecessor vehicle, we have a directed edge $(v_i, v_j) \in \mathcal{E}$.

The matrices $n \times n$ associated with the graph \mathcal{G} : Pinning, Adjacency, Degree, and Laplacian are used to describe a communication topology. The \mathcal{G} graph matrices (square of order n equal to the number of following vehicles) are presented in the following topics. After each instruction on how to obtain the matrices associated with \mathcal{G} , an example of assembling a numerical matrix is presented according to the connection topology of the vehicles of the platoon represented in the figure 3.1 composed of five followers vehicles and the leader.

Pinning Matrix P

The pinning matrix denotes the communication link between the leader and other follower vehicles. It is a diagonal matrix with entries that depend on the communication range of each follower vehicle. When the distance between the i -th vehicle and the leader is less than the sensor range of the i -th vehicle, the position (i, i) of the diagonal of the pinning matrix is

set to a value equal to 1, so that

$$P_i = \begin{cases} 1 & \text{if } (p_0 - p_i) \leq R_i \quad \forall i = 1, \dots, n, \\ 0 & \text{otherwise,} \end{cases}$$

where the index 0 represents the leader vehicle (p_0 is the position variable of this first vehicle in the platoon) and R_i represents the sensor range of each follower.

Example for Matrix Pinning:

The green arrow in figure 3.1 indicates that vehicles $i = 1$ and $i = 3$ receive information from the leader. Then the pinning matrix has the coordinates (1,1) and (3,3) set to 1 and its other positions are zero.

$$\mathbf{P} = \begin{bmatrix} 1 & 0 & 0 & 0 & 0 \\ 0 & 0 & 0 & 0 & 0 \\ 0 & 0 & 1 & 0 & 0 \\ 0 & 0 & 0 & 0 & 0 \\ 0 & 0 & 0 & 0 & 0 \end{bmatrix}.$$

Another format to present the pinning matrix using $\Omega^{i,j} \in \mathfrak{R}^{n \times n}$ that is a single-entry matrix, where the only non-null element is equal to 1 and it is located at i -th row and the j -th column:

$$\mathbf{P} = \sum_{i=1}^n \mathbf{P}_i = \sum_{i=1}^n \Omega^{i,i} P_i \in \mathfrak{R}^{n \times n}$$

Adjacency Matrix \mathbf{M}

The adjacency matrix \mathbf{M} indicates the sharing links among the follower vehicles, whose possible non-zero entries are

$$M_{ij} = \begin{cases} 1 & \text{if } (p_j - p_i) \leq R_i, \\ 0 & \text{otherwise,} \end{cases}$$

where, in the topological order, j -th vehicle precedes the i -th one, i.e. $i > j$.

Example for Matrix Adjacency:

In the communication topology of figure 3.1 the orange arrow indicates the communication link between vehicles in blue receiving information from predecessor vehicles also in blue that are within their communication ranges. The adjacency matrix is obtained by setting column j to 1 for each predecessor vehicle that sends information to i , i.e. to fill line 3, referring to vehicle $i = 3$, columns 1 and 2 are set to 1. Filling each line i of the adjacency matrix in

relation to the respective follower and doing this for all vehicles, a matrix is built lower triangle.

$$\mathbf{M} = \begin{bmatrix} 0 & 0 & 0 & 0 & 0 \\ 1 & 0 & 0 & 0 & 0 \\ 1 & 1 & 0 & 0 & 0 \\ 1 & 1 & 1 & 0 & 0 \\ 0 & 0 & 0 & 1 & 0 \end{bmatrix}.$$

Degree Matrix \mathbf{D}

The degree matrix \mathbf{D} is a diagonal with the elements

$$D_i = \sum_{j=1}^n M_{ij}.$$

Example for Matrix Degree:

The matrix degree is obtained as the result of the sum of each line of the adjacency matrix in the position corresponding to the i of the diagonal.

$$\mathbf{D} = \begin{bmatrix} 0 & 0 & 0 & 0 & 0 \\ 0 & 1 & 0 & 0 & 0 \\ 0 & 0 & 2 & 0 & 0 \\ 0 & 0 & 0 & 3 & 0 \\ 0 & 0 & 0 & 0 & 1 \end{bmatrix}.$$

Laplacian Matrix \mathbf{L}

The Laplacian matrix is

$$\mathbf{L} = \mathbf{D} - \mathbf{M}.$$

Example for Matrix Laplacian:

$$\mathbf{L} = \begin{bmatrix} 0 & 0 & 0 & 0 & 0 \\ -1 & 1 & 0 & 0 & 0 \\ -1 & -1 & 2 & 0 & 0 \\ -1 & -1 & -1 & 3 & 0 \\ 0 & 0 & 0 & -1 & 1 \end{bmatrix}.$$

This graph-based model is subsequently used to analyze the stabilization of the spacing error dynamics of the platoon vehicles described by the linear model (3.3). Since the communication topology is directed, the resulting Laplacian matrix is generally non-symmetric, and the stability analysis relies on the structure of the predecessor–follower interconnection rather than on spectral symmetry.

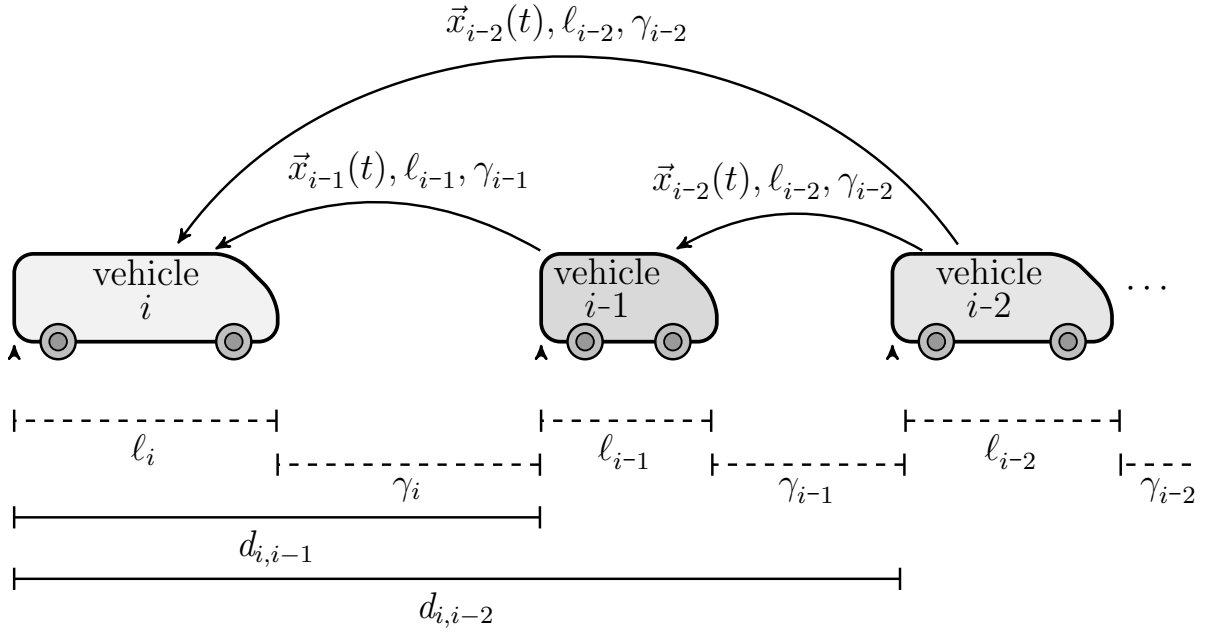


Figure 3.2 – Metric parameters in the platoon. The position p_i of the i -th vehicle is referenced on its rear bumper. The vehicle i must keep the fixed distance $d_{i,i-1} = \gamma_i + l_i$ from its first immediately preceding neighbor, the distance $d_{i,i-2} = \gamma_i + l_i + \gamma_{i-1} + l_{i-1}$ to its second immediately preceding neighbor ($i-2$), and so on.

3.3 Definitions for the steady state: Platoon formation

The platoon is considered to be in steady-state formation when each vehicle maintains the desired distance from its immediately preceding vehicle. Stability refers to the property that this condition is reached asymptotically over time. As a mathematical abstraction, the spacing error employed in the control formulation is defined as As a mathematical abstraction, the spacing error variable for optimization is defined as

$$e_i = p_{i-1}(t) - p_i(t) - l_i - \gamma_i, \quad i = 1, \dots, N \quad (3.4)$$

where N denotes the number of follower vehicles, and p_i and p_{i-1} represent the longitudinal positions of vehicle i and its immediate predecessor, respectively. As shown in the figure 3.2 the length of each vehicle is l_i and the desired distance γ_i is the spacing among the vehicle i and $i-1$.

The velocity error Ev_i is defined as the difference between the velocity of the i -th vehicle and the cruising velocity of the leader v_0 , i.e.,

$$Ev_i = v_i - v_0. \quad (3.5)$$

Stability of the platoon formation is achieved when both the spacing error and the cruising velocity error converge to zero, that is,

$$\lim_{t \rightarrow \infty} e_i(t) = 0, \quad \lim_{t \rightarrow \infty} Ev_i(t) = 0. \quad (3.6)$$

4 HETEROGENEOUS PLATOON VEHICLES WITH FIXED COMMUNICATION TOPOLOGY

This part of the thesis presents the main results on decentralized control of vehicle platoons, organized into three chapters. Chapter 4 introduces the low-level control hierarchy and presents formulations for decentralized control laws applied to platoons composed of vehicles with heterogeneous dynamics. In addition to the control formulation and stability analysis, this chapter provides the basis for discussing structural properties arising from the adopted predecessor–follower communication topology.

In the subsequent chapters, the contributions of this work are addressed at a higher level of the control hierarchy. Chapter 5 presents a protocol for platoon reconfiguration in response to vehicle entry and exit events. Chapter 6 introduces a recovery protocol that enables a vehicle to recompose the platoon after communication loss, which may occur when inter-vehicle distances exceed the sensing or communication range.

Within this context, Chapter 4 presents the decentralized control law developed for vehicle platoons under three communication scenarios: without communication delay, with fixed communication delay, and with heterogeneous fixed delays. The chapter is organized into three main parts. First, graph-theoretic tools are employed to construct the augmented system matrices resulting from the interconnection of individual vehicle models. Based on this formulation, the decentralized control law is expressed in an augmented matrix form.

In the second part, the dynamics of the augmented formation error are derived and analyzed. Finally, Theorem 4.1 establishes admissible gain limits for the decentralized control law applied to each vehicle in the platoon, considering a fixed communication topology defined by the sensing range of the vehicles and the absence of communication delays.

4.1 Decentralized Control Law

4.1.1 A: Platoon free of communication delay

In this work, each vehicle in the platoon is conducted by the local control law:

$$u_i(t) = -\mathbf{K}_i \mathbf{u}_i(t) = -\mathbf{K}_i \sum_{j \in \mathcal{N}_i} (\mathbf{x}_i(t) - \mathbf{x}_j(t) + \delta_{ij}), \quad (4.1)$$

where $\mathbf{K}_i = [\kappa_1^i \ \kappa_2^i \ \kappa_3^i]$ is the control gain vector, and in $\delta_{ij} = [d_{ij} \ 0 \ 0]^\top$, d_{ij} is the constant desirable rear bumper-to-rear bumper distance between the vehicle i and all $j \in \mathcal{N}_i$. The set \mathcal{N}_i is composed of all vehicles that share information with the vehicle i along the transient regime until the platoon achieves the desired formation. In other words, the constant spacing policy implies that fixed distances between vehicles must be ensured in steady state.

Since we are dealing with heterogeneous agents, this inter-vehicle space may be different for every pair (i, j) .

In order to assemble the platoon control model, initially, we apply the control law (4.1) in (3.3), which yields

$$\dot{\mathbf{x}}_i(t) = \mathbf{A}_i \mathbf{x}_i(t) - \mathbf{F}_i \mathbf{u}_i(t), \quad (4.2)$$

with $\mathbf{F}_i = \mathbf{B}_i \mathbf{K}_i$. Therefore the augmented longitudinal dynamics of the formation can be described as:

$$\dot{\mathbf{X}}(t) = \widehat{\mathbf{A}} \mathbf{X}(t) + \widehat{\mathbf{B}} \mathbf{U}(t), \quad \text{with} \quad (4.3)$$

$$\mathbf{X}(t) = \left[\mathbf{x}_1^T(t) \ \dots \ \mathbf{x}_n^T(t) \right]^T, \quad \text{and} \quad \mathbf{U}(t) = \left[\mathbf{u}_1^T(t) \ \dots \ \mathbf{u}_n^T(t) \right]^T \quad (4.4)$$

are the augmented state and control vectors of the n -vehicles platoon, respectively,

$$\begin{aligned} \widehat{\mathbf{A}} &= \sum_{i=1}^n (\boldsymbol{\Omega}_i \otimes \mathbf{A}_i) = \text{diag}\{\mathbf{A}_1, \mathbf{A}_2, \dots, \mathbf{A}_n\} \quad \text{and} \\ \widehat{\mathbf{B}} &= \sum_{i=1}^n (\boldsymbol{\Omega}_i \otimes \mathbf{F}_i) = \text{diag}\{\mathbf{F}_1, \mathbf{F}_2, \dots, \mathbf{F}_n\}, \end{aligned}$$

where $\boldsymbol{\Omega}_i$ is a single-entry $n \times n$ matrix which the non-zero entry is equal 1 in the i -th diagonal position.

Now, considering that $\delta_{ij} = \delta_{0i} - \delta_{0j}$, the control law (4.1) can be rewritten as the augmented vector:

$$\begin{aligned} \mathbf{U}(t) &= - \left[(\mathbf{P} + \mathbf{D}) \otimes \mathbf{I}_3 \right] \mathbf{X}(t) + (\mathbf{M} \otimes \mathbf{I}_3) \mathbf{X}(t) \\ &\quad + (\mathbf{P} \otimes \mathbf{I}_3) \mathbf{X}_0(t) - \left[(\mathbf{P} + \mathbf{D} - \mathbf{M}) \otimes \mathbf{I}_3 \right] \boldsymbol{\Delta}_0, \end{aligned} \quad (4.5)$$

where the desired formation distances between all followers and the leader are concatenated in $\boldsymbol{\Delta}_0$ and the augmented vector of n copies of the leader states are defined as, respectively:

$$\boldsymbol{\Delta}_0 = \begin{bmatrix} \delta_{01} \\ \delta_{02} \\ \vdots \\ \delta_{0n} \end{bmatrix}, \quad \text{and} \quad \mathbf{X}_0(t) = \begin{bmatrix} \mathbf{x}_0(t) \\ \mathbf{x}_0(t) \\ \vdots \\ \mathbf{x}_0(t) \end{bmatrix}.$$

4.1.2 B: Communication with fixed constant delay

To stabilize the platoon, we have used a distributed control law based on a constant spacing policy between the vehicles. This law was extended from our previous work (NETO; MOZELLI; SOUZA, 2019), where we have addressed heterogeneity just for two types of vehicles (aerial and ground robots). Basically, when agent i receives information from one or more teammates, it is governed by:

$$\begin{aligned} u_i(t) &= -\mathbf{K}_i \mathbf{u}_i(t) \\ &= -\mathbf{K}_i \sum_{j \in \mathcal{N}_i} \left(\mathbf{x}_i(t) - \mathbf{x}_j(t - \tau) + \delta_{ij} - \tau \mathbf{W} \mathbf{x}_i(t) \right), \end{aligned} \quad (4.6)$$

where $\mathbf{K}_i = [\kappa_1^i \ \kappa_2^i \ \kappa_3^i]$ represents the control gain vector, $\mathbf{W} = [1 \ 0 \ 0]^\top [0 \ 1 \ 0]$, τ is the communication delay, and $\delta_{ij} = [d_{ij} \ 0 \ 0]^\top$, with d_{ij} being the constant desirable rear bumper-to-rear bumper distance between the vehicle i and all $j \in \mathcal{N}_i$. The set $j \in \mathcal{N}_i$ is composed of all vehicles that share information with the vehicle i along the transient regime until the platoon achieves the desired formation. This means that fixed distances among vehicles must be ensured in steady-state, independent of their velocities. However, since we are dealing with heterogeneous agents, this inter-vehicle distance may be different for every pair (i, j) . Similar to what was discussed in (Souza *et al.*, 2019) for homogeneous vehicles, to work around the problem of communication delay, the portion $\tau \mathbf{W} \mathbf{x}_i(t)$ is added to the control law to compensate for the error of spacing in permanent regime, as demonstrated below

$$\tau \mathbf{W} \mathbf{x}_i(t) = \tau \begin{bmatrix} 1 \\ 0 \\ 0 \end{bmatrix} \begin{bmatrix} 0 & 1 & 0 \end{bmatrix} \begin{bmatrix} p_i(t) \\ v_i(t) \\ a_i(t) \end{bmatrix} = \tau \begin{bmatrix} 0 & 1 & 0 \\ 0 & 0 & 0 \\ 0 & 0 & 0 \end{bmatrix} \begin{bmatrix} p_i(t) \\ v_i(t) \\ a_i(t) \end{bmatrix} = \tau \begin{bmatrix} v_i(t) \\ 0 \\ 0 \end{bmatrix} = \begin{bmatrix} \tau v_i(t) \\ 0 \\ 0 \end{bmatrix}$$

then considering the control law for the i -th vehicle following only one connected vehicle in its communication range, we have

$$u_i(t) = - \begin{bmatrix} \kappa_1^i & \kappa_2^i & \kappa_3^i \end{bmatrix} \left(\begin{bmatrix} p_i(t) \\ v_i(t) \\ a_i(t) \end{bmatrix} - \begin{bmatrix} p_j(t - \tau) \\ v_j(t - \tau) \\ a_j(t - \tau) \end{bmatrix} + \begin{bmatrix} d_{ij} \\ 0 \\ 0 \end{bmatrix} - \begin{bmatrix} \tau v_i(t) \\ 0 \\ 0 \end{bmatrix} \right) \quad (4.7)$$

$$= - \begin{bmatrix} \kappa_1^i & \kappa_2^i & \kappa_3^i \end{bmatrix} \begin{bmatrix} p_i(t) - p_j(t - \tau) + d_{ij} - \tau v_i(t) \\ v_i(t) - v_j(t - \tau) \\ a_i(t) - a_j(t - \tau) \end{bmatrix} \quad (4.8)$$

$$= - \left(\kappa_1^i (p_i(t) - p_j(t - \tau) + d_{ij} - \tau v_i(t)) + \kappa_2^i (v_i(t) - v_j(t - \tau)) \right) \quad (4.9)$$

$$+ \kappa_3^i (a_i(t) - a_j(t - \tau)) \quad (4.10)$$

To assemble the platoon control model, initially we apply the control law (4.6) in (3.3), that yields:

$$\dot{\mathbf{x}}_i(t) = \mathbf{A}_i \mathbf{x}_i(t) - \mathbf{F}_i \mathbf{u}_i(t), \quad (4.11)$$

with $\mathbf{F}_i = \mathbf{B}_i \mathbf{K}_i$. As \mathbf{F}_i is independent for each agent, the results present in (NETO; MOZELLI; SOUZA, 2019) are extended in this thesis to a more general case of heterogeneous platoon. Therefore, the augmented longitudinal dynamics of the formation can then be described in the compact form:

$$\dot{\mathbf{X}}(t) = \widehat{\mathbf{A}} \mathbf{X}(t) + \widehat{\mathbf{B}} \mathbf{U}(t) \quad (4.12)$$

with $\mathbf{X}(t)$ representing the vector augmented state, and $\mathbf{U}(t)$ the control vectors of the n team

members

$$\mathbf{X}(t) = \begin{bmatrix} \mathbf{x}_1(t) \\ \mathbf{x}_2(t) \\ \vdots \\ \mathbf{x}_n(t) \end{bmatrix} \quad \text{and} \quad \mathbf{U}(t) = \begin{bmatrix} \mathbf{u}_1(t) \\ \mathbf{u}_2(t) \\ \vdots \\ \mathbf{u}_n(t) \end{bmatrix},$$

and matrices of constant parameters are formed like this

$$\hat{\mathbf{A}} = \sum_{i=1}^n (\mathbf{\Omega}_i \otimes \mathbf{A}_i) = \begin{bmatrix} \mathbf{A}_1 & 0 & \cdots & 0 & \cdots & 0 \\ 0 & \mathbf{A}_2 & \cdots & 0 & \cdots & 0 \\ \vdots & \vdots & \ddots & \vdots & & \vdots \\ 0 & 0 & \cdots & \mathbf{A}_i & \cdots & 0 \\ \vdots & \vdots & & \vdots & \ddots & \vdots \\ 0 & 0 & \cdots & 0 & \cdots & \mathbf{A}_n \end{bmatrix}, \quad \text{and}$$

$$\hat{\mathbf{B}} = \sum_{i=1}^n (\mathbf{\Omega}_i \otimes \mathbf{F}_i) = \begin{bmatrix} \mathbf{F}_1 & 0 & \cdots & 0 & \cdots & 0 \\ 0 & \mathbf{F}_2 & \cdots & 0 & \cdots & 0 \\ \vdots & \vdots & \ddots & \vdots & & \vdots \\ 0 & 0 & \cdots & \mathbf{F}_i & \cdots & 0 \\ \vdots & \vdots & & \vdots & \ddots & \vdots \\ 0 & 0 & \cdots & 0 & \cdots & \mathbf{F}_n \end{bmatrix},$$

where $\mathbf{\Omega}_i$ is a single-entry $n \times n$ matrix with all elements null, except for the diagonal element $\Omega_i = 1$. As demonstrated below

$$\mathbf{\Omega}_1 = \begin{bmatrix} 1 & 0 & \cdots & 0 & \cdots & 0 \\ 0 & 0 & \cdots & 0 & \cdots & 0 \\ \vdots & \vdots & \ddots & \vdots & & \vdots \\ 0 & 0 & \cdots & 0 & \cdots & 0 \\ \vdots & \vdots & & \vdots & \ddots & \vdots \\ 0 & 0 & \cdots & 0 & \cdots & 0 \end{bmatrix}, \quad \mathbf{\Omega}_2 = \begin{bmatrix} 0 & 0 & \cdots & 0 & \cdots & 0 \\ 0 & 1 & \cdots & 0 & \cdots & 0 \\ \vdots & \vdots & \ddots & \vdots & & \vdots \\ 0 & 0 & \cdots & 0 & \cdots & 0 \\ \vdots & \vdots & & \vdots & \ddots & \vdots \\ 0 & 0 & \cdots & 0 & \cdots & 0 \end{bmatrix},$$

$$\mathbf{\Omega}_i = \begin{bmatrix} 0 & 0 & \cdots & 0 & \cdots & 0 \\ 0 & 0 & \cdots & 0 & \cdots & 0 \\ \vdots & \vdots & \ddots & \vdots & & \vdots \\ 0 & 0 & \cdots & 1 & \cdots & 0 \\ \vdots & \vdots & & \vdots & \ddots & \vdots \\ 0 & 0 & \cdots & 0 & \cdots & 0 \end{bmatrix}, \quad \mathbf{\Omega}_n = \begin{bmatrix} 0 & 0 & \cdots & 0 & \cdots & 0 \\ 0 & 0 & \cdots & 0 & \cdots & 0 \\ \vdots & \vdots & \ddots & \vdots & & \vdots \\ 0 & 0 & \cdots & 0 & \cdots & 0 \\ \vdots & \vdots & & \vdots & \ddots & \vdots \\ 0 & 0 & \cdots & 0 & \cdots & 1 \end{bmatrix}.$$

The control law (4.6) can be rewritten as the augmented vector, whereas $\delta_{ij} = \delta_{0i} - \delta_{0j}$, results in

$$\begin{aligned} \mathbf{U}(t) = & - [(\mathbf{P} + \mathbf{D}) \otimes \mathbf{I}_3] \mathbf{X}(t) + (\mathbf{M} \otimes \mathbf{I}_3) \mathbf{X}(t-\tau) + (\mathbf{P} \otimes \mathbf{I}_3) \mathbf{X}_0(t-\tau) \\ & - [(\mathbf{P} + \mathbf{D} - \mathbf{M}) \otimes \mathbf{I}_3] \Delta_0 + [(\mathbf{D} + \mathbf{P}) \otimes \tau \mathbf{W}] \mathbf{X}(t), \end{aligned} \quad (4.13)$$

in that the desired formation distances between all followers vehicle and the leader are concatenated in Δ_0 and the augmented vector of n copies of the leader vehicle states $\mathbf{X}_0(t)$, are defined as:

$$\Delta_0 = \begin{bmatrix} \delta_{01} \\ \delta_{02} \\ \vdots \\ \delta_{0n} \end{bmatrix}, \text{ and } \mathbf{X}_0(t) = \begin{bmatrix} \mathbf{x}_0(t) \\ \mathbf{x}_0(t) \\ \vdots \\ \mathbf{x}_0(t) \end{bmatrix}.$$

4.1.3 C: Communication with heterogeneous constant delay

All vehicles in the platoon have a fixed delay in receiving information from neighboring vehicles. As it is a communication network with heterogeneous delay, each vehicle receives information with different delay times.

To stabilize the platoon, we have used a distributed control law based on a constant spacing policy between the vehicles. Basically, when agent i receives information from one or more teammates, it is governed by:

$$\begin{aligned} u_i(t) = & -\mathbf{K}_i \mathbf{u}_i(t), \\ = & -\mathbf{K}_i \sum_{j \in \mathcal{N}_i} \left(\mathbf{x}_i(t) - \mathbf{x}_j(t-\tau_{ij}) + \delta_{ij} - \tau_{ij} \mathbf{W} \mathbf{x}_i(t) \right), \end{aligned} \quad (4.14)$$

where $\mathbf{K}_i = [\kappa_1^i \ \kappa_2^i \ \kappa_3^i]$ represents the control gain vector, $\mathbf{W} = [1 \ 0 \ 0]^\top [0 \ 1 \ 0]$, τ_{ij} is the heterogeneous constant delay in the communication link from vehicle j to vehicle i , and $\delta_{ij} = [d_{ij} \ 0 \ 0]^\top$, with d_{ij} being the constant desirable front bumper-to-rear bumper distance between the vehicle i and all $j \in \mathcal{N}_i$. The set \mathcal{N}_i is defined as

$$\mathcal{N}_i = \begin{cases} \mathcal{C}_i, & \text{if } i \text{ does not detect any obstacle in its trajectory;} \\ \emptyset, & \text{otherwise;} \end{cases}$$

where the set \mathcal{C}_i is composed of all vehicles that share information with the vehicle i along the transient regime. In the case when $\mathcal{N}_i = \emptyset$ the control law (4.14) is computed taking into account virtual reference states, see Thm. 6.1.

The proposed control law implies that fixed distances between vehicles must be ensured in a steady-state condition, independent of their speeds. However, since we are dealing with heterogeneous agents, this inter-vehicle distance may be different for every pair (i, j) . The $\tau_{ij} \mathbf{W} \mathbf{x}_i(t)$ term was added to the control law (4.1) to compensate the permanent regime spacing error caused by the delays, as addressed in (Souza *et al.*, 2019) for homogeneous

vehicles. To assemble the platoon control model, we initially apply the control law (4.14) in (3.3), which yields:

$$\dot{\mathbf{x}}_i(t) = \mathbf{A}_i \mathbf{x}_i(t) - \mathbf{F}_i \mathbf{u}_i(t), \quad (4.15)$$

with $\mathbf{F}_i = \mathbf{B}_i \mathbf{K}_i$. As \mathbf{F}_i is independent for each agent, the results present in (NETO; MOZELLI; SOUZA, 2019) are extended in this thesis to a more general case of heterogeneous platoon. Therefore, the augmented longitudinal dynamics of the formation can then be described in the compact form:

$$\dot{\mathbf{X}}(t) = \widehat{\mathbf{A}} \mathbf{X}(t) + \widehat{\mathbf{B}} \mathbf{U}(t) \quad (4.16)$$

with $\mathbf{X}(t)$ representing the vector augmented state, and $\mathbf{U}(t)$ the control vectors of the n team members

$$\mathbf{X}(t) = \begin{bmatrix} \mathbf{x}_1(t) \\ \mathbf{x}_2(t) \\ \vdots \\ \mathbf{x}_n(t) \end{bmatrix} \quad \text{and} \quad \mathbf{U}(t) = \begin{bmatrix} \mathbf{u}_1(t) \\ \mathbf{u}_2(t) \\ \vdots \\ \mathbf{u}_n(t) \end{bmatrix},$$

and matrices of constant parameters are:

$$\widehat{\mathbf{A}} = \sum_{i=1}^n \left(\boldsymbol{\Omega}^{i,i} \otimes \mathbf{A}_i \right) = \begin{bmatrix} \mathbf{A}_1 & 0 & \cdots & 0 \\ 0 & \mathbf{A}_2 & \cdots & 0 \\ \vdots & \vdots & \ddots & 0 \\ 0 & 0 & 0 & \mathbf{A}_n \end{bmatrix},$$

$$\widehat{\mathbf{B}} = \sum_{i=1}^n \left(\boldsymbol{\Omega}^{i,i} \otimes \mathbf{F}_i \right) = \begin{bmatrix} \mathbf{F}_1 & 0 & \cdots & 0 \\ 0 & \mathbf{F}_2 & \cdots & 0 \\ \vdots & \vdots & \ddots & 0 \\ 0 & 0 & 0 & \mathbf{F}_n \end{bmatrix}.$$

Further, the control law (4.14) can be vectorized, provided that

$$\delta_{ij} = \delta_{i0} - \sum_{j=i-1}^1 (\delta_{j,j-1} + \ell_j),$$

where ℓ_j is the j th vehicle length, resulting in

$$\begin{aligned} \mathbf{U}(t) = & - [(\mathbf{P} + \mathbf{D}) \otimes \mathbf{I}_3] \mathbf{X}(t) + \sum_{i=1}^n (\mathbf{P}_i \otimes \mathbf{I}_3) \mathbf{X}_0(t - \tau_{i0}) \\ & + \sum_{i=1}^n \sum_{j=1}^n (\mathbf{M}_{i,j} \otimes \mathbf{I}_3) \mathbf{X}(t - \tau_{ij}) - [(\mathbf{P} + \mathbf{L}) \otimes \mathbf{I}_3] \boldsymbol{\Delta}_0 \\ & + \sum_{i=1}^n \left[(\tau_{i0} \mathbf{P}_i + \boldsymbol{\Omega}^{i,i} \sum_{j=1}^n \tau_{ij} \mathbf{M}_{i,j}) \otimes \mathbf{W} \right] \mathbf{X}(t), \end{aligned} \quad (4.17)$$

where $\Delta_0^\top = \left[\delta_{10}^\top \ \delta_{20}^\top \ \cdots \ \delta_{n0}^\top \right]$ concatenates the desired formation distances between all follower vehicles and the leader, while vector $\mathbf{X}_0^\top(t) = \left[\mathbf{x}_0^\top(t) \ \mathbf{x}_0^\top(t) \ \cdots \ \mathbf{x}_0^\top(t) \right]$ contains n copies of the leader vehicle states.

4.2 Formation error dynamics

This section presents the formation error dynamics associated with the decentralized control law introduced in the previous section. In line with the problem formulation described in the Introduction, the formation error is expressed using an augmented state-space model that captures the collective behavior of the platoon while preserving the decentralized structure of the control law. The objective is to formulate compact augmented representations of the formation error dynamics under different communication conditions, which will be used in the subsequent stability analysis. The presentation is organized progressively, starting with the case of communication without delay and subsequently addressing fixed and heterogeneous communication delays.

4.2.1 A: Platoon free of communication delay

Next, we present a compact representation for the formation error, which can be written as:

$$\tilde{\mathbf{X}}(t) = \mathbf{X}(t) - \mathbf{X}^*(t), \quad (4.18)$$

where $\mathbf{X}^*(t) = \mathbf{X}_0(t) - \Delta_0$ is the reference value dependent on the difference between the leader state and the set-point distances. Since we are restricted to look-ahead communication topologies, the leader vehicle dynamics is not ruled by the control law in (4.1), thus we have:

$$\dot{\tilde{\mathbf{X}}}(t) = \dot{\mathbf{X}}(t) - \dot{\mathbf{X}}^*(t) = \dot{\mathbf{X}}(t) - \hat{\mathbf{A}}_0 \mathbf{X}^*(t), \quad (4.19)$$

where $\hat{\mathbf{A}}_0$ is an augmented matrix with copies of the leader dynamics, expressed by $\hat{\mathbf{A}}_0 = \mathbf{I}_n \otimes \mathbf{A}_0$, in which n is the number of followers. Replacing (4.3) in (4.19),

$$\begin{aligned} \dot{\tilde{\mathbf{X}}}(t) &= \hat{\mathbf{A}}\mathbf{X}(t) + \hat{\mathbf{B}}\mathbf{U}(t) - \hat{\mathbf{A}}_0\mathbf{X}^*(t) \\ &= \hat{\mathbf{A}} \left[\tilde{\mathbf{X}}(t) + \mathbf{X}^*(t) \right] + \hat{\mathbf{B}}\mathbf{U}(t) - \hat{\mathbf{A}}_0\mathbf{X}^*(t) \\ &= \hat{\mathbf{A}}\tilde{\mathbf{X}}(t) + \hat{\mathbf{B}}\mathbf{U}(t) + \left[\hat{\mathbf{A}} - \hat{\mathbf{A}}_0 \right] \mathbf{X}^*(t). \end{aligned} \quad (4.20)$$

Because $\mathbf{L} = \mathbf{D} - \mathbf{M}$, the control law (4.5) is rewritten as:

$$\mathbf{U}(t) = - \left[(\mathbf{P} + \mathbf{D}) \otimes \mathbf{I}_3 \right] \mathbf{X}(t) + (\mathbf{M} \otimes \mathbf{I}_3) \mathbf{X}(t) + (\mathbf{P} \otimes \mathbf{I}_3) [\mathbf{X}_0(t) - \Delta_0] - (\mathbf{L} \otimes \mathbf{I}_3) \Delta_0 \quad (4.21)$$

and adding it with the null term $(\mathbf{L} \otimes \mathbf{I}_3)\mathbf{X}_0(t)$, keeping in mind that the sum of the line elements of the Laplacian matrix is null, we have:

$$\begin{aligned}
\mathbf{U}(t) &= - [(\mathbf{P} + \mathbf{D}) \otimes \mathbf{I}_3]\mathbf{X}(t) + (\mathbf{M} \otimes \mathbf{I}_3)\mathbf{X}(t) + (\mathbf{P} \otimes \mathbf{I}_3)[\mathbf{X}_0(t) - \Delta_0] + \\
&\quad + (\mathbf{L} \otimes \mathbf{I}_3)[\mathbf{X}_0(t) - \Delta_0] \\
&= - (\mathbf{D} \otimes \mathbf{I}_3)\mathbf{X}(t) - (\mathbf{P} \otimes \mathbf{I}_3)\mathbf{X}(t) + (\mathbf{D} \otimes \mathbf{I}_3)\mathbf{X}(t) - (\mathbf{L} \otimes \mathbf{I}_3)\mathbf{X}(t) + \\
&\quad + [(\mathbf{P} + \mathbf{L}) \otimes \mathbf{I}_3]\mathbf{X}^*(t) \\
&= - [(\mathbf{P} + \mathbf{L}) \otimes \mathbf{I}_3][\mathbf{X}(t) - \mathbf{X}^*(t)]. \tag{4.22}
\end{aligned}$$

Then, the formation error dynamics in closed-loop is obtained applying (4.22) in (4.20), resulting

$$\begin{aligned}
\dot{\tilde{\mathbf{X}}}(t) &= \tilde{\mathbf{A}}\tilde{\mathbf{X}}(t) + \tilde{\mathbf{A}}^*\mathbf{X}^*(t) \tag{4.23} \\
\dot{\tilde{\mathbf{X}}}(t) &= \left\{ \hat{\mathbf{A}} - \hat{\mathbf{B}}[(\mathbf{P} + \mathbf{L}) \otimes \mathbf{I}_3] \right\} \tilde{\mathbf{X}}(t) + \left[\hat{\mathbf{A}} - \hat{\mathbf{A}}_0 \right] \mathbf{X}^*(t).
\end{aligned}$$

4.2.2 B: Communication with fixed constant delay

To obtain the dynamics of the formation error, we initially started from the compact representation for the formation error:

$$\tilde{\mathbf{X}}(t) = \mathbf{X}(t) - \mathbf{X}^*(t), \tag{4.24}$$

where $\mathbf{X}^*(t) = \mathbf{X}_0(t) - \Delta_0$ is the reference value dependent on the difference between the leader states and the set-point distance. As the communication topologies, in this thesis, are look-ahead, the dynamics of the leader are independent of other vehicles, and are not governed by the control law (4.6). Thus, the formation error dynamics can be represented by:

$$\dot{\tilde{\mathbf{X}}}(t) = \dot{\mathbf{X}}(t) - \dot{\mathbf{X}}^*(t) = \dot{\mathbf{X}}(t) - \hat{\mathbf{A}}_0\mathbf{X}^*(t), \tag{4.25}$$

where $\hat{\mathbf{A}}_0$ is a augmented matrix of the leader \mathbf{A}_0 matrix expressed by $\hat{\mathbf{A}}_0 = \mathbf{I}_n \otimes \mathbf{A}_0$, in which n is the number of vehicles following. Replacing (4.12) in (4.25),

$$\dot{\tilde{\mathbf{X}}}(t) = \hat{\mathbf{A}}\tilde{\mathbf{X}}(t) + \hat{\mathbf{B}}\mathbf{U}(t) - \hat{\mathbf{A}}_0\mathbf{X}^*(t). \tag{4.26}$$

Based on the fact that $\mathbf{L} = \mathbf{D} - \mathbf{M}$, and that the sum of the line elements of the Laplacian matrix is null, we add the null term $(\mathbf{L} \otimes \mathbf{I}_3)\mathbf{X}_0(t)$ to the control law (4.13) which is rewritten as:

$$\begin{aligned}
\mathbf{U}(t) &= - [(\mathbf{P} + \mathbf{D}) \otimes \mathbf{I}_3]\mathbf{X}(t) + (\mathbf{M} \otimes \mathbf{I}_3)\mathbf{X}(t - \tau) + (\mathbf{P} \otimes \mathbf{I}_3)[\mathbf{X}_0(t - \tau) - \Delta_0] \\
&\quad - (\mathbf{L} \otimes \mathbf{I}_3)[\Delta_0 - \mathbf{X}_0(t)] + [(\mathbf{P} + \mathbf{D}) \otimes \tau\mathbf{W}]\mathbf{X}(t). \tag{4.27}
\end{aligned}$$

Considering the definition of the formation error in (4.24) and its delayed variant, the following replacements can be performed:

$$\begin{aligned}
\mathbf{X}(t) &= \tilde{\mathbf{X}}(t) + \mathbf{X}^*(t), \text{ and} \\
\mathbf{X}(t - \tau) &= \tilde{\mathbf{X}}(t - \tau) + \mathbf{X}^*(t - \tau), \\
\mathbf{X}_0(t - \tau) - \Delta_0 &= \mathbf{X}^*(t - \tau), \text{ and} \\
\Delta_0 - \mathbf{X}_0(t) &= -\mathbf{X}^*(t).
\end{aligned}$$

Then, the control law in the augmented form results in

$$\begin{aligned} \mathbf{U}(t) &= - [(\mathbf{P}+\mathbf{D}) \otimes \mathbf{I}_3 - (\mathbf{P}+\mathbf{D}) \otimes \tau\mathbf{W}] [\tilde{\mathbf{X}}(t) + \mathbf{X}^*(t)] + (\mathbf{L} \otimes \mathbf{I}_3)\mathbf{X}^*(t) \\ &\quad + (\mathbf{M} \otimes \mathbf{I}_3) [\tilde{\mathbf{X}}(t-\tau) + \mathbf{X}^*(t-\tau)] + (\mathbf{P} \otimes \mathbf{I}_3) \mathbf{X}^*(t-\tau) \\ &= - [(\mathbf{P}+\mathbf{D}) \otimes (\mathbf{I}_3 - \tau\mathbf{W})] \tilde{\mathbf{X}}(t) + (\mathbf{M} \otimes \mathbf{I}_3) \tilde{\mathbf{X}}(t-\tau) \\ &\quad + [\mathbf{L} \otimes \mathbf{I}_3 - (\mathbf{P}+\mathbf{D}) \otimes (\mathbf{I}_3 - \tau\mathbf{W})] \mathbf{X}^*(t) + [(\mathbf{P} + \mathbf{M}) \otimes \mathbf{I}_3] \mathbf{X}^*(t-\tau). \end{aligned} \quad (4.28)$$

Replacing the formation error $\mathbf{X}(t) = \tilde{\mathbf{X}}(t) + \mathbf{X}^*(t)$ in (4.26), the dynamics of the formation error is rewritten as:

$$\dot{\tilde{\mathbf{X}}}(t) = \hat{\mathbf{A}}[\tilde{\mathbf{X}}(t) + \mathbf{X}^*(t)] + \hat{\mathbf{B}}\mathbf{U}(t) - \hat{\mathbf{A}}_0\mathbf{X}^*(t). \quad (4.29)$$

Therefore, the formation error dynamics in closed-loop is obtained applying the control law (4.28) in (4.29),

$$\begin{aligned} \dot{\tilde{\mathbf{X}}}(t) &= \{\hat{\mathbf{A}} - \hat{\mathbf{B}}[(\mathbf{P}+\mathbf{D}) \otimes (\mathbf{I}_3 - \tau\mathbf{W})]\} \tilde{\mathbf{X}}(t) + \hat{\mathbf{B}}(\mathbf{M} \otimes \mathbf{I}_3) \tilde{\mathbf{X}}(t-\tau) \\ &\quad + \{\hat{\mathbf{A}} - \hat{\mathbf{A}}_0 + \hat{\mathbf{B}}[\mathbf{L} \otimes \mathbf{I}_3 - (\mathbf{P}+\mathbf{D}) \otimes (\mathbf{I}_3 - \tau\mathbf{W})]\} \mathbf{X}^*(t) + \hat{\mathbf{B}}[(\mathbf{P} + \mathbf{M}) \otimes \mathbf{I}_3] \mathbf{X}^*(t-\tau). \end{aligned}$$

Grouping the matrices contained in each term the formation error dynamics is presented as

$$\dot{\tilde{\mathbf{X}}}(t) = \tilde{\mathbf{A}}\tilde{\mathbf{X}}(t) + \tilde{\mathbf{A}}_\tau\tilde{\mathbf{X}}(t-\tau) + \mathbf{A}^*\mathbf{X}^*(t) + \mathbf{A}_\tau^*\mathbf{X}^*(t-\tau). \quad (4.30)$$

4.2.3 C: Communication with heterogeneous constant delay

To obtain the dynamics of the formation error, we initially started from the compact representation for the formation error:

$$\tilde{\mathbf{X}}(t) = \mathbf{X}(t) - \mathbf{X}^*(t), \quad (4.31)$$

where $\mathbf{X}^*(t) = \mathbf{X}_0(t) - \Delta_0$ is the reference value dependent on the difference between the leader states and the set-point distance. Since in this thesis we have look-ahead communication topologies, the dynamic of the leader is not governed by the control law (4.14). Thus, the formation error dynamics can be represented by:

$$\dot{\tilde{\mathbf{X}}}(t) = \dot{\mathbf{X}}(t) - \dot{\mathbf{X}}^*(t) = \dot{\mathbf{X}}(t) - \hat{\mathbf{A}}_0\mathbf{X}^*(t), \quad (4.32)$$

where $\hat{\mathbf{A}}_0$ is a augmented matrix of the leader \mathbf{A}_0 matrix expressed by $\hat{\mathbf{A}}_0 = \mathbf{I}_n \otimes \mathbf{A}_0$. Replacing (4.16) in (4.32),

$$\dot{\tilde{\mathbf{X}}}(t) = \hat{\mathbf{A}}\mathbf{X}(t) + \hat{\mathbf{B}}\mathbf{U}(t) - \hat{\mathbf{A}}_0\mathbf{X}^*(t). \quad (4.33)$$

Based on the fact that $\mathbf{L} = \mathbf{D} - \mathbf{M}$, $\mathbf{P} = \sum_{i=1}^n \mathbf{P}_i$, and the sum of the line elements of the \mathbf{L} is null, we add the null term $(\mathbf{L} \otimes \mathbf{I}_3)\mathbf{X}_0(t)$ to the control law (4.17) which is rewritten

as:

$$\begin{aligned}
\mathbf{U}(t) = & - [(\mathbf{P} + \mathbf{D}) \otimes \mathbf{I}_3] \mathbf{X}(t) - (\mathbf{L} \otimes \mathbf{I}_3) (\Delta_0 - \mathbf{X}_0(t)) \\
& + \sum_{i=1}^n (\mathbf{P}_i \otimes \mathbf{I}_3) (\mathbf{X}_0(t - \tau_{i0}) - \Delta_0) \\
& + \sum_{i=1}^n \sum_{j=1}^n (\mathbf{M}_{i,j} \otimes \mathbf{I}_3) \mathbf{X}(t - \tau_{ij}) \\
& + \sum_{i=1}^n \left[(\tau_{i0} \mathbf{P}_i + \Omega^{i,i} \sum_{j=1}^n \tau_{ij} \mathbf{M}_{i,j}) \otimes \mathbf{W} \right] \mathbf{X}(t). \tag{4.34}
\end{aligned}$$

Then, considering the identities:

$$\mathbf{X}(t) = \tilde{\mathbf{X}}(t) + \mathbf{X}^*(t),$$

$$\mathbf{X}(t - \tau_{ij}) = \tilde{\mathbf{X}}(t - \tau_{ij}) + \mathbf{X}^*(t - \tau_{ij}),$$

$$\mathbf{X}^*(t) = \mathbf{X}_0(t) - \Delta_0,$$

and

$$\mathbf{X}^*(t - \tau_{i0}) = \mathbf{X}_0(t - \tau_{i0}) - \Delta_0,$$

which follows from (4.31), yields

$$\begin{aligned}
\mathbf{U}(t) = & - [(\mathbf{P} + \mathbf{D}) \otimes \mathbf{I}_3] \tilde{\mathbf{X}}(t) + \sum_{i=1}^n (\mathbf{P}_i \otimes \mathbf{I}_3) \mathbf{X}^*(t - \tau_{i0}) \\
& + \sum_{i=1}^n \sum_{j=1}^n (\mathbf{M}_{i,j} \otimes \mathbf{I}_3) \tilde{\mathbf{X}}(t - \tau_{ij}) \\
& + \sum_{i=1}^n \left[(\tau_{i0} \mathbf{P}_i + \Omega^{i,i} \sum_{j=1}^n \tau_{ij} \mathbf{M}_{i,j}) \otimes \mathbf{W} \right] \tilde{\mathbf{X}}(t) \\
& - [(\mathbf{P} + \mathbf{D}) \otimes \mathbf{I}_3] \mathbf{X}^*(t) + (\mathbf{L} \otimes \mathbf{I}_3) \mathbf{X}^*(t) \\
& + \sum_{i=1}^n \left[(\tau_{i0} \mathbf{P}_i + \Omega^{i,i} \sum_{j=1}^n \tau_{ij} \mathbf{M}_{i,j}) \otimes \mathbf{W} \right] \mathbf{X}^*(t) \\
& + \sum_{i=1}^n \sum_{j=1}^n (\mathbf{M}_{i,j} \otimes \mathbf{I}_3) \mathbf{X}^*(t - \tau_{ij}). \tag{4.35}
\end{aligned}$$

Now, replacing the formation error $\mathbf{X}(t) = \tilde{\mathbf{X}}(t) + \mathbf{X}^*(t)$ in (4.20), the dynamics of the formation error is rewritten as:

$$\dot{\tilde{\mathbf{X}}}(t) = \hat{\mathbf{A}} \tilde{\mathbf{X}}(t) + \hat{\mathbf{B}} \mathbf{U}(t) + (\hat{\mathbf{A}} - \hat{\mathbf{A}}_0) \mathbf{X}^*(t). \tag{4.36}$$

Therefore, the formation error dynamics in closed-loop is obtained applying the control law (4.35) in (4.36),

$$\begin{aligned}
\dot{\tilde{\mathbf{X}}}(t) = & \left\{ \hat{\mathbf{A}} - \hat{\mathbf{B}}[(\mathbf{P} + \mathbf{D}) \otimes \mathbf{I}_3] \right. \\
& + \hat{\mathbf{B}} \sum_{i=1}^n \left[(\tau_{i0} \mathbf{P}_i + \mathbf{\Omega}^{i,i} \sum_{j=1}^n \tau_{ij} \mathbf{M}_{i,j}) \otimes \mathbf{W} \right] \tilde{\mathbf{X}}(t) \\
& + \sum_{i=1}^n \sum_{j=1}^n \left(\hat{\mathbf{B}} \mathbf{M}_{i,j} \otimes \mathbf{I}_3 \right) \tilde{\mathbf{X}}(t - \tau_{ij}) \\
& + \left\{ \hat{\mathbf{A}} - \hat{\mathbf{A}}_0 - \hat{\mathbf{B}}[(\mathbf{P} + \mathbf{M}) \otimes \mathbf{I}_3] \right. \\
& + \hat{\mathbf{B}} \sum_{i=1}^n \left[(\tau_{i0} \mathbf{P}_i + \mathbf{\Omega}^{i,i} \sum_{j=1}^n \tau_{ij} \mathbf{M}_{i,j}) \otimes \mathbf{W} \right] \mathbf{X}^*(t) \\
& + \sum_{i=1}^n \hat{\mathbf{B}} (\mathbf{P}_i \otimes \mathbf{I}_3) \mathbf{X}^*(t - \tau_{i0}) \\
& \left. + \sum_{i=1}^n \sum_{j=1}^n \hat{\mathbf{B}} (\mathbf{M}_{i,j} \otimes \mathbf{I}_3) \mathbf{X}^*(t - \tau_{ij}), \right.
\end{aligned} \tag{4.37}$$

which can be rewritten in the following compact form:

$$\begin{aligned}
\dot{\tilde{\mathbf{X}}}(t) = & \tilde{\mathbf{A}} \tilde{\mathbf{X}}(t) + \sum_{i=1}^n \sum_{j=1}^n \tilde{\mathbf{A}}_{\tau_{ij}} \tilde{\mathbf{X}}(t - \tau_{ij}) + \mathbf{A}^* \mathbf{X}^*(t) \\
& + \sum_{i=1}^n \mathbf{A}_{\tau_{i0}}^* \mathbf{X}^*(t - \tau_{i0}) + \sum_{i=1}^n \sum_{j=1}^n \mathbf{A}_{\tau_{ij}}^* \mathbf{X}^*(t - \tau_{ij}),
\end{aligned} \tag{4.38}$$

where the matrices definitions follow directly by comparison with (4.37).

4.3 Platoon under fixed communication topology

It is clear that, in most cases, the number of vehicles in the platoon does not change as does the communication topology. In this scenario, although the control law of each vehicle is decentralized, it is possible to impose constraints over those control gains to ensure the global stability of the platoon, enabling the following results for communication without time-delay and with constant fixed delay for all vehicles.

4.3.1 A: Platoon free of communication delay

Theorem 4.1. *Let a vehicular platoon composed of n heterogeneous vehicles, with dynamics described by model (3.3), ruled by the distributed control law (4.1), and with a fixed known*

predecessor-based DAG communication topology. Then, the platoon is asymptotically stable, with null formation error, if and only if:

$$\kappa_1^i > 0, \quad \kappa_2^i > \frac{\zeta_i}{n_i} + \frac{\zeta_i \kappa_1^i}{n_i \kappa_3^i + 1}, \quad \kappa_3^i > \frac{\zeta_i - 1}{n_i}, \quad (4.39)$$

$\forall i = 1, \dots, n$, where ζ_i is the i -th vehicle powertrain time constant and $n_i = |\mathcal{N}_i|$ denotes the cardinality of \mathcal{N}_i , i.e. the number of vehicles connected with the vehicle i .

Proof. Based on the development presented in Sec. 4.2.1, the formation error dynamics is asymptotically stable if all eigenvalues of $\tilde{\mathbf{A}}$ in (4.23) are in the left half of the complex plane. To guarantee the Bounded-Input Bounded-Output (BIBO) stability, the portion in $\mathbf{X}^*(t)$ of (4.23) can be neglected, since it is an exogenous input, depending only on the leader states. Equivalently, all roots of the characteristic equation

$$0 = \det \left(\lambda \mathbf{I}_{3n} - \left\{ \hat{\mathbf{A}} - \hat{\mathbf{B}}[(\mathbf{P} + \mathbf{L}) \otimes \mathbf{I}_3] \right\} \right),$$

must have negative real parts. Note that matrices $\hat{\mathbf{A}}$ and $\hat{\mathbf{B}}$ are block diagonal, and the matrix $(\mathbf{P} + \mathbf{L})$ is lower triangular, once we are constrained to predecessor-follower topologies that are described by DAG. In this case, $\tilde{\mathbf{A}}$ is also lower block triangular, and the following holds:

$$\det \left(\lambda \mathbf{I}_{3n} - \tilde{\mathbf{A}} \right) = \prod_{i=1}^n \det \left(\lambda \mathbf{I}_3 - \mathbf{A}_i + (P_i + D_i) \mathbf{F}_i \right),$$

revealing that the asymptotic stability of the formation error dynamics is dictated by the stability of each vehicle in the platoon, ruled by the control law (4.1). Furthermore,

$$\begin{aligned} 0 &= \det \left(\lambda \mathbf{I}_3 - \mathbf{A}_i + (P_i + D_i) \mathbf{F}_i \right) \\ &= \lambda^3 + \frac{n_i \kappa_3^i + 1}{\zeta_i} \lambda^2 + \frac{n_i \kappa_2^i}{\zeta_i} \lambda + \frac{n_i \kappa_1^i}{\zeta_i}. \end{aligned}$$

In the latter equation, we have used the fact that $n_i = P_i + D_i$. Then, the Routh-Hurwitz array

$$\begin{array}{l|ll} \lambda^3 & 1 & n_i \kappa_2^i / \zeta_i \\ \lambda^2 & (n_i \kappa_3^i + 1) / \zeta_i & n_i \kappa_1^i / \zeta_i \\ \lambda^1 & \frac{(n_i \kappa_2^i)(n_i \kappa_3^i + 1) - \zeta_i (n_i \kappa_1^i)}{\zeta_i (n_i \kappa_3^i + 1)} & \\ \lambda^0 & n_i \kappa_1^i / \zeta_i & \end{array}$$

with $\zeta_i > 0$ and $n_i > 0$, leading to the stability conditions in the theorem statement, which concludes the proof. \square

The previous theorem provides necessary and sufficient conditions to ensure the platoon's asymptotic stability with null formation error. It establishes lower bounds for the admissible

control gains related to the i -th vehicle constant time and for the numbers of vehicles sharing information with it. Thus, the design rules presented in Thm. 4.1 are dependent on the communication topology. Further, note that, if a vehicle in the platoon does not have any neighbor in its sensing range, then $n_i = 0$ and the conditions in the previous theorem are unfeasible.

In the following corollary, we present similar design rules valid for any predecessor-follower topology.

Corollary 4.1. *Let a vehicular platoon composed of n heterogeneous vehicles with dynamics described by the linearized model in (3.3), governed by the distributed control law in (4.1), and subject to any fixed predecessor-based communication network topology. Besides, we assume that each vehicle in the platoon is connected with at least one of the other vehicles in the platoon. Then, the platoon is asymptotically stable with null formation error if and only if the following inequalities hold for all $i = 1, \dots, n$:*

$$\kappa_1^i > 0, \quad \kappa_2^i > \zeta_i + \frac{\zeta_i \kappa_1^i}{\kappa_3^i + 1}, \quad \kappa_3^i > \zeta_i - 1. \quad (4.40)$$

Proof. The result follows directly from Theorem 4.1, noting that the maximum of the right side of the inequalities (4.39) are obtained by setting $n_i = 1$. \square

The design rules conditions presented so far are essential in proving the main result of this thesis. However, the analysis of the resilience is incomplete without invoking new ideas. In the next section, we present a reconfiguration protocol that is fundamental to obtain this condition.

4.3.2 B: Communication with fixed constant delay

Theorem 4.2. *Consider a vehicular platoon composed of n heterogeneous vehicles, with dynamics described by the model (3.3), governed by the distributed control law (4.6), subject to communication time delay and a fixed known predecessor-based DAG communication topology. Thus, the platoon is asymptotically stable, with zero formation error, if and only if the following inequalities hold:*

$$\begin{aligned} \kappa_1^i &> 0, \\ \kappa_2^i &> \frac{\zeta_i \kappa_1^i}{n_i \kappa_3^i + 1} + \tau \kappa_1^i, \\ \kappa_3^i &> -\frac{1}{n_i}, \\ \tau &< \frac{\kappa_2^i}{\kappa_1^i} - \frac{\zeta_i}{n_i \kappa_3^i + 1}, \quad \forall i = 1, \dots, n, \end{aligned} \quad (4.41)$$

where $n_i = |\mathcal{N}_i|$ denotes the cardinality of \mathcal{N}_i , i.e. the number of vehicles connected with i .

thm. 4.2. In order to guarantee BIBO (Bounded-Input Bounded-Output) stability of the formation error dynamics (4.30), the state vectors, $\mathbf{X}^*(t)$ and $\mathbf{X}^*(t - \tau)$, which are inputs from the leader are considered exogenous. Then, the dynamics of the error is asymptotically stable if and only if all roots of the characteristic polynomial

$$\det(\lambda \mathbf{I}_{3n} - \tilde{\mathbf{A}} - \tilde{\mathbf{A}}_{\tau} e^{-\tau\lambda}) = 0 \quad (4.42)$$

have the negative real part. Notice that $\tilde{\mathbf{A}}_{\tau}$ is strictly lower triangular, then

$$\det(\lambda \mathbf{I}_{3n} - \tilde{\mathbf{A}} - \tilde{\mathbf{A}}_{\tau} e^{-\tau\lambda}) = \det(\lambda \mathbf{I}_{3n} - \tilde{\mathbf{A}}) = 0. \quad (4.43)$$

Therefore, to determine the BIBO stability of the dynamics of the formation error is necessary only if

$$\tilde{\mathbf{A}} = \hat{\mathbf{A}} - \hat{\mathbf{B}}[(\mathbf{P} + \mathbf{D}) \otimes (\mathbf{I}_3 - \tau\mathbf{W})]. \quad (4.44)$$

Expanding $\hat{\mathbf{A}}$ and $\hat{\mathbf{B}}$ in (4.44), results in

$$\tilde{\mathbf{A}} = \sum_{i=1}^n (\boldsymbol{\Omega}_i \otimes \mathbf{A}_i) - \left[\sum_{i=1}^n (\boldsymbol{\Omega}_i \otimes \mathbf{F}_i) \right] [(\mathbf{P} + \mathbf{D}) \otimes (\mathbf{I}_3 - \tau\mathbf{W})],$$

with $\mathbf{F}_i = \mathbf{B}_i \mathbf{K}_i$. Passing $(\mathbf{P} + \mathbf{D}) \otimes (\mathbf{I}_3 - \tau\mathbf{W})$ into the sum, and grouping the elements of the summation together, we have

$$\tilde{\mathbf{A}} = \sum_{i=1}^n \boldsymbol{\Omega}_i \otimes [\mathbf{A}_i - ([\mathbf{P}]_{ii} + [\mathbf{D}]_{ii}) \mathbf{F}_i (\mathbf{I}_3 - \tau\mathbf{W})]. \quad (4.45)$$

Since $\tilde{\mathbf{A}}$ is a diagonal block, and as the determinant of a diagonal block matrix is the product of the block determinants, calculating the determinant at (4.43) results in

$$\det(\lambda \mathbf{I}_{3n} - \tilde{\mathbf{A}}) = \prod_{i=1}^n \det[\lambda \mathbf{I}_3 - \mathbf{A}_i + ([\mathbf{P}]_{ii} + [\mathbf{D}]_{ii}) \mathbf{F}_i (\mathbf{I}_3 - \tau\mathbf{W})]. \quad (4.46)$$

This determinant equal to zero is the characteristic polynomial of the formation error dynamics in close-loop. The formation of the platoon will only be reached if this dynamic tends to zero in the worst case in infinite time. For this, all the λ eigenvalues of the characteristic equations associated with all the i -th vehicles must have a real part less than zero:

$$\begin{aligned} 0 &= \det \left(\lambda \mathbf{I}_3 - \mathbf{A}_i + (P_i + D_i) \mathbf{F}_i (\mathbf{I}_3 - \tau\mathbf{W}) \right) \\ &= \det \left(\lambda \mathbf{I}_3 - \begin{bmatrix} 0 & 1 & 0 \\ 0 & 0 & 1 \\ 0 & 0 & -\frac{1}{\zeta_i} \end{bmatrix} + \frac{n_i}{\zeta_i} \begin{bmatrix} 0 & 0 & 0 \\ 0 & 0 & 0 \\ \kappa_1^i & \kappa_2^i & \kappa_3^i \end{bmatrix} \begin{bmatrix} 1 & -\tau & 0 \\ 0 & 1 & 0 \\ 0 & 0 & 1 \end{bmatrix} \right) \\ &= \lambda^3 + \frac{n_i \kappa_3^i + 1}{\zeta_i} \lambda^2 + \frac{n_i (\kappa_2^i - \tau \kappa_1^i)}{\zeta_i} \lambda + \frac{n_i \kappa_1^i}{\zeta_i}, \end{aligned} \quad (4.47)$$

with $n_i = P_i + D_i$. Finally, the Routh-Hurwitz method for finding the limits of stability was chosen because it is a tool that has sufficient conditions for choosing the variables of the

consensus gain control vector and provides the maximum communication delay time in which the formation stability is guaranteed:

$$\begin{array}{l|l} \lambda^3 & 1 & \frac{n_i(\kappa_2^i - \tau\kappa_1^i)}{\zeta_i} \\ \lambda^2 & (n_i\kappa_3^i + 1)/\zeta_i & n_i\kappa_1^i/\zeta_i \\ \lambda^1 & \frac{(n_i\kappa_3^i + 1)(n_i\kappa_2^i - n_i\tau\kappa_1^i) - \zeta_i(n_i\kappa_1^i)}{\zeta_i(n_i\kappa_3^i + 1)} & \\ \lambda^0 & n_i\kappa_1^i/\zeta_i & \end{array}$$

with power-train inertial time $\zeta_i > 0$, and the number of followed vehicle for i $n_i > 0$.

Based on (4.46) we conclude that the decentralized control system studied in this thesis only depends on local information for its stability. However, it is obvious that for the stability of the platoon, all vehicles must reach the desired formation distance, which is guaranteed by the appropriate choice of parameters in (4.41). We reach the result presented by theorem 4.2, and the proof is concluded. \square

4.4 Structural Properties of Local Stabilization under a Predecessor–Follower Topology

Building upon the control formulation and stability analysis presented in the previous sections, this section discusses a structural property that emerges from the adopted predecessor–follower communication topology.

Under this configuration, each vehicle computes its control action using only locally available variables, obtained from onboard measurements and information exchanged with neighboring vehicles. This structure leads to a form of local regulation in which the stabilization of each vehicle can be addressed independently at the control design level, while the overall platoon behavior arises from the interconnection of these locally regulated subsystems (BULLO; CORTÉS; MARTÍNEZ, 2009b).

From a control-theoretic perspective, this property can be interpreted as a form of structural decoupling at the vehicle level. Although the platoon remains a dynamically interconnected system, the predecessor–follower topology allows the closed-loop dynamics of each vehicle to be expressed primarily in terms of its own state and relative information with respect to adjacent vehicles. As a result, stability analysis and controller tuning can be carried out locally, without requiring explicit knowledge of the full platoon model or the dynamics of non-neighboring vehicles (MESBAHI; EGERSTEDT, 2010).

This local stabilization property is particularly relevant in heterogeneous platoons, where vehicles may present distinct dynamic characteristics, actuation capabilities, and sensing configurations. In such scenarios, centralized or globally coupled control strategies typically require accurate modeling of all vehicles, which becomes impractical as the platoon size increases

or when vehicles join and leave the formation dynamically. In contrast, the predecessor–follower structure enables each vehicle to regulate its behavior based on its own dynamics, while preserving coordinated motion through relative measurements and local communication.

It is important to emphasize that this property does not imply complete dynamic decoupling of the platoon. The vehicles remain interconnected through the communication topology, and global platoon behavior (such as disturbance propagation and transient performance) still depends on the interaction structure. Nevertheless, the possibility of enforcing stability conditions at the vehicle level represents a significant simplification from a design and analysis standpoint and contributes to the scalability of the proposed approach, in line with classical results on the stability of interconnected systems ([SILJAK, 1978](#)).

The emergence of coordinated platoon behavior from locally stabilized dynamics is also consistent with consensus-based interpretations of distributed control. In this context, local control laws ensure regulation of relative states, while the communication topology governs how information propagates through the platoon. The predecessor–follower configuration plays a central role in shaping this propagation, allowing coordinated motion to be achieved without centralized coordination or global state information ([MESBAHI; EGERSTEDT, 2010](#)).

Finally, this structural property has direct implications for platoon reconfiguration and recovery scenarios addressed in the subsequent chapters. Since stability conditions are formulated locally, vehicles can be added to or removed from the platoon with limited impact on the control laws of the remaining vehicles. Likewise, in situations where communication is temporarily lost, the local control structure allows vehicles to maintain stable behavior and subsequently reestablish coordinated motion once communication is restored. These aspects contribute to the resilience of the platoon under realistic operating conditions. The formulation developed in this chapter provides the mathematical foundation for the analysis of platoon reconfiguration and recovery mechanisms under communication constraints, which are addressed in the following chapters.

5 PROTOCOL OF RECONFIGURATION AFTER ENTRY AND EXIT OF VEHICLES.

Situations such as mechanical problems, cyber attacks, malicious agents, or changing lanes to the side lane can cause a vehicle to leave the platoon and leave a space greater than the desired distance: the formation distance. When a vehicle leaves the platoon, the other vehicles that received information from it start to have complications with its stabilization, which is performed at the lowest hierarchical level of control. The departure of the vehicle is a problem because the control law, in particular cases of communication delay in 4.1, 4.6 and 4.14 depends on the information from the vehicle that left. To solve this problem, we propose a protocol that changes the entry of the consensus law to a new queue position pointer reference: the state vector of the vehicle immediately ahead of the one that left. This chapter focuses on structural reconfiguration of the communication topology, while preserving the same low-level control law derived in Chapter 4.

In order to certify the asymptotic stability of the platoon by the procedure of the tests carried out in this thesis, according to the classical control theory, it is necessary to guarantee that the events, both input and output, occur only in steady state. This means that the protocol at a level above the control hierarchy can only modify the communication topology of the vehicles when all are in formation, traveling at cruising speed and with zero acceleration. The vehicles being aligned according to the consensus law at the desired distance between all vehicles means that there is no effort acted by the control law in the sense of modifying the acceleration of the car: the control law is equal to zero and all vehicles travel at the same cruising speed. The condition that every vehicle entry or exit occurs only when the platoon travels in a steady state, restricts the application of the proposed method to occurrences that can be planned to be performed after the stabilization dynamics of the train of connected vehicles. Which is very reasonable to do in traffic where defensive driving is adopted.

Thus, we present here a reconfiguration protocol that, based on this approach, provides stability and resilience in the face of changes in the number of vehicles in the platoon. The protocol action is performed on each vehicle to properly adjust d_{ij} in δ_{ij} and \mathcal{N}_i in the control law 4.1, 4.6 and 4.14, whenever a reorganization becomes necessary. Figure 3.2 represents the desirable rear bumper-to-rear bumper distance denoted by the parameter d_{ij} . The vehicle's rear bumper reference is only a marked reference point for other vehicles. The choice of this point on the rear bumper can be changed as long as the new reference is updated for all vehicles that depend on it. As illustrated, the length of the i -th vehicle is given by ℓ_i , while the gap between i and $i - 1$ is given by γ_i . Thus, the target distance to the first immediately preceding neighbor is $d_{i,i-1} = \ell_i + \gamma_i$, to the second one is $d_{i,i-2} = \ell_{i-1} + \gamma_{i-1} + d_{i,i-1}$, and so on. Then,

Algorithm 1 reconfiguration protocol

-
- 1: $\mathcal{D}_i \leftarrow \langle \mathbf{x}_j(t), \gamma_j, \ell_j \rangle$ for every j inside R_i
 - 2: define the desired inter-spacing d_{ij} using Eq. (5.1)
 - 3: $\mathcal{N}_i \leftarrow$ every element in \mathcal{D}_i with associated $d_{ij} \leq R_i$
 - 4: $u_i(t) \leftarrow$ control law (4.1) using δ_{ij} and \mathcal{N}_i
 - 5: **repeat**
 - 6: $\mathcal{D}_i \leftarrow \langle \mathbf{x}_j(t), \gamma_j, \ell_j \rangle$ for every j inside R_i
 - 7: **if** $|u_i(t)| < \epsilon$ **and** $|\mathcal{D}_i| \neq |\mathcal{N}_i|$ **then**
 - 8: define the inter-spacing d_{ij} using Eq. (5.1)
 - 9: $\mathcal{N}_i \leftarrow$ every element in \mathcal{D}_i with related $d_{ij} \leq R_i$
 - 10: **end if**
 - 11: $u_i(t) \leftarrow$ control law (4.1) using δ_{ij} and \mathcal{N}_i
 - 12: **until** vehicle i leaves the platoon
-

equivalently, we have the iterative formula:

$$d_{i,j} = \ell_{j+1} + \gamma_{j+1} + d_{i,j+1}, \quad (5.1)$$

for any $j \in \{i-1, i-2, \dots, 0\}$, setting the starting term as $d_{i,i} = 0$. Here it must be clear that each vehicle needs to broadcast its states information $\mathbf{x}_i(t)$, its length ℓ_i , and its desired distance to its first ahead vehicle γ_i , as in Fig. 3.2.

Based on the previous setup of calculation the Algorithm 1 performs locally a reconfiguration in the parameters of the control law in (4.1) that guarantees the platoon stability and reorganization.

The reconfiguration protocol updates the control law whenever vehicles leave or enter the platoon. In the case of entrances, vehicles choose places to get in, and then they start to send/receive information to/from the nearby vehicles. The Alg. 1 proceeds as follows. In the line 1 it is created a set \mathcal{D}_i with data received by the vehicle i from all others inside its communication range, R_i , and the desired inter-spacing distances are calculated in line 2. The set \mathcal{N}_i is determined in the line 3 by selecting from \mathcal{D}_i only the vehicles that will keep connection with the vehicle i when the platoon reaches the desired formation. Then the vehicle i begins to run its control law, as presented in line 4.

The control action is used to test the stationary condition, line 7, then if $|u_i(t)| > \epsilon$, for some small $\epsilon > 0$, the vehicle is not in steady-state. Thus, in the main loop, the agent will execute the control law at line 11 until condition in line 7 is satisfied. It ensures that the network topology remains unchanged during a transient regime.

The line 6 updates the set \mathcal{D}_i . Note that, when the platoon reaches the desired formation and no new vehicle connects to vehicle i , or alternatively, no vehicle disconnects from vehicle i , we have $|\mathcal{D}_i| = |\mathcal{N}_i|$.

In line 7 is tested if the steady-state regime is reached and if the number of vehicles detected by the vehicle i changes. Then, if the conditions hold, the reconfiguration protocol

effectively starts. The desired inter-vehicle space is updated according to line 8 and the set \mathcal{N}_i is updated in line 9; leading to the computation of the control law (4.1) in line 11. Alternatively, if the number of neighbors detected is unchanged or if the platoon is not in steady-state, the parameters are not reconfigured and the control law is computed as in the previous iteration, restarting the loop.

In practical terms of exits, every vehicle moves up to the preceding vehicle position, which is graphically depicted in Fig. 1.2, filling any gaps that are left because of the purposeful exists of unwanted failures. Analogously, in the case of entries, some following vehicles leave a room to allow new vehicles to join the platoon.

5.1 Resilience condition for platoon stability

Results in Sec. 4.3 demonstrate that platoons with fixed network connections reach null formation error in steady-state, as long as control gains are designed in accordance with inequalities (4.39) or (4.40). Therefore, they are valid for any invariant look-ahead communication topology and any number of vehicles in the platoon.

The main assumption considered here, allowing those previous results to be applied in the case of switching topologies, is that the communication network switches only when the platoon is in a stationary condition, which justifies the reconfiguration protocol previously proposed.

Under the aforementioned assumption, platoon states are time-independent, and they can be simply regarded as a set of new initial conditions for the new configuration, in case of the entrance or exit of vehicles in the formation. Therefore, based on the results presented in Sec. 4.3, the reconfiguration protocol, and on all previous discussion, we can state the main result:

Theorem 5.1. *Let a vehicular platoon composed of heterogeneous vehicles, with dynamics described by (3.3), ruled by the distributed control law (4.1), and subject to a predecessor-based communication topology. Then, the formation is asymptotically stable, with null formation error, and resilience to the entry or the exit of members if:*

- (i) *control gains are designed in accordance with the inequalities (4.39) or (4.40); and*
- (ii) *any entrance or exit of vehicles occurs when the platoon is in a steady-state, and each vehicle control law is updated by the reconfiguration protocol in Sec. 5.*

The previous theorem presents sufficient conditions that guarantee stability, null formation error, and resilience under the entry and exit of vehicles for platoons in a decentralized manner. It is worth mentioning that before condition can be satisfied using the inequalities (4.39), where the design rules are based on the connectivity of each vehicle. Thus, at each entrance or exit of a vehicle in the platoon, the control law gains of the vehicles may be

updated. It is possible because under steady-state the distributed control law in (4.1) is null independently of the control gains.

Finally, it remains to emphasize that the conditions presented so far in this thesis assume the existence of connection among vehicles, a basic requirement for the autonomous platoon. In the worst scenario, each vehicle needs to be connected at least to one other, then in the case of vehicles exiting from the platoon such minimum connection requirement needs to hold, that is $n_i \geq 1 \forall i$. Otherwise, some vehicle connections may be broken, and then the platoon itself. We illustrate such a case and the application of our resilient control strategy using simulated experiments in the next section.

5.2 Numerical examples

This chapter presents simulated results to illustrate the effectiveness of our protocol. We have performed: i) linear simulation (4.2) subject to multiple exits and entrances of vehicles; and ii) nonlinear simulation with resilience analysis in a robotic simulator. All trials were executed on Python/NumPy language at Ubuntu 20.04.

5.2.1 Linear simulation: multiple entries and exits

In this simulation, we have started the platoon with 8 vehicles, adding 2 more at 50 s, removing other 2 at 100 s and, finally, removing 3 more at 150 s. Most of the vehicles parameters were extracted from (ZHENG *et al.*, 2019) as shown in Tab. 5.1.

Table 5.1 – Vehicle parameters extracted from (ZHENG *et al.*, 2019).

Parameter values	
$m_i = 1500 + 100i$ [kg]	$r_i = 0.25 + 0.005i$ [m]
$\eta_i = 80 + i$ [%]	$\zeta_i = 0.3 + 0.02i$
$C_i = 0.4 + 0.01i$	$\mu_i = 0.015 + 0.001i$
$\ell_i = 4.0 + 0.5i$ [m]	$\gamma_i = 10.0 + 0.25i$ [m]
$\rho = 1.23$ [kg/m ³]	$g = 9.78$ [m/s ²]

To maintain each teammate connected with at least one other when two consecutive vehicles leave the platoon simultaneously, we have set $R_i = 64 + i$. In addition, the leader executes the following trajectory:

$$u_0(t) = \begin{cases} 2 \text{ m/s}^2 & \text{for } 10 \text{ s} \leq t \leq 15 \text{ s}, \\ 1 \text{ m/s}^2 & \text{for } 160 \text{ s} \leq t \leq 165 \text{ s}, \\ 0 \text{ m/s}^2 & \text{otherwise,} \end{cases} \quad (5.2)$$

inducing local disturbances at the beginning. Moreover, in accordance with the stability conditions in (4.39), control gains were set by $\mathbf{K}_i = (\zeta_i/\zeta_0) \begin{bmatrix} 4.0 & 15.0 & 8.0 \end{bmatrix}$, which is based on the ratio between the inertial time constant of the i -th follower and the leader vehicle.

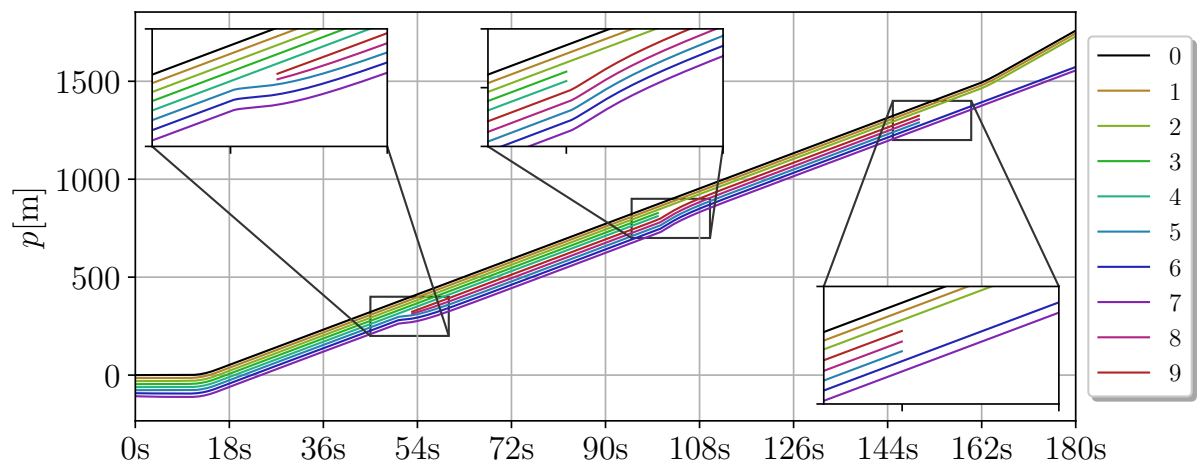


Figure 5.1 – Vehicles position with multiple entries and exits.

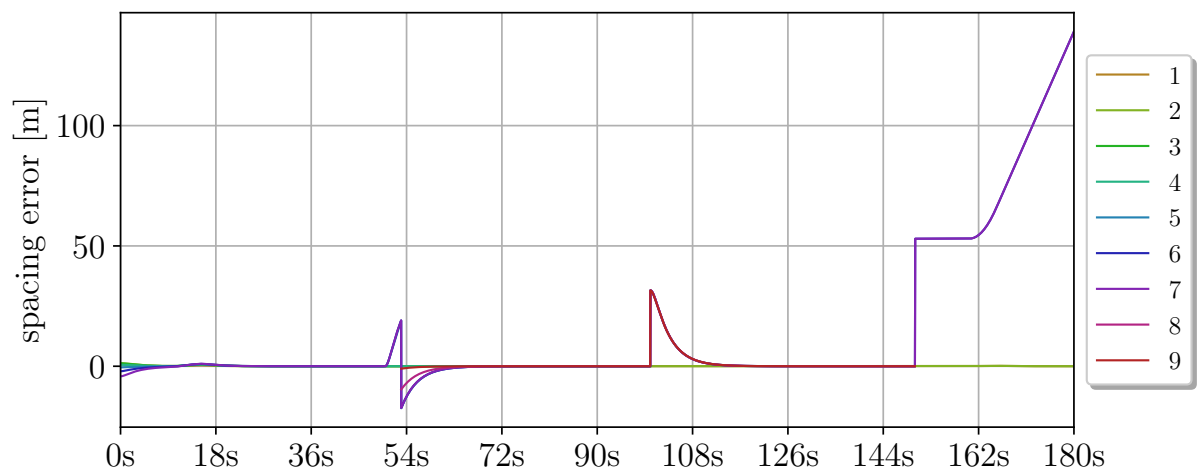


Figure 5.2 – Formation error. At 150s, 3 vehicles exit simultaneously splitting the platoon.

Figures 5.1 and 5.2 present the results obtained. Initially, we see the platoon reaching formation and then in steady-state at 50s two vehicles join it. After that, the platoon starts its reorganization, and already in stationary regime at 100s two vehicles leave. Once again the platoon reaches formation, but at 150s more three vehicles leave. This caused a communication breakdown in the team because one vehicle lost its connection with the others. As consequence at this time, the platoon does not reorganize itself and between 160 and 165s when the leader vehicle accelerates once again the last two vehicles are left behind.

Fig. 5.2 presents the spacing error related to the leader position. Resilience was guaranteed whenever the conditions established by Corollary 4.1 were met. The platoon does not recover its formation only after the simultaneous exit of three vehicles because one vehicle lost its connection with all others, violating Corollary 4.1.

5.2.2 Nonlinear simulation: comparative analysis

In this simulation, the aim is twofold: *i*) illustrate how the controller can overcome nonlinear dynamics and *ii*) compare the performance of our methodology with a state-of-the-art similar one proposed in (PIRANI *et al.*, 2018). The nonlinear simulation was performed with *CoppeliaSim* simulator¹ and its built-in *Manta* platform, a relatively complex Ackermann model with suspension and steering command. Here the platoon is homogeneous and it starts with 6 vehicles, whose parameters are given in Tab. 5.2 and $R_i = 16$ m.

Table 5.2 – Parameters extracted from the CoppeliaSim.

Parameter	Value	Parameter	Value
m_i [kg]	30.0	r_i [m]	0.09
η_i [%]	80.0	ζ_i	0.5
C_i	0.01	μ_i	0.003
ℓ_i [m]	0.6	γ_i [m]	7.0

Here, the leader was commanded to accelerate until it reaches the constant velocity of $v_0(t) \approx 4.2$ m/s. At 35 s and 70 s, vehicles 3 and 4 leave the platoon, respectively. The Figs. 5.3 and 5.4 presents the results obtained by applying the W-MSR algorithm in (PIRANI *et al.*, 2018) and our proposed methodology.

Fig.5.3 shows that the W-MSR algorithm can reorganize the platoon after vehicle 3 exits, but not after the exit of vehicle 4 when vehicle 5 is disconnected from the platoon. On the other hand, Fig. 5.4 shows that the proposed reconfiguration protocol governed the platoon to formation after both exits. The result concerning the W-MSR algorithm was foreseen because in the present setup it ensures resilience for $\lfloor (k+1)/2 \rfloor = 1$ failing agent, since in steady-state the number of connected neighbors is $k = 2$ due the vehicles connection range.

In Figs. 5.5 and 5.6 compares the spacing error of both approaches. Fig. 5.5 shows that the spacing error grows up after the second failure, while Fig. 5.6 demonstrate the effectiveness of the proposed protocol. That occurs because the proposed reconfiguration protocol updates the set of connected neighbors vehicles after every entrance or exit of vehicle (Alg.1, line 9). Unlike resilient consensus strategies based on W-MSR, the proposed approach does not assume a minimum level of k -connectivity nor the presence of malicious agents.

This chapter shows that topology reconfiguration events can be handled without modifying the underlying control law, paving the way for the recovery mechanisms introduced in the next chapter.

¹ <https://www.coppeliarobotics.com/>

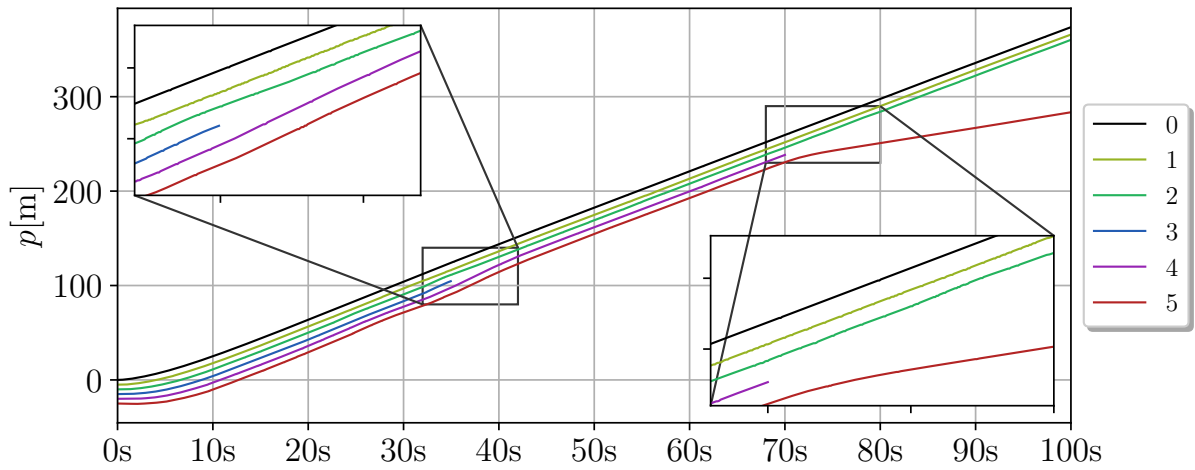


Figure 5.3 – W-MSR method in (PIRANI *et al.*, 2018). Comparative analysis between (PIRANI *et al.*, 2018) and our approach: position over time.

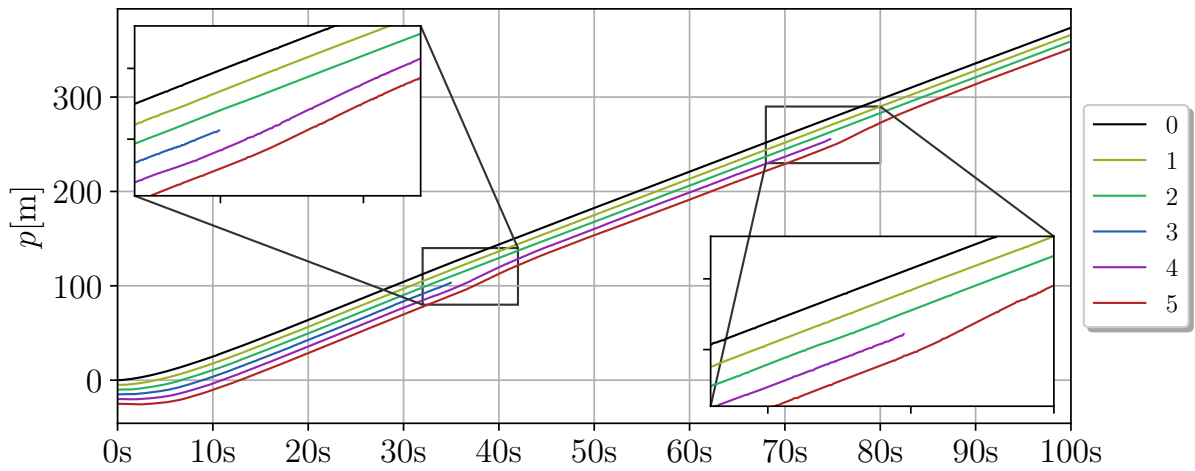


Figure 5.4 – Our reconfiguration protocol. Comparative analysis between (PIRANI *et al.*, 2018) and our approach: position over time.

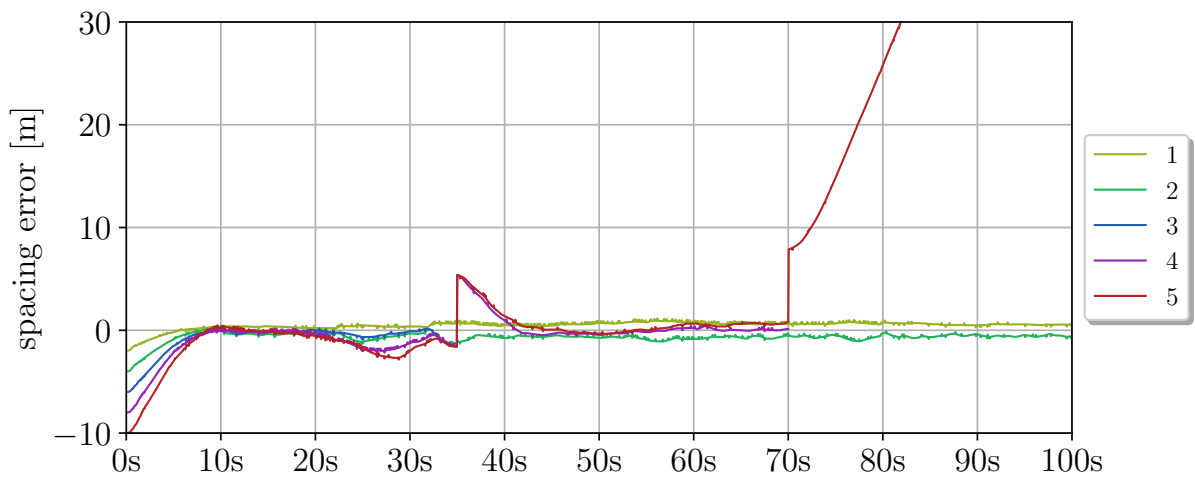


Figure 5.5 – Comparative analysis between (PIRANI *et al.*, 2018) and our approach: spacing over time. W-MSR method in (PIRANI *et al.*, 2018).

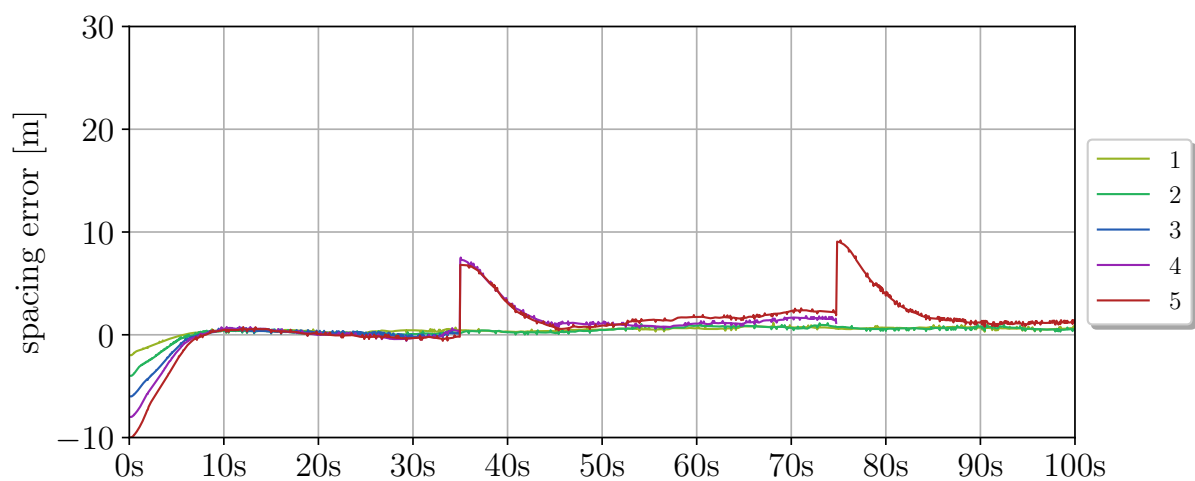


Figure 5.6 – Comparative analysis between (PIRANI *et al.*, 2018) and our approach: spacing over time. Our reconfiguration protocol.

6 PROTOCOL FOR RECOVERY OF VEHICLE TO THE PLATOON

6.1 Problem definition

The platoon reaches its main objective when all vehicles reach a formation consensus with their neighbors, such that the spacing errors asymptotically converge to zero. Concerning the aforementioned characteristics, we can formally define the scope of this thesis according to the following problems:

Problem 6.1 (Resilient connection). *Consider a heterogeneous platoon where each vehicle i is ruled by dynamic Eq. (3.3) and subjected to communication time-delay τ_{ij} and even communication breakdowns. In addition, assume that the vehicle i can start completely unplugged from the other ones, or it can be temporarily disconnected from the team due to failing vehicles or external disturbances (e.g., traffic lights). Then, the main problem is to compute an input command $u_i(t)$ such that i will join or rejoin the platoon (modeled as a DAG), even if lost communication with the preceding teammates.*

Problem 6.2 (Platoon stability). *Assuming that vehicle i was capable of reaching the platoon, the following problem is to compute an input command $u_i(t)$ such that it will be able to achieve the steady-state condition with the neighbors. When any disturbance or event causes the complete disconnection of i with the agents ahead, we return to the scope of Prob. 6.1.*

6.2 Main results

6.2.1 Proposed approach

Typical consensus protocols in the literature generally assume that each team member always receives information from at least one neighbor. However, depending on the current platoon behavior or some adverse road condition, the i -th vehicle, or a subset composed of itself and its followers, can be completely disconnected from the preceding vehicles. For instance, this situation occurs when the platoon travels on a road devoid of connected infrastructure, and a traffic light changes when the platoon is passing by. Some vehicles keep going and others are stopped at the red light. Another adverse situation occurs when the platoon is connected, but there is an obstacle that prevents the succeeding vehicles to follow closely. For example, HDV may change lanes and enter the gap between two members of the platoon, behaving in a non-cooperative manner. Either way, in this thesis, whenever a vehicle has lost the connection link with the platoon or there is no free path toward a neighbor, we assume that connectivity is lost.

Therefore, in this section, we propose a strategy that solves both, Prob. 6.1 and 6.2. Our method is based on the state-machine shown in Fig. 6.1, which is composed of three

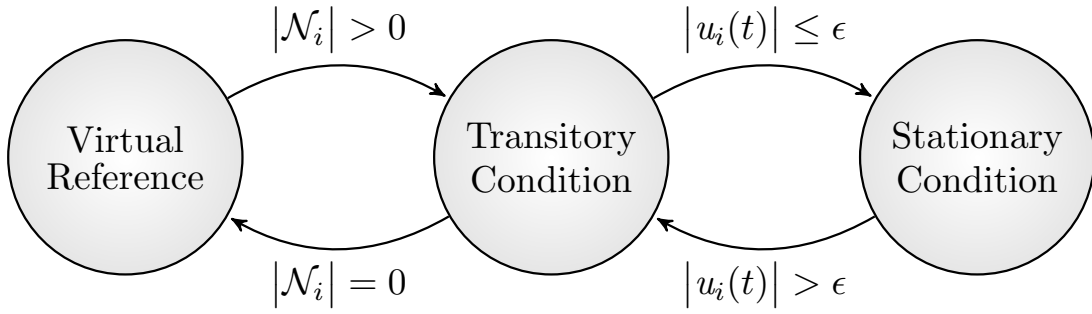


Figure 6.1 – Switching protocol: in the *Virtual Reference* state, the vehicle is completely disconnected from the platoon; when it reaches one agent at its front, it switches to the *Transitory Condition*, using the state information provided by its new neighbor to reduce the state error; when the error is small enough, the vehicle goes to the *Stationary Condition*, following the entire platoon.

states and the transitions among them:

- (i) in the *Virtual Reference* state, there are two possibilities: i) no teammates are connected with the i -th vehicle or ii) there are teammates connected, but there are some obstacles ahead. In both cases, this vehicle will start to follow a virtual leader if, $\mathcal{N}_i = \emptyset$.
- (ii) in the *Transitory Condition* state, i -th vehicle regains connectivity with another agent, which is enough for it to reduce its spacing error related to this neighbor. Here, however, a steady-state condition has not yet been achieved.
- (iii) finally, in the *Stationary Condition* state, the error to its first predecessor neighbor is so small that it regains full connectivity with the platoon.

Here, we assume that the vehicles are equipped with collision avoidance assistance and enough instruments to identify obstacles in their trajectory traffic, such as traffic lights, signs, and HDVs. Whenever it is safe to do so a vehicle in the *Virtual Reference* state, $\mathcal{N}_i = \emptyset$, will keep using the same control law as before. However, it starts to follow a kind of virtual leader, whose position and speed varies according to road conditions (see Thm. 6.1). If the conditions are safe, this virtual leader assumes that it is trailing the platoon, and accelerates to the maximum road speed without any issues.

As it can be seen, transitions between *Virtual Reference* and *Transitory Condition* depend on existence of at least one vehicle in the communication range and no presence of obstacles. Once a vehicle is in *Transitory Condition* the control law (4.14) will act in order to drive the vehicle to the *Stationary Condition*. However, transitions between *Transitory Condition* and *Stationary Condition* depend on disturbances, such as agent failures, abrupt changes in the leader speed, or external events like changes in the road slope, which force an acceleration command to be higher than a small positive value ϵ .

Moreover note that, since the proposed protocol is local, only the vehicle with $\mathcal{N}_i = \emptyset$

can activate the virtual reference. For example, suppose the agent i -th has m followers and is disconnected from its predecessors or there is an obstacle preventing it from following them. Then, when it is safe, the i -th agent will activate the *Virtual Reference* state, but this does not mean that its followers will do so. They might be in the *Transitory Condition* or even *Stationary Condition*. In this situation, we have a subset of the original platoon forming a platoon with size $m + 1$ vehicles, whose practical leader is the i -th vehicle of the former platoon, that is constrained to follow the *Virtual Reference*.

6.2.2 Reconnection protocol

The recovery protocol does not introduce a new control law; instead, it switches the reference information used by the same distributed controller derived in Chapter 4. To demonstrate that our approach ensures the *resilient* incorporation of agent i to the platoon, let us first consider the following assumption:

Assumption 6.1. *In steady-state, the leader travels at constant speed $0 < v_0 \leq \alpha v_{max}$, where v_{max} is the speed limit value for the road and $0 < \alpha < 1$ is a constant factor.*

This is a fundamental assumption since in Thm. 1 of (ZHENG *et al.*, 2019), it is demonstrated that a steady state consensus can only be achieved when the leader acceleration is null. This assumption for mixed-traffic scenarios is also supported by previous works in the literature, see (LIANG *et al.*, 2015) for instance. In a heterogeneous platoon, a leader vehicle traveling above the maximum speed of at least one following vehicle will make the null formation error unfeasible in the entire platoon. On the other hand, a very slow leading vehicle is likely to be inefficient from the platoon perspective. Therefore, there is an optimal value for α that is an open topic explored in the platoon literature.

As previously stated, at the *Virtual Reference*, agent i has no feedback information about other members of the platoon, so it can not properly compute $u_i(t)$ to reduce the spacing error using Eq. (4.14). That can happen at the start, when the vehicle is powered on, or when its connection is temporarily lost due to system disturbances. So, to solve the Problem 6.1, it is proposed to use a *virtual agent*; a new numerical reference created to emulate the communication of the agent i with a direct neighbor further ahead of i . Figure 6.2 illustrates the idea when the preceding vehicles are out of communication range and there is a clear path. For simplicity in the following, we set $\delta_{i^*} = 0$.

In this context, let us present the following statement:

Theorem 6.1. *Suppose a platoon at the equilibrium point accordingly with Assumption 6.1 and let the virtual reference states be given by $\mathbf{x}_*(t) := [p_i(t) \quad \beta v_{max} \quad 0]^T$. Then a vehicle i in the Virtual Reference state governed by the control law (4.14), setting $j = *$, $\delta_{i^*} = \tau_{i^*} = 0$, will reach the Transitory Condition state as $t \rightarrow \infty$ if it has a free path to its first predecessor*

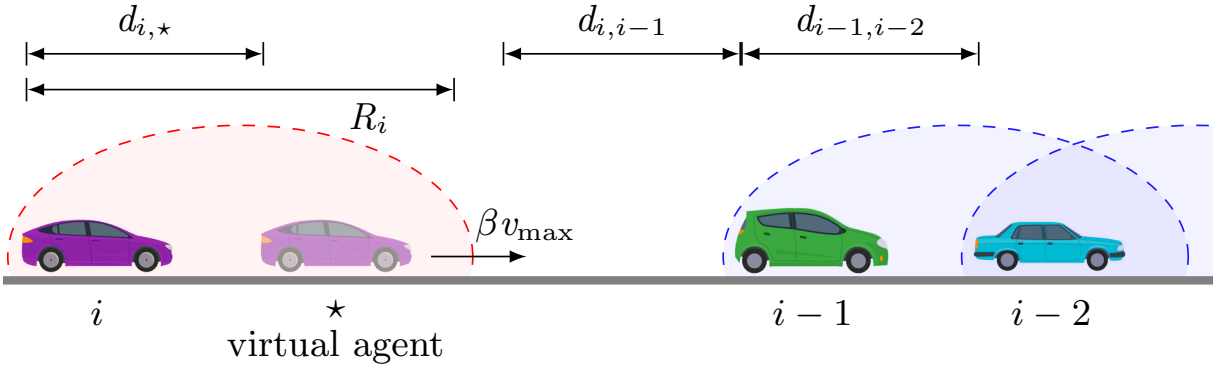


Figure 6.2 – Virtual agent used to ensure connectivity with the platoon in the *Virtual Reference* state: when no communication is available and there is a free path, vehicle i uses a virtual neighbor traveling ahead to run the proposed control law. R_i represents the vehicle i communication range.

neighbor and the following conditions hold

$$k_2 > 0, \kappa_3^i > -1 \text{ and } \alpha < \beta \frac{\kappa_3^i + 1}{\kappa_2^i} \leq 1; \quad (6.1)$$

where β is a tuning parameter to adjust the final speed of the vehicle in the *Virtual Reference* state and αv_{\max} defines the platoon speed.

thm. 6.1. Setting $j = \star$ in (4.14) and $\delta_{i\star} = \tau_{i\star} = 0$ we get

$$\begin{aligned} u_i(t) &= -\mathbf{K}_i \left(\mathbf{x}_i(t) - \mathbf{x}_\star(t) + \delta_{i\star} \right), \\ &= \kappa_2^i \left(\beta v_{\max} - v_i(t) \right) - \kappa_3^i a_i(t), \end{aligned} \quad (6.2)$$

which reveals that the control law (4.14) plugged with the virtual reference states provides a positive acceleration command. In the Laplace domain, focusing on the speed output, we have

$$v_i(\lambda) = G(\lambda) \frac{v_{\max}}{\lambda} \text{ with } G(\lambda) = \frac{\beta(\lambda + (\kappa_3^i + 1)/\zeta_i)}{\lambda^2 + (\kappa_3^i + 1)/\zeta_i \lambda + \kappa_2^i/\zeta_i}.$$

Thus the first two inequalities in the theorem statement ensure the vehicle stability. The final value theorem yields the third one that guarantees $\alpha v_{\max} < v_i(t)|_{t \rightarrow \infty} \leq v_{\max}$.

Then, if the conditions in the theorem hold, a vehicle commanded by (6.2) decreases its spacing error to its predecessor neighbor up to switch to the *Transitory Condition* because the platoon speed in steady-state is higher than αv_{\max} , the leader vehicle speed (Asm.6.1). \square

This result shows that, in the absence of information and with a free path, vehicle i will travel at a speed higher than the platoon speed. Moreover, it is important to mention that the vehicle's transient speed can reach values higher than the road speed limit. Therefore, to avoid such a scenario extra constraints in the control law can be added if $v_i(t) \geq v_{\max}$. It is worth emphasizing that the proposed recovery mechanism is fully local and does not require any global information about the platoon topology or size.

6.2.3 Formation error

Now, still concerning the switching protocol, Fig. 6.1, let us state the following:

Theorem 6.2. *Suppose the platoon with the leader vehicle at the equilibrium point (Asm. 6.1), and assume that the formation error dynamics (4.38) is asymptotically stable. If a vehicle i is in the Transitory Condition state and it has free path to its first predecessor neighbor, the control law (4.14) will govern it to reach the Stationary Condition state as $t \rightarrow \infty$.*

thm. 6.2. Let us prove it by induction. Assuming that the first follower governed by the distributed control law (4.14) is connected and has a free path to the leader. Then, if the formation error dynamics (4.38) is asymptotically stable, the vehicle will approach the leader up to $|u_i(t)| < \epsilon$ (for some small $\epsilon > 0$) as $t \rightarrow \infty$ and reach the *Stationary Condition* state. Following this reasoning, if the $(i-1)$ -th agent is in the *Stationary Condition*, the i -th agent will be able to reach a null spacing error as t tends to ∞ and the *Stationary Condition*. \square

In the following, we establish design conditions for the control law (4.14) that guarantee formation error dynamics (4.38) asymptotically stable, the main assumption in the previous theorem. We start with the following result.

Theorem 6.3. *Consider a connected vehicular platoon free of obstacles in its trajectory composed of n heterogeneous vehicles, with dynamics in (3.3), governed by the control law (4.14), subject to communication delays and a fixed known predecessor-based DAG communication topology. Thus, the platoon is asymptotically stable if and only if the following hold:*

$$\kappa_1^i > 0, \quad \kappa_2^i > \frac{\zeta_i \kappa_1^i}{n_i \kappa_3^i + 1} + \frac{\bar{\tau}_i}{n_i} \kappa_1^i, \quad \kappa_3^i > -\frac{1}{n_i}, \quad (6.3)$$

for all $i = 1, \dots, n$, where $n_i = |\mathcal{N}_i|$ is the number of vehicles connected to vehicle i , and $\bar{\tau}_i$ is the sum of all delays in the information shared with the vehicle i , i.e. $\bar{\tau}_i = \sum_{j \in \mathcal{N}_i} \tau_{ij}$.

thm. 6.3. In order to guarantee the BIBO (Bounded-Input Bounded-Output) stability of the formation error dynamics (4.38), we first note that the entries related to the leader, $\mathbf{X}^*(t)$ and $\mathbf{X}^*(t - \tau_{ij})$, are exogenous. Then, the error dynamics is asymptotically stable if and only if all roots of the characteristic polynomial $\Delta(\lambda) = 0$, with

$$\Delta(\lambda) := \det \left(\lambda \mathbf{I}_{3n} - \tilde{\mathbf{A}} - \sum_{i=1}^n \sum_{j=1}^n \tilde{\mathbf{A}}_{\tau_{ij}} e^{-\tau_{ij} \lambda} \right),$$

having a negative real part. To investigate such roots, note that $\tilde{\mathbf{A}}_{\tau_{ij}}$ is strictly lower triangular and

$$\tilde{\mathbf{A}} = \hat{\mathbf{A}} - \hat{\mathbf{B}}[(\mathbf{P} + \mathbf{D}) \otimes \mathbf{I}_3]$$

$$\begin{aligned}
& + \widehat{\mathbf{B}} \sum_{i=1}^n (\tau_{i0} \mathbf{P}_i + \boldsymbol{\Omega}^{i,i} \sum_{j=1}^n \tau_{ij} M_{i,j}) \otimes \mathbf{W} \\
& = \widehat{\mathbf{A}} - \sum_{i=1}^n (\boldsymbol{\Omega}^{i,i} \otimes \mathbf{F}_i) \left[\sum_{i=1}^n \boldsymbol{\Omega}^{i,i} (P_i + D_i) \otimes \mathbf{I}_3 \right] \\
& + \sum_{i=1}^n (\boldsymbol{\Omega}^{i,i} \otimes \mathbf{F}_i) \sum_{i=1}^n \boldsymbol{\Omega}^{i,i} (\tau_{i0} P_i + \sum_{j=1}^n \tau_{ij} M_{i,j}) \otimes \mathbf{W}.
\end{aligned}$$

Defining $n_i = P_i + D_i$ and $\bar{\tau}_i = \tau_{i0} P_i + \sum_{j=1}^n \tau_{ij} M_{i,j}$ we have that

$$\begin{aligned}
\tilde{\mathbf{A}} & = \sum_{i=1}^n \boldsymbol{\Omega}^{i,i} \otimes \mathbf{A}_i - \sum_{i=1}^n (\boldsymbol{\Omega}^{i,i} \otimes \mathbf{F}_i) \sum_{i=1}^n (\boldsymbol{\Omega}^{i,i} \otimes n_i \mathbf{I}_3) \\
& + \sum_{i=1}^n (\boldsymbol{\Omega}^{i,i} \otimes \mathbf{F}_i) \sum_{i=1}^n (\boldsymbol{\Omega}^{i,i} \otimes \bar{\tau}_i \mathbf{W}) \\
& = \sum_{i=1}^n \boldsymbol{\Omega}^{i,i} \otimes \mathbf{A}_i - \sum_{i=1}^n \boldsymbol{\Omega}^{i,i} \otimes n_i \mathbf{F}_i + \sum_{i=1}^n \boldsymbol{\Omega}^{i,i} \otimes \bar{\tau}_i \mathbf{F}_i \mathbf{W} \\
& = \sum_{i=1}^n \boldsymbol{\Omega}^{i,i} \otimes [\mathbf{A}_i + \mathbf{F}_i (\bar{\tau}_i \mathbf{W} - n_i \mathbf{I}_3)],
\end{aligned}$$

which implies that $\tilde{\mathbf{A}}$ is a block diagonal matrix. Therefore,

$$\begin{aligned}
\Delta(\lambda) & = \det \left(\lambda \mathbf{I}_{3n} - \tilde{\mathbf{A}} - \sum_{i=1}^n \sum_{j=1}^n \tilde{\mathbf{A}}_{\tau_{ij}} e^{-\tau_{ij} \lambda} \right) \\
& = \det (\lambda \mathbf{I}_{3n} - \tilde{\mathbf{A}}) \\
& = \prod_{i=1}^n \det (\lambda \mathbf{I}_{3n} - \mathbf{A}_i - \mathbf{F}_i (\bar{\tau}_i \mathbf{W} - n_i \mathbf{I}_3)) \\
& = \prod_{i=1}^n \left(\lambda^3 + \frac{n_i \kappa_3^i + 1}{\zeta_i} \lambda^2 + \frac{n_i \kappa_2^i - \bar{\tau}_i \kappa_1^i}{\zeta_i} \lambda + \frac{n_i \kappa_1^i}{\zeta_i} \right),
\end{aligned}$$

which reveals that the platoon's stability is dictated by the stability of each individual vehicle.

Finally, we apply the Routh-Hurwitz method for finding the limits of stability as a function of the control gains and communication time-delays:

$$\begin{array}{l|l}
\lambda^3 & \begin{array}{l} 1 \\ \frac{n_i \kappa_3^i + 1}{\zeta_i} \\ \frac{(n_i \kappa_3^i + 1)(n_i \kappa_2^i - \bar{\tau}_i \kappa_1^i) - \zeta_i n_i \kappa_1^i}{\zeta_i (n_i \kappa_3^i + 1)} \end{array} \\
\lambda^2 & \begin{array}{l} \frac{n_i \kappa_2^i - \bar{\tau}_i \kappa_1^i}{\zeta_i} \\ \frac{n_i \kappa_1^i}{\zeta_i} \end{array} \\
\lambda^1 & \frac{n_i \kappa_1^i}{\zeta_i} \\
\lambda^0 & \zeta_i
\end{array}$$

which leads to the conditions in Thm. 6.3 concluding the proof. \square

The previous theorem establishes conditions to ensure the formation error asymptotically stability, assumption of Theorem 6.2. A disadvantage of this result is the necessity to know beforehand the parameters of the network topology, i.e., the number of neighbor vehicles and the communication delay values. To overcome this problem, we can analyze the worst-case scenario to obtain a stability certificate according to Eq. (6.3), leading to the following Corollary.

Corollary 6.1. *Consider a vehicular platoon composed of heterogeneous vehicles, with dynamics described in (3.3), governed by the distributed control law (4.14), subject to a maximum communication delay τ_{\max} . Thus, if the following conditions hold*

$$\kappa_1^i > 0, \quad \kappa_2^i > \frac{\zeta_i \kappa_1^i}{\kappa_3^i + 1} + \tau_{\max} \kappa_1^i, \quad \kappa_3^i > 0, \quad (6.4)$$

for all $i = 1, \dots, n$, the platoon is asymptotically stable.

The result in the previous corollary follows directly from Eq. (6.3), setting $n_i = 1$ and bounding the average communication delay term by the maximum communication delay allowed by the network, i.e. $\bar{\tau}_i/n_i \leq \tau_{\max}$. Such conditions, easy to check, reveal that the control law (4.14) of each vehicle depends only on its motor efficiency ζ_i and the upper bound for the communication delay, τ_{\max} , enabling a design procedure that is independent of prior knowledge of the platoon structure.

6.3 Simulation and analysis results for the platoon of vehicles with communication with heterogeneous delay.

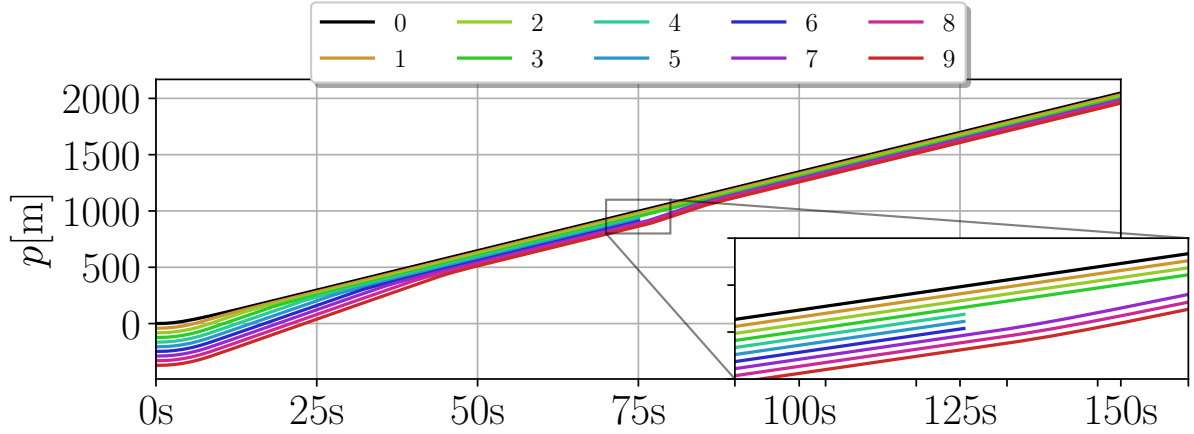
In this chapter, we present the results of our control protocol. Here, we evaluate characteristics such as agent exits, mixed-traffic external disturbances (such as traffic lights and Human-driven Vehicles (HDVs)), and nonlinear simulations. The protocol and the linear model of the agents have been calculated using the *Numpy* library for *Python* language, running at *Ubuntu 20.04*. Meanwhile, for the nonlinear example, the dynamic of the vehicles was emulated using the *CARLA* simulator.

6.3.1 Simulation: disconnection

In this first experiment, we begin by demonstrating that our method provides a platooning formation even under the following circumstances: (i) all vehicles start disconnected, and (ii) three agents leave the team, simultaneously. The simulation considers a team with one leader and 9 followers, with the parameters detailed in Table 6.1, whose values and heterogeneous characteristics have been extracted from (ZHENG *et al.*, 2019). Note that the parameter values in Table 6.1 are defined as a function of the vehicle position in the platoon in order to try to make it easier to identify the effect of different physical parameters on the vehicles. Besides, the parameters indicate that, in steady-state, the platoon travels in a 2PF communication topology.

Table 6.1 – Vehicle parameters extracted from (ZHENG *et al.*, 2019).

Parameter values	
$m_i = 1500 + 100 i$ [kg]	$r_i = 0.25 + 0.005 i$ [m]
$\eta_i = 80 + i$ [%]	$\zeta_i = 0.3 + 0.02 i$
$C_i = 0.4 + 0.01 i$	$\mu_i = 0.015 + 0.001 i$
$\epsilon = 0.1$	$R_i = 35.0 + 0.5 i$ [m]
$\rho = 1.23$ [kg/m ³]	$g = 9.81$ [m/s ²]

**Figure 6.3** – (experiment 1) position of the vehicles over time. All agents start disconnected and, over time, they are capable of stabilizing the platoon. After the exit of three vehicles simultaneously, there is a momentary split, but a new steady state condition is reached.

For all simulations, we defined the maximum allowed road speed of $v_{\max} = 20$ m/s (72 km/h), with the leader accelerating from zero to 70 % of v_{\max} ($\alpha = 0.7$). Moreover, under the conditions in (6.1) and (6.4), the control gains for all follower vehicles were selected using $\beta = 1$ and the formula $\mathbf{K}_i = (\zeta_i / \zeta_0) \begin{bmatrix} 1.0 & 4.0 & 2.0 \end{bmatrix}$. The delays were set to $\tau_{ij} = 0.2 + 0.02 i$ [s], which are typical values for VANETs (ABDELGADIR; SAEED; BABIKER, 2016a), while the spacing distances were set to $d_{ij} = 15$ m for all agents. For simulation proposes the parameter R_i denotes the communication range of the i -th vehicle. Finally, we set $u_i(t) = 0$ whenever $v_i(t) \geq v_{\max}$ to avoid the vehicle's transient speed reaching values much higher than the road speed limit.

Fig. 6.3 presents the position of all vehicles over time. At $t = 0$, the followers are completely disconnected, but, as they accelerate, they are capable of recovering connection and the platoon is kept stable, as illustrated by the spacing error in Fig. 6.4. When agents 4, 5, and 6 simultaneously leave the platoon at 75 s, agent 7 switches to the *Virtual Reference* state (Fig. 6.5) and begins to accelerate. Agents 8 and 9 do not lose connection with agent 7, however, the perturbation forces agent 8 to activate the *Transitory Condition*. Eventually, these three vehicles travel fast until recover communication with other teammates, that have not been affected by the disturbance. Fig. 6.6 presents the speed of the vehicles. there it is possible to see that, at the start, the agents accelerate to v_{\max} in the *Transitory Condition*

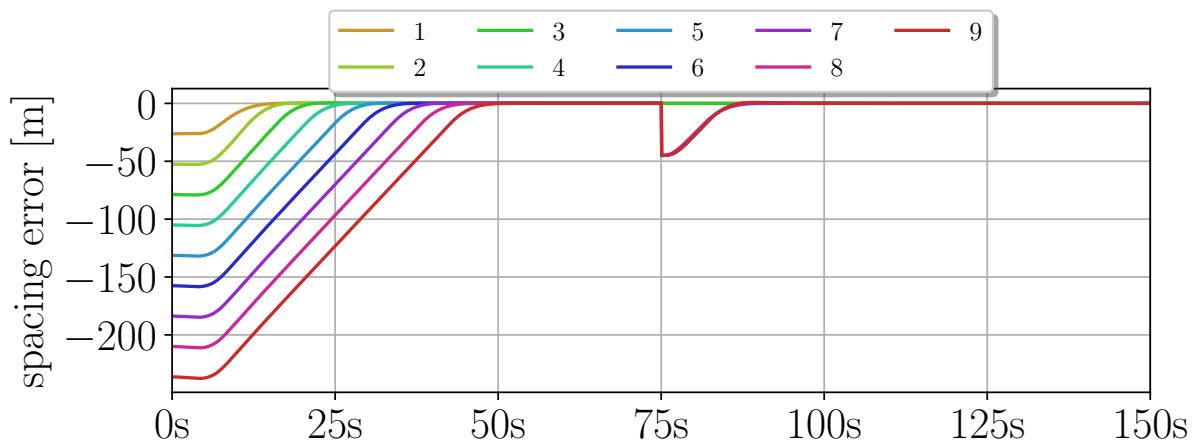


Figure 6.4 – (experiment 1) spacing error of the vehicles over time according to the leader. All followers start disconnected, but they can reach their forwarding neighbors. The platoon presented a null error when three vehicles exited, but the disturbance is quickly compensated.

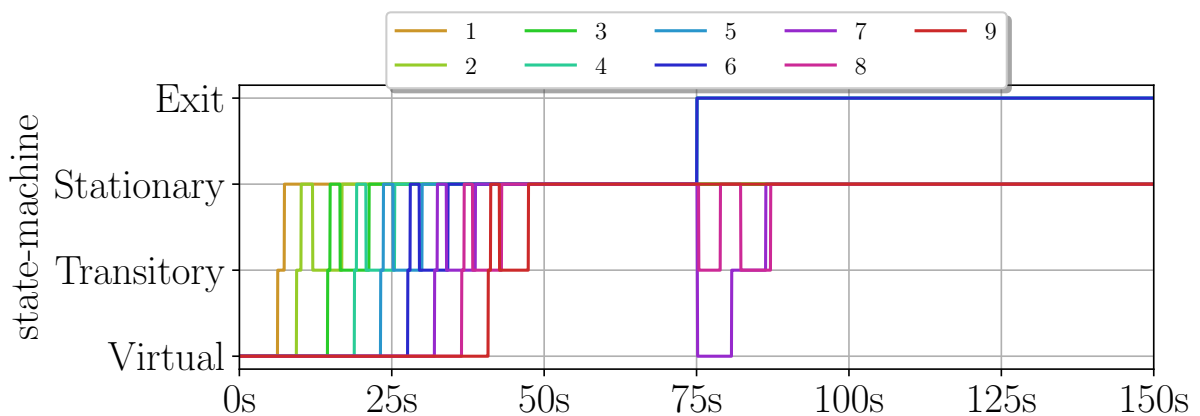


Figure 6.5 – (experiment 1) state behavior of the vehicles over time. After the stabilization, all followers reach the stationary condition, until the disturbance, when vehicle 7 assumes the *Virtual Reference* state and accelerates to reach again the *Stationary Condition* state.

state. Then, with data provided by forwarding neighbors, they track the leader speed with a null error.

6.3.2 Simulation: traffic light

In this second experiment, we evaluate the influence of external events on the formation. This time, the 9 followers start connected (with a null spacing error), but after 40 s, we simulate a traffic light that splits the platoon during 20 s. Figures 6.7 and 6.8 show the position and the spacing error of the agents over time. Here, it is possible to see that two teams were temporarily created after the disconnection, but they merged later.

Fig. 6.10 represents the speed profile of the vehicles, where it is possible to see that some vehicles decelerate and stop at the traffic light, some of them running at v_{\max} . About

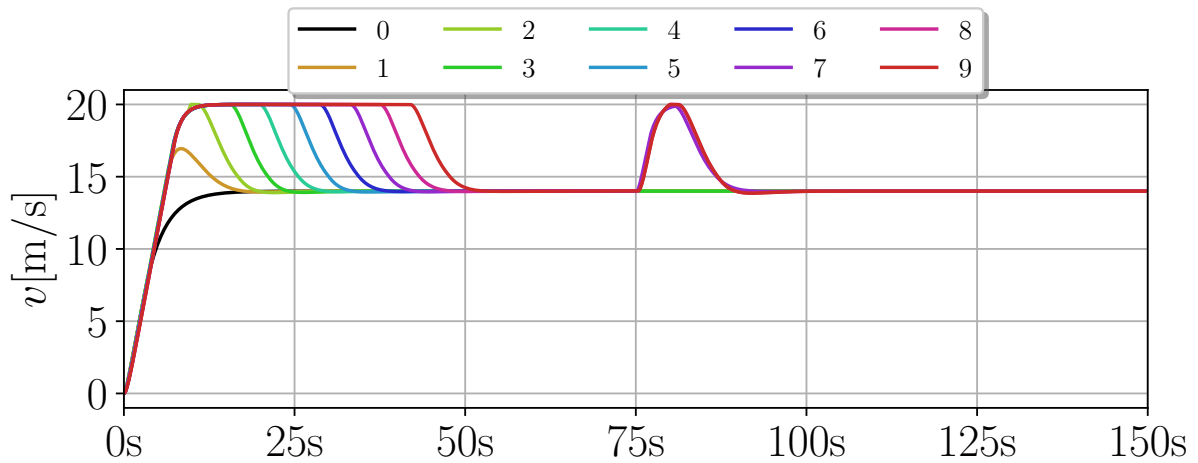


Figure 6.6 – (experiment 1) speed of the vehicles over time. Even with the disturbances caused by the disconnection, the followers were able to track the leader's speed.

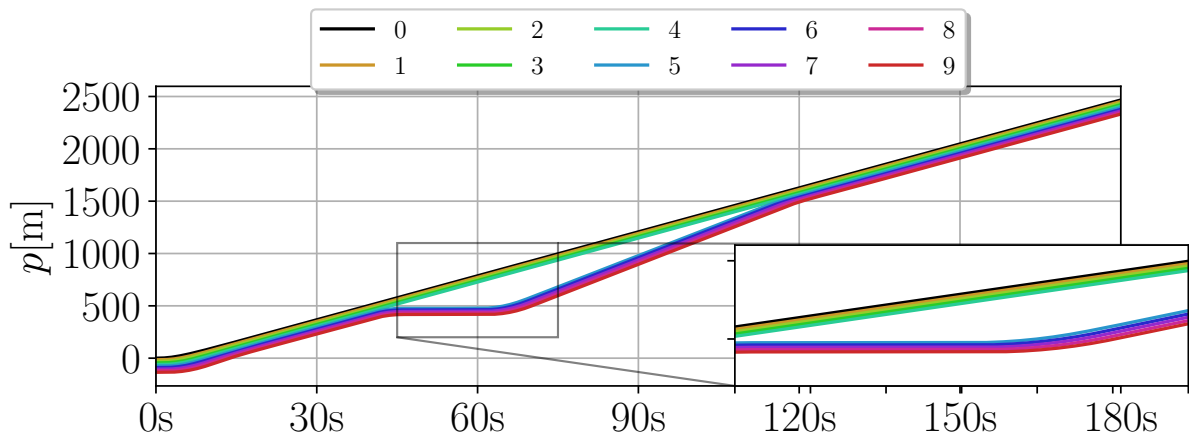


Figure 6.7 – (experiment 2) position of the vehicles over time. The agents start connected and the platoon moves on until 40 s when a traffic light splits it. Then, the leader and the first 4 followers travel freely, while the rest are held at the red light during 20 s. Even so, after the green light, the platooning formation is reestablished.

20 s after being held in the red light, vehicle 5 operates in the *Virtual Reference* mode, while the others follow it in the *Transitory Condition* state, as presented in Fig. 6.9. It is important to notice that, under the step reference of the virtual agent, the overshoots of all vehicles are independent of their position in the platoon. On the other hand, when the reference is a forwarding neighbor, as happens with the step reference after the traffic light, the overshoot influence is propagated backward. So, it is fundamental to adjust the control gains properly to avoid collision effects or to propose a more smooth profile for the acceleration of the virtual leader.

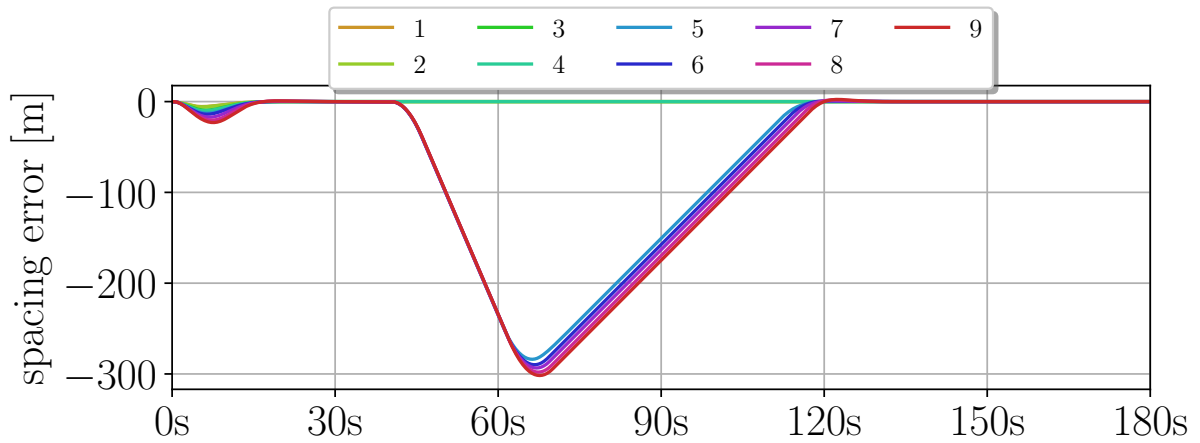


Figure 6.8 – (experiment 2) spacing error of the vehicles over time according to the leader. After some members are stuck at the traffic light, they manage to reach the vehicles ahead.

6.3.3 Nonlinear simulation: human-driven vehicle

In this last experiment, we have implemented our strategy with a heterogeneous team composed of the leader and 9 followers, but this time in the *CARLA* simulator¹ (DOSOVITSKIY *et al.*, 2017), an open-source tool for autonomous driving research that provides a client/server interface allowing for external communication with many languages, including Python. Here, also, we set the fourth follower in the team to behave like an HDV, whose time-varying speed is given by

$$v_4(t) = (0.8 + 0.1 \sin 0.5t) \alpha v_{\max},$$

for $t \geq 20s$, the instant in which the platoon is interrupted. Also, to make the simulation more realistic, we have used typical values for the time-varying communication delay, i.e a uniform random distribution $\tau_{ij}(t) \in [0.1s, 0.3s]$ [s] (ABDELGADIR; SAEED; BABIKER, 2016b).

The setup is illustrated as follows, Fig. 6.11 shows the start when all vehicles are connected to their neighbors, and the HDV is in the parallel lane. After 20 s, the external vehicle performs a lane change maneuver, and one can observe that its subsequent lower velocity, below the leader's speed, forces a split in the platoon. Then, after 50 s, the non-cooperative agent leaves the road, as illustrated in Fig. 6.12, the moment in which the fifth follower is allowed to accelerate until it reaches the team in Fig. 6.13. Once again, by applying our heuristics, we can recover the communication and reach a stable condition, even in mixed traffic scenarios. Figures 6.14, 6.15, and 6.17 show in detail the position, spacing error, and speed of the vehicles over time. Particularly with the speed profile, it is possible to see the effects of the time-varying delay (small fluctuations) and the oscillatory behavior of the HDV, but our controller is shown to be string stable and ensures asymptotic stability of the closed-loop formation dynamics under such conditions.

¹ <<https://carla.org/>>

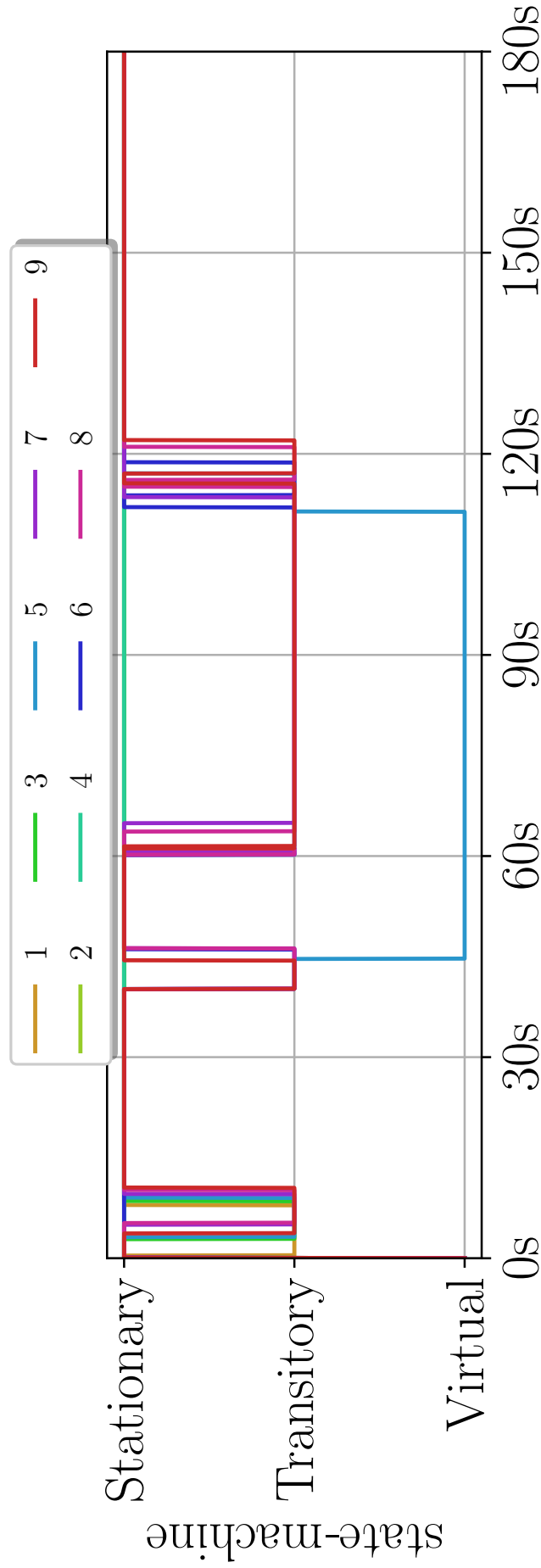


Figure 6.9 – (Experiment 2) Vehicle state evolution over time. After stabilization, all followers reach the *Stationary* state until the traffic light event, when vehicle 5 assumes the *Virtual Reference* state. At the green light, this vehicle accelerates and returns to the *Stationary* state.

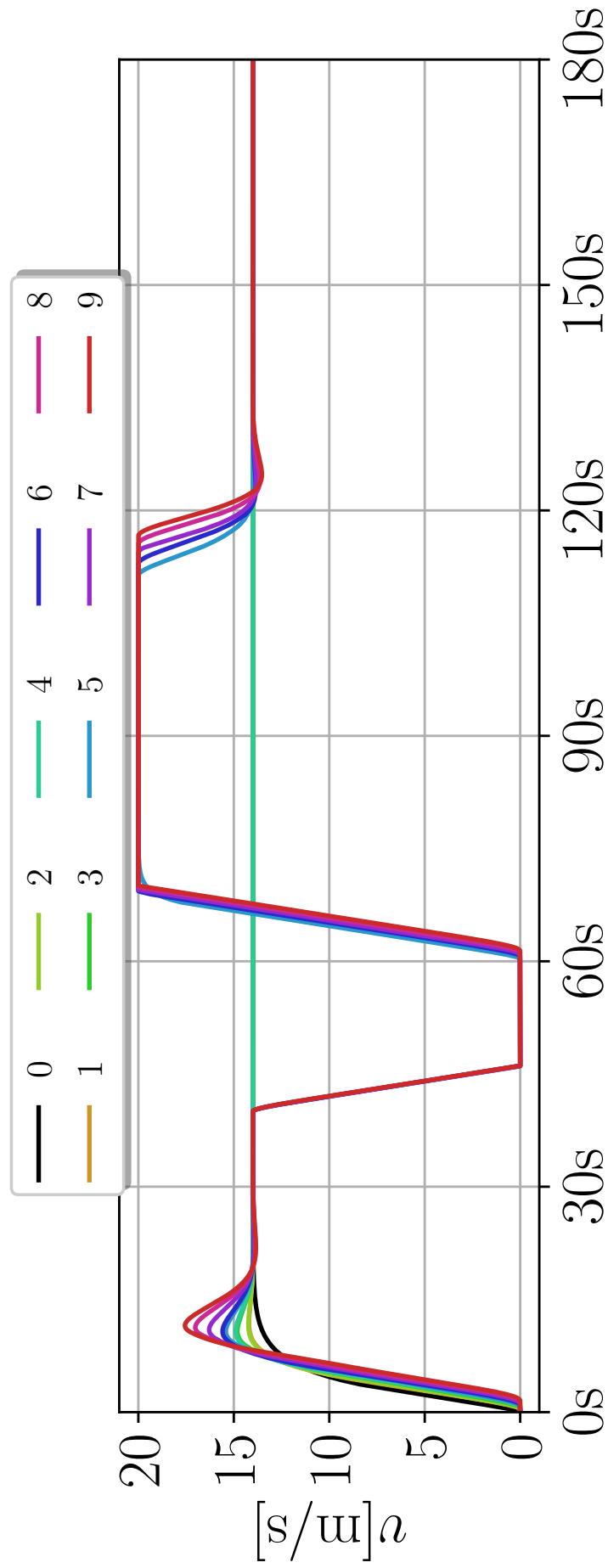


Figure 6.10 – (Experiment 2) Vehicle speeds over time. After leaving the traffic light, the follower vehicles successfully track the leader speed.

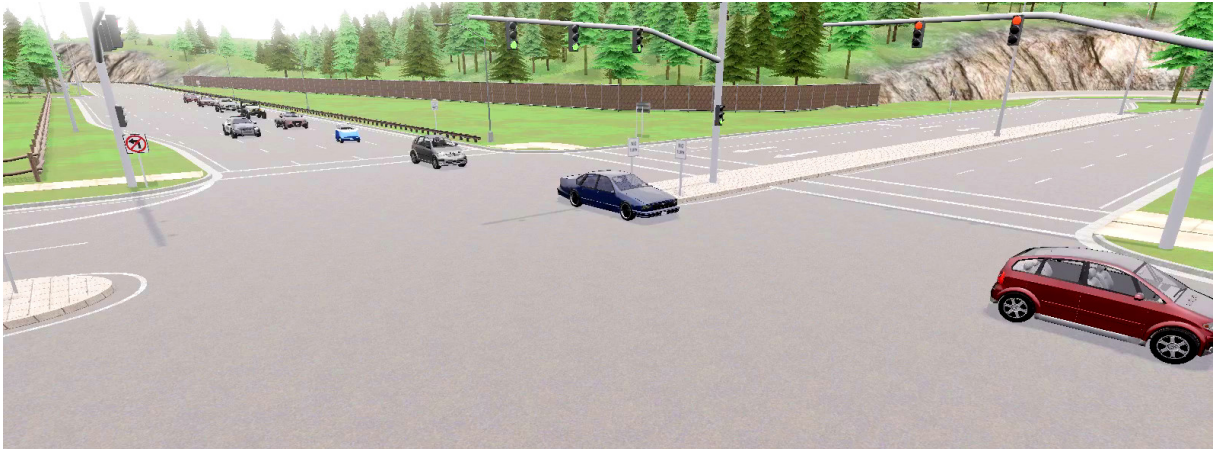


Figure 6.11 – experiment 3) platoon composed of the leader and 9 followers implemented in the *CARLA* simulator: (a) the robots start connected, but the fourth follower (an HDV) delays its predecessors with a low speed;



Figure 6.12 – experiment 3) platoon composed of the leader and 9 followers implemented in the *CARLA* simulator: (b) the HDV leaves the road

These results demonstrate that platoon recovery can be achieved without explicit split/merge maneuvers, relying solely on local measurements and communication. This chapter concludes the proposed reorganization framework by addressing scenarios in which vehicles must autonomously recover connectivity after complete communication loss. These results show that the proposed distributed controller, combined with the recovery protocol, enables autonomous reintegration of vehicles after complete communication loss, without requiring global information or controller redesign.



Figure 6.13 – experiment 3) platoon composed of the leader and 9 followers implemented in the *CARLA* simulator: (c) the last agents recover connection and reaches null spacing error.

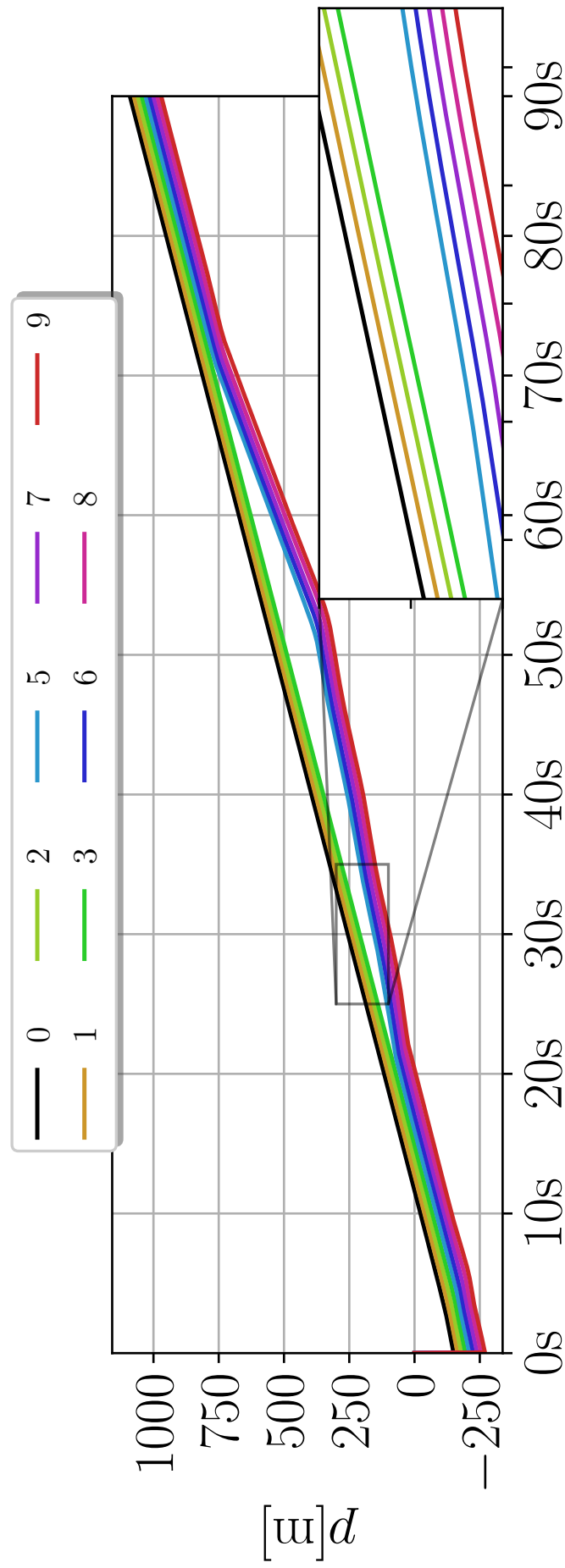


Figure 6.14 – (Experiment 3) Vehicle positions in the CARLA simulator. All agents start connected. After $t = 20s$, the HDV splits the platoon, leaving the road at $t = 50s$ and allowing the predecessor vehicles to recover communication after approximately $t = 70s$.

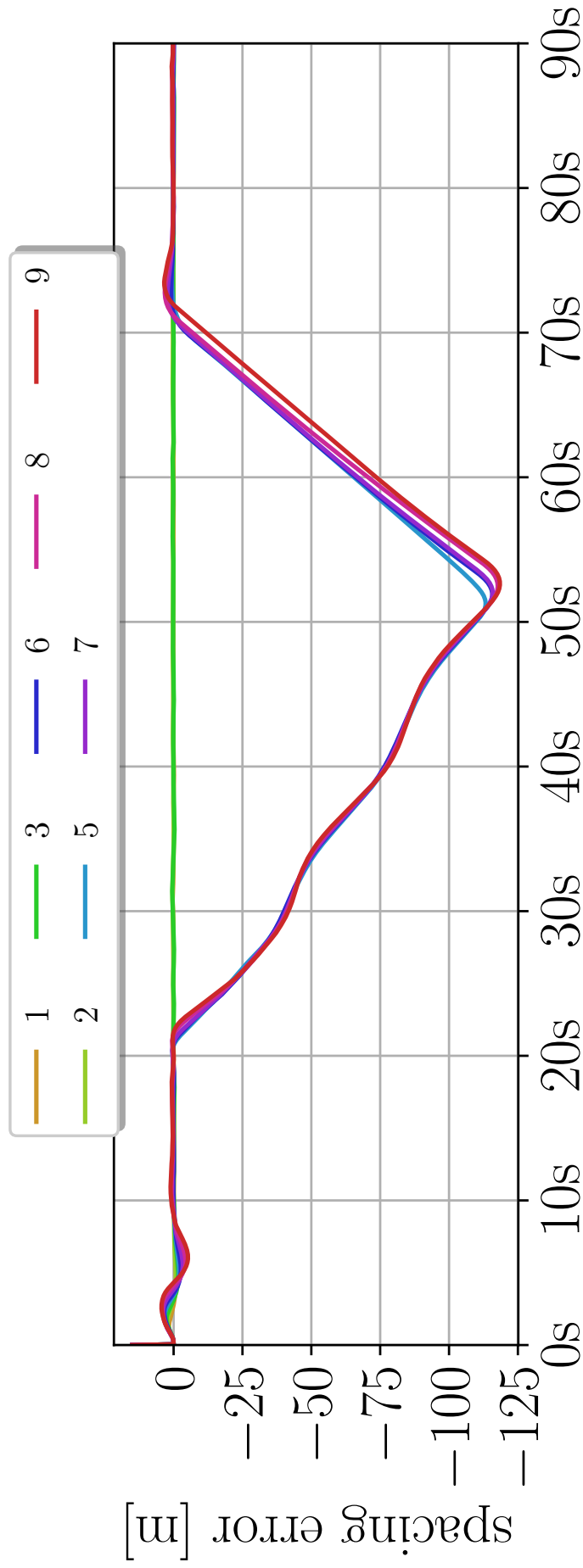


Figure 6.15 – (Experiment 3) Spacing error of the vehicles with respect to the leader in the CARLA simulator. After the initial stationary condition of the platoon, the HDV enters and leaves the road; however, the resulting disturbance is completely rejected by the proposed protocol.

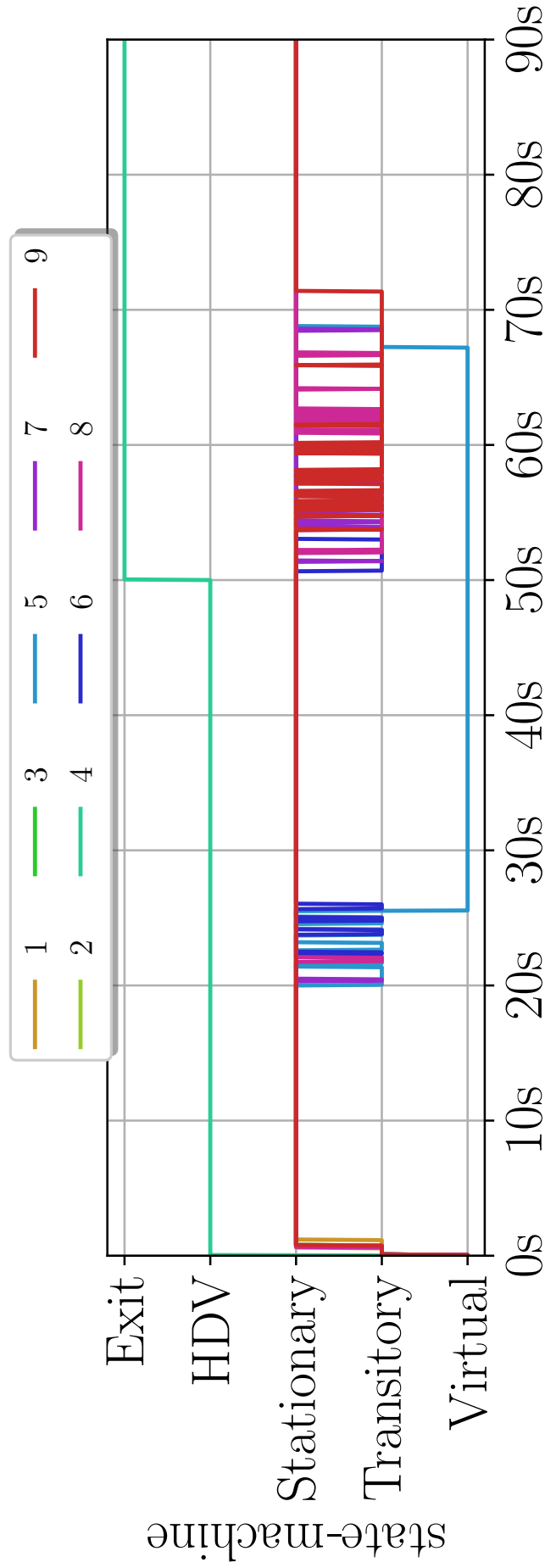


Figure 6.16 – (Experiment 3) Vehicle states in the CARLA simulator. All agents remain in the *Stationary* state until the interference of the HDV, whose lower speed forces the disconnection of follower 5. This vehicle remains in the *Virtual* state until it rejoins the platoon, after the exit of the disturbing agent at $t = 50s$.

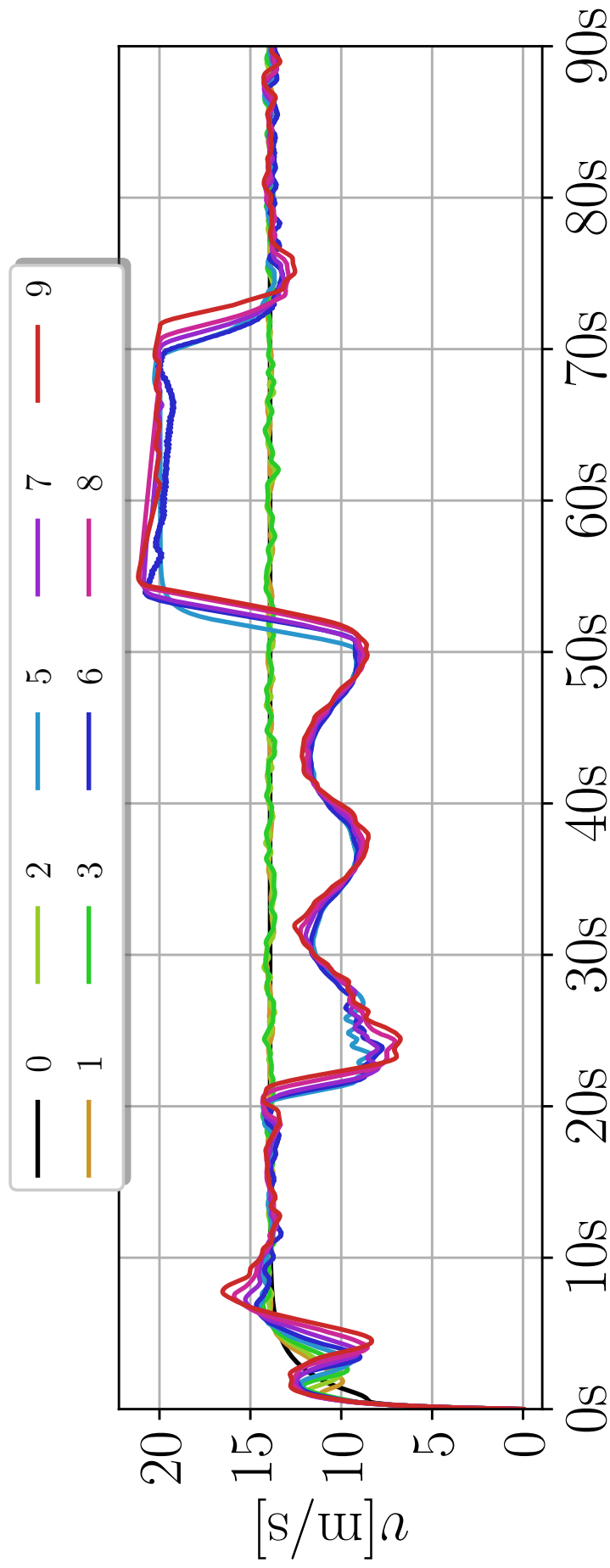


Figure 6.17 – (Experiment 3) Vehicle speeds in the CARLA simulator. All follower vehicles track the leader speed before and after the exit of the HDV.

7 CONCLUSIONS AND FUTURE DIRECTIONS

7.1 Conclusions

This thesis investigated the problem of distributed control and reorganization of heterogeneous autonomous vehicles organized in platoons under realistic communication constraints. The main objective was to develop decentralized control strategies capable of supporting stable platoon formation, reorganization, and recovery behaviors based on local information exchange among vehicles.

First, a distributed control framework was developed for the formation of heterogeneous vehicle platoons. The proposed approach relies on local measurements and information received from neighboring vehicles, adopting a predecessor–follower communication topology. The results show that, under this framework, stable platoon formation can be achieved even in the presence of heterogeneous vehicle dynamics. This indicates that global information or centralized coordination is not required to achieve convergence of the inter-vehicle spacing error, provided that appropriate local control laws are employed.

Second, reorganization protocols were designed to address structural changes in the platoon resulting from vehicle entry and exit events. These protocols enable autonomous reconfiguration of the communication topology while preserving closed-loop stability. The results indicate that, following such events, the platoon is able to restore the desired inter-vehicle spacing and reach a new steady-state configuration without external intervention. This reorganization process is performed in a distributed manner and does not depend on prior knowledge of the platoon size, highlighting the scalability of the proposed approach.

Third, recovery strategies were proposed to address scenarios in which a vehicle becomes temporarily disconnected from the platoon due to communication constraints, including limited communication range and time delays. In these situations, a recovery protocol modifies the control law of the disconnected vehicle, allowing it to reestablish communication and reintegrate into the platoon. The analysis and simulation results demonstrate that the proposed strategy enables the restoration of the desired formation after communication loss, characterizing a self-recovery capability emerging from the decentralized control structure.

The control design and stability analysis were conducted within the framework of linear time-invariant (LTI) systems. Classical control theory tools, including pole placement and the Routh–Hurwitz stability criterion, were employed to establish conditions for asymptotic stability of the closed-loop system. The analysis considered communication scenarios without delay, with fixed delays, and with heterogeneous delays, providing admissible bounds on control gains and delay values that preserve stability.

Overall, the results presented in this thesis indicate that decentralized control strategies based on locally available information are sufficient to support the formation, reorganization, and recovery of heterogeneous vehicle platoons under realistic communication constraints. These findings contribute to the understanding of cooperative vehicular systems and provide a foundation for the development of resilient platooning strategies applicable to real-world traffic scenarios.

7.2 Future research directions

Future research directions include the extension of the proposed distributed control framework to more general communication topologies, relaxing the predecessor–follower assumption adopted in this thesis. In addition, the incorporation of lateral vehicle dynamics represents a natural progression of the present work, allowing the analysis of more complex maneuvers such as lane changes and merges under cooperative control strategies.

Another important direction concerns the experimental validation of the proposed methodologies using real vehicles. Such validation would allow the assessment of the proposed control and reorganization protocols under practical uncertainties, sensor noise, and communication imperfections not fully captured in simulation environments.

Future research directions also include the extension of the proposed framework to cooperative systems composed of vehicles with increasingly diverse dynamic characteristics, including multimodal platforms operating in land, aerial, and aquatic environments. In this context, heterogeneous platoons may be envisioned not only as formations of vehicles sharing the same physical domain, but also as cooperative transportation systems in which cargo or passengers transition between different vehicles when changing routes or environments. For underwater vehicle modeling and control, the approach presented in (SHOJAEI; CHATRAEI, 2021) provides a relevant reference for extending the proposed strategies to such scenarios.

Furthermore, the investigation of coupled longitudinal and lateral vehicle dynamics constitutes an important direction for future work, enabling a more comprehensive representation of vehicle motion under cooperative control. Related approaches can be found in (GUO *et al.*, 2020), where adaptive control strategies are developed for connected autonomous distributed electric vehicles.

Finally, the integration of collision avoidance mechanisms based on Lyapunov stability theory represents a promising extension aimed at enhancing safety guarantees in cooperative vehicular systems. In this context, the methodology presented in (WANG *et al.*, 2019) offers a suitable reference for incorporating formal safety constraints into the distributed control framework.

Overall, these extensions aim to broaden the applicability of the proposed distributed control and reorganization strategies while preserving their fundamental properties of scalability,

resilience, and reliance on local information.

7.3 Publications

The studies that generated this thesis contributed to two publications in scientific journals. The first paper was published in the International Journal of Control, Automation and Systems (IJCAS) we present a resilient control strategy that ensures the reorganization of a platoon after vehicle entries and/or exits. In IEEE Transactions on Intelligent Transportation Systems, we have the results of the vehicle reconnection strategy to the platoon out of communication range and with heterogeneous communication delay. These are the papers:

Godinho, Daniel Almeida, Armando Alves Neto, Leonardo Amaral Mozelli, and Fernando de Oliveira Souza. "Control and Reorganization of Heterogeneous Vehicle Platoons after Vehicle Exits and Entrances." *International Journal of Control, Automation and Systems* 20, no. 8 (2022): 2437-2446.

<https://doi.org/10.1007/s12555-021-0106-0> (GODINHO *et al.*, 2022)

D. A. Godinho, A. Alves Neto, L. A. Mozelli and F. de Oliveira Souza, "A Strategy for Traffic Safety of Vehicular Platoons Under Connection Loss and Time-Delay," in *IEEE Transactions on Intelligent Transportation Systems*, vol. 24, no. 6, pp. 6627-6638, June 2023, doi: 10.1109/TITS.2023.3258633. (GODINHO *et al.*, 2023)

BIBLIOGRAPHY

- ABDELGADIR, M.; SAEED, R.; BABIKER, A. Vehicular ad-hoc networks (vanets) dynamic performance estimation routing model for city scenarios. In: **Int. Conf. Inform. Sci. Commun. Technol. (ICISCT)**. [S.l.: s.n.], 2016. p. 1–8. Page [68](#).
- ABDELGADIR, M.; SAEED, R.; BABIKER, A. Vehicular ad-hoc networks (vanets) dynamic performance estimation routing model for city scenarios. In: **Int. Conf. Inform. Sci. Commun. Technol. (ICISCT)**. [S.l.: s.n.], 2016. p. 1–8. Page [71](#).
- Abunei, A.; Comşa, C. R.; Caruntu, C. F.; Bogdan, I. Redundancy based v2v communication platform for vehicle platooning. In: **Int. Symp. on Signals, Circuits and Systems, ISSCS**. [S.l.: s.n.], 2019. p. 1–4. Page [26](#).
- ALEXIS, Kostas. **Towards a Science of Resilient Robotic Autonomy**. 2020. Pages [25](#) and [27](#).
- AMOOZADEH, Mani; DENG, Hui; CHUAH, Chen-Nee; ZHANG, H Michael; GHOSAL, Dipak. Platoon management with cooperative adaptive cruise control enabled by vanet. **Vehicular Communications**, Elsevier, v. 2, n. 2, p. 110–123, 2015. Page [30](#).
- Antonelli, G.; Chiaverini, S. Kinematic control of platoons of autonomous vehicles. **IEEE Trans. on Robotics**, v. 22, n. 6, p. 1285–1292, 2006. Page [26](#).
- BADNAVA, Sareh; MESKIN, Nader; GASTLI, Adel; AL-HITMI, Mohammed A.; GHOMMAM, Jawhar; MESBAH, Mostefa; MNIF, Faiçal. Platoon transitional maneuver control system: A review. **IEEE Access**, v. 9, p. 88327–88347, 2021. Page [30](#).
- BIAN, Yougang; ZHENG, Yang; LI, Shengbo; XU, Qing; WANG, Jianqiang; LI, Keqiang. Behavioral cooperation of multiple connected vehicles with directed acyclic interactions using feedforward-feedback control. In: **Int. Symp. on Advanced Vehicle Control, AVEC**. [S.l.: s.n.], 2019. Pages [28](#) and [32](#).
- BIRON, Zoliekha Abdollahi; DEY, Satadru; PISU, Pierluigi. Resilient control strategy under denial of service in connected vehicles. In: **IEEE. 2017 American Control Conference (ACC)**. [S.l.], 2017. p. 4971–4976. Page [26](#).
- BULLO, Francesco; CORTÉS, Jorge; MARTÍNEZ, Sonia. **Distributed Control of Robotic Networks**. Princeton: Princeton University Press, 2009. Page [18](#).
- BULLO, F.; CORTÉS, J.; MARTÍNEZ, S. **Distributed Control of Robotic Networks**. Princeton: Princeton University Press, 2009. Pages [28](#) and [51](#).
- CHEHARDOLI, Hossein; HOMAINEZHAD, MR. Stable control of a heterogeneous platoon of vehicles with switched interaction topology, time-varying communication delay and lag of actuator. **Institution of Mechanical Engineers, Part C: Journal of Mechanical Engineering Science**, v. 231, n. 22, p. 4197–4208, 2017. Pages [27](#) and [28](#).
- Dey, K. C.; Yan, L.; Wang, X.; Wang, Y.; Shen, H.; Chowdhury, M.; Yu, L.; Qiu, C.; Soundararaj, V. A review of communication, driver characteristics, and controls aspects of cooperative adaptive cruise control (CACC). **IEEE Trans. on Intelligent Transportation Systems**, v. 17, n. 2, p. 491–509, Feb 2016. ISSN 1558-0016. Page [25](#).

DOSOVITSKIY, Alexey; ROS, German; CODEVILLA, Felipe; LOPEZ, Antonio; KOLTUN, Vladlen. CARLA: An open urban driving simulator. In: **Proc. of the 1st Annual Conf. on Robot Learning**. [S.l.: s.n.], 2017. p. 1–16. Page 71.

ELAHI, Arezou; ALFI, Alireza; MODARES, Hamidreza. H_∞ consensus of homogeneous vehicular platooning systems with packet dropout and communication delay. **IEEE Trans. on Systems, Man, and Cybernetics: Systems**, v. 52, n. 6, p. 3680–3691, 2022. Pages 27 and 30.

FENG, Shuo; ZHANG, Yi; LI, Shengbo Eben; CAO, Zhong; LIU, Henry X.; LI, Li. String stability for vehicular platoon control: Definitions and analysis methods. **Annual Reviews in Control**, v. 47, p. 81–97, 2019. ISSN 1367-5788. Page 19.

GAO, Feng; DANG, Dongfang; LI, Shengbo Eben. Control of a heterogeneous vehicular platoon with uniform communication delay. In: IEEE. **2015 IEEE International Conference on Information and Automation**. [S.l.], 2015. p. 2419–2424. Page 18.

GHAEDSHARAF, Yaser; SOMARAKIS, Christoforos; MOTEE, Nader. Performance of second-order platoon of vehicles in presence of time-delay and noise. In: IEEE. **2018 Annual American Control Conference (ACC)**. [S.l.], 2018. p. 4887–4892. Page 27.

GODINHO, Daniel Almeida; NETO, Armando Alves; MOZELLI, Leonardo Amaral; SOUZA, Fernando de Oliveira. Control and reorganization of heterogeneous vehicle platoons after vehicle exits and entrances. **International Journal of Control, Automation and Systems**, Springer, v. 20, n. 8, p. 2437–2446, 2022. Page 82.

GODINHO, Daniel Almeida; NETO, Armando Alves; MOZELLI, Leonardo Amaral; SOUZA, Fernando de Oliveira. A strategy for traffic safety of vehicular platoons under connection loss and time-delay. **IEEE Transactions on Intelligent Transportation Systems**, v. 24, n. 6, p. 6627–6638, 2023. Page 82.

GOLI, Mohammad; ESKANDARIAN, Azim. Merging strategies, trajectory planning and controls for platoon of connected, and autonomous vehicles. **Int. Journal of Intelligent Transportation Systems Research**, Springer, v. 18, n. 1, p. 153–173, 2020. Page 30.

GRAVINA, Antoniel Peixoto Guelber. **Estudo do efeito do atraso de comunicação em comboio de veículos autônomos**. Tese (Doutorado) — Universidade Federal de Minas Gerais, 2017. Page 27.

GUNGOR, Osman Erman; SHE, Ruifeng; AL-QADI, Imad L; OUYANG, Yanfeng. One for all: Decentralized optimization of lateral position of autonomous trucks in a platoon to improve roadway infrastructure sustainability. **Transportation Research Part C: Emerging Technologies**, Elsevier, v. 120, p. 102783, 2020. Page 18.

GUO, Ge; YUE, Wei. Autonomous platoon control allowing range-limited sensors. **IEEE Trans. on Vehicular Technology**, IEEE, v. 61, n. 7, p. 2901–2912, 2012. Page 27.

GUO, Jinghua; JINGYAO, Wang; LI, Keqiang; LUO, Yugong. Adaptive non-linear coordinated optimal dynamic platoon control of connected autonomous distributed electric vehicles on curved roads. **IET Intelligent Transport Systems**, IET, v. 14, n. 12, p. 1626–1637, 2020. Page 81.

Hu, J.; Bhowmick, P.; Arvin, F.; Lanzon, A.; Lennox, B. Cooperative control of heterogeneous connected vehicle platoons: An adaptive leader-following approach. **IEEE Robotics and Automation Letters**, v. 5, n. 2, p. 977–984, 2020. Page 18.

Huang, J.; Tseng, Y. The steady-state distribution of rehealing delay in an intermittently connected highway vanet. **International Journal of Control, Automation and Systems**, v. 67, n. 10, p. 10010–10021, 2018. Page 27.

JIN, I Ge; OROSZ, Gábor. Optimal control of connected vehicle systems with communication delay and driver reaction time. **IEEE Transactions on Intelligent Transportation Systems**, IEEE, v. 18, n. 8, p. 2056–2070, 2016. Page 18.

LeBlanc, H. J.; Zhang, H.; Koutsoukos, X.; Sundaram, S. Resilient asymptotic consensus in robust networks. **IEEE Journal on Selected Areas in Communications**, v. 31, n. 4, p. 766–781, 2013. Page 26.

LI, Shengbo Eben; ZHENG, Yang; LI, Keqiang; WANG, Jianqiang. An overview of vehicular platoon control under the four-component framework. In: IEEE. **2015 IEEE Intelligent Vehicles Symposium (IV)**. [S.l.], 2015. p. 286–291. Page 18.

Li, Y.; Tang, C.; Peeta, S.; Wang, Y. Nonlinear consensus-based connected vehicle platoon control incorporating car-following interactions and heterogeneous time delays. **IEEE Trans. on Intelligent Transportation Systems**, v. 20, n. 6, p. 2209–2219, 2019. Page 27.

LIANG, Kuo-Yun; DENG, Qichen; MÅRTENSSON, Jonas; MA, Xiaoliang; JOHANSSON, Karl H. The influence of traffic on heavy-duty vehicle platoon formation. In: IEEE. **2015 IEEE Intelligent Vehicles Symposium (IV)**. [S.l.], 2015. p. 150–155. Page 63.

LIU, Bao; GAO, Feng; CHEN, Tao; YANG, Cai. Decoupled control of vehicular platoon with heterogeneous communication delay. In: **SAE Technical Paper**. [S.l.]: SAE Int., 2018. Page 27.

LIU, Bing; KAMEL, Abdelkader El. V2x-based decentralized cooperative adaptive cruise control in the vicinity of intersections. **IEEE Transactions on Intelligent Transportation Systems**, v. 17, n. 3, p. 644–658, 2016. Page 18.

Maiti, S.; Winter, S.; Kulik, L.; Sarkar, S. The impact of flexible platoon formation operations. **IEEE Trans. on Intelligent Vehicles**, v. 5, n. 2, p. 229–239, 2020. Page 30.

Merco, R.; Ferrante, F.; Pisu, P. Dos-resilient hybrid controller for string-stable connected vehicles. In: **2019 IEEE Intelligent Vehicles Symp. (IV)**. [S.l.: s.n.], 2019. p. 1639–1644. Page 26.

MESBAHI, M.; EGERSTEDT, M. **Graph Theoretic Methods in Multiagent Networks**. Princeton: Princeton University Press, 2010. Pages 18, 28, 51, and 52.

MIDDLETON, Richard H; BRASLAVSKY, Julio H. String instability in classes of linear time invariant formation control with limited communication range. **IEEE Trans. on Automatic Control**, IEEE, v. 55, n. 7, p. 1519–1530, 2010. Page 27.

NETO, Armando Alves; MOZELLI, Leonardo A.; SOUZA, Fernando O. Control of air-ground convoy subject to communication time delay. **Computers & Electrical Engineering**, v. 76, p. 213 – 224, 2019. ISSN 0045-7906. Pages 27, 38, 39, and 42.

NOEI, Shirin; SARGOLZAEI, Arman; ABBASPOUR, Alireza; YEN, Kang. A decision support system for improving resiliency of cooperative adaptive cruise control systems. **Procedia Computer Science**, v. 95, p. 489 – 496, 2016. ISSN 1877-0509. Complex Adaptive Systems Los Angeles, CA November 2-4, 2016. Page 26.

OLFATI-SABER, R.; FAX, J. A.; MURRAY, R. M. Consensus and cooperation in networked multi-agent systems. **Proceedings of the IEEE**, v. 95, n. 1, p. 215–233, 2007. Page 29.

PARANJOTHI, Anirudh; ATIQUZZAMAN, Mohammed; KHAN, Mohammad S. Pmcd: Platoon - merging approach for cooperative driving. **Internet Technology Letters**, v. 3, n. 1, p. e139, 2020. Page 30.

PARK, Hyongju; HUTCHINSON, Seth A. Fault-tolerant rendezvous of multirobot systems. **IEEE Trans. on Robotics**, IEEE, v. 33, n. 3, p. 565–582, 2017. Page 26.

Parkinson, S.; Ward, P.; Wilson, K.; Miller, J. Cyber threats facing autonomous and connected vehicles: Future challenges. **IEEE Trans. on Intelligent Transportation Systems**, v. 18, n. 11, p. 2898–2915, Nov 2017. ISSN 1558-0016. Page 26.

Patounas, G.; Zhang, Y.; Gjessing, S. Evaluating defence schemes against jamming in vehicle platoon networks. In: **IEEE Int. Conf. on Intelligent Transportation Systems**. [S.l.: s.n.], 2015. p. 2153–2158. Page 26.

PI, Dawei; XUE, Pengyu; WANG, Weihua; XIE, Boyuan; WANG, Hongliang; WANG, Xianhui; YIN, Guodong. Automotive platoon energy-saving: A review. **Renewable and Sustainable Energy Reviews**, Elsevier, v. 179, p. 113268, 2023. Page 18.

PIRANI, Mohammad; HASHEMI, Ehsan; FIDAN, Baris; SIMPSON-PORCO, John W; SANDBERG, Henrik; JOHANSSON, Karl Henrik. Resilient estimation and control on k-nearest neighbor platoons: A network-theoretic approach. **IFAC-PapersOnLine**, Elsevier, v. 51, n. 23, p. 22–27, 2018. Pages 9, 26, 58, 59, and 60.

PLOEG, J.; SHUKLA, D. P.; WOUW, N. van de; NIJMEIJER, H. Controller synthesis for string stability of vehicle platoons. **IEEE Transactions on Intelligent Transportation Systems**, v. 15, n. 2, p. 854–865, 2014. Page 29.

RAJAMANI, Rajesh. **Vehicle dynamics and control**. [S.l.]: Springer Science & Business Media, 2011. Page 31.

RAJAMANI, Rajesh; RAJAMANI, Rajesh. Longitudinal vehicle dynamics. **Vehicle dynamics and control**, Springer, p. 87–111, 2012. Page 31.

REN, W.; BEARD, R. W. **Distributed Consensus in Multi-Vehicle Cooperative Control**. London: Springer, 2008. Page 29.

SANTINI, Stefania; SALVI, Alessandro; VALENTE, Antonio Saverio; PESCAPÈ, Antonio; SEGATA, Michele; CIGNO, Renato Lo. Platooning maneuvers in vehicular networks: A distributed and consensus-based approach. **IEEE Trans. on Intelligent Vehicles**, v. 4, n. 1, p. 59–72, 2019. Page 28.

SAULNIER, Kelsey; SALDANA, David; PROROK, Amanda; PAPPAS, George J; KUMAR, Vijay. Resilient flocking for mobile robot teams. **IEEE Robotics and Automation Letters**, IEEE, v. 2, n. 2, p. 1039–1046, 2017. Pages 26 and 28.

SAVINO, Heitor Judiss. New methods for consensus in multiagent systems. Universidade Federal de Minas Gerais, 2016. Page 27.

SEN, Indranil; MATOLAK, David W. Vehicle–vehicle channel models for the 5-ghz band. **IEEE Transactions on Intelligent Transportation Systems**, v. 9, n. 2, p. 235–245, 2008. Page [27](#).

SHOJAEI, Khoshnam; CHATRAEI, Abbas. Robust platoon control of underactuated autonomous underwater vehicles subjected to nonlinearities, uncertainties and range and angle constraints. **Applied Ocean Research**, Elsevier, v. 110, p. 102594, 2021. Page [81](#).

Souza, F. O.; Torres, L. A. B.; Mozelli, L. A.; Neto, A. A. Stability and formation error of homogeneous vehicular platoons with communication time delays. **IEEE Trans. on Intelligent Transportation Systems**, p. 1–12, 2019. Pages [27](#), [31](#), [32](#), [39](#), and [41](#).

SWAROOP, D.; HEDRICK, J. K. String stability of interconnected systems. **IEEE Transactions on Automatic Control**, v. 41, n. 3, p. 349–357, 1996. Page [29](#).

SILJAK, Dragoslav D. **Large-Scale Systems: Stability and Structure**. New York: North-Holland, 1978. Pages [18](#) and [52](#).

WANG, Jiange; LUO, Xiaoyuan; WONG, Wai-Choong; GUAN, Xinping. Specified-time vehicular platoon control with flexible safe distance constraint. **IEEE Transactions on Vehicular Technology**, v. 68, n. 11, p. 10489–10503, 2019. Page [81](#).

WANG, Ziran; WU, Guoyuan; BARTH, Matthew J. Developing a distributed consensus-based cooperative adaptive cruise control system for heterogeneous vehicles with predecessor following topology. **Journal of Advanced Transportation**, v. 2017, n. 1, p. 1–16, 2017. Page [30](#).

XU, Liwei; ZHUANG, Weichao; YIN, Guodong; BIAN, Chentong. Stable longitudinal control of heterogeneous vehicular platoon with disturbances and information delays. **IEEE Access**, IEEE, v. 6, p. 69794–69806, 2018. Page [18](#).

Yan, Z.; Jiang, H.; Shen, Z.; Chang, Y.; Huang, L. k -connectivity analysis of one-dimensional linear vanets. **International Journal of Control, Automation and Systems**, v. 61, n. 1, p. 426–433, 2012. Page [28](#).

YANG, Panpan; TANG, Ye; YAN, Maode; ZHU, Xu. Consensus based control algorithm for nonlinear vehicle platoons in the presence of time delay. **Int. Journal of Control, Automation and Systems**, v. 17, p. 752–764, 02 2019. Page [27](#).

Zhang, H.; Chen, Z.; Mo, X. Effect of adding edges to consensus networks with directed acyclic graphs. **IEEE Trans. on Automatic Control**, v. 62, n. 9, p. 4891–4897, 2017. Page [28](#).

Zhang, L.; Orosz, G. Motif-based design for connected vehicle systems in presence of heterogeneous connectivity structures and time delays. **IEEE Trans. on Intelligent Transportation Systems**, v. 17, n. 6, p. 1638–1651, 2016. Pages [27](#) and [28](#).

ZHENG, Yang; BIAN, Yougang; LI, Shen; LI, Shengbo Eben. Cooperative control of heterogeneous connected vehicles with directed acyclic interactions. **IEEE Intelligent Transportation Systems Magazine**, Institute of Electrical and Electronics Engineers (IEEE), p. 1–1, 2019. ISSN 1941-1197. Pages [12](#), [27](#), [28](#), [33](#), [56](#), [63](#), [67](#), and [68](#).

ZHENG, Yang; LI, Shengbo Eben; LI, Keqiang; REN, Wei. Platooning of connected vehicles with undirected topologies: Robustness analysis and distributed H-infinity controller synthesis. **IEEE Trans. on Intelligent Transportation Systems**, v. 19, n. 5, p. 1353–1364, 2018. Page [30](#).

ZHOU, Yang; AHN, Soyoung; WANG, Meng; HOOGENDOORN, Serge. Stabilizing mixed vehicular platoons with connected automated vehicles: An H-infinity approach. **Journal of Transportation Research Procedia**, v. 38, p. 441–461, 2019. ISSN 2352-1465. Pages [28](#) and [30](#).